AD 607769

/APL TDR 64-117

FLOW STABILITY IN MULTITUBE FORCED-CONVECTION VAPORIZERS

TECHNICAL DOCUMENTARY REPORT NO. APL TDR 64-117

October 1964

Air Force Aero Propulsion Laboratory
Research and Technology Division
Air Force Systems Command
Wright-Patterson Air Force Base, Ohio

BPSN 4(6399-675A)

(Prepared under Contract No. AF 33(615)-1551 by the
AiResearch Manufacturing Division, The Garrett Corporation
Los Angeles, California; P. J. Berenson, author)

NOTICES

When Government drawings, specifications, or other data are used for any purpose other than in connection with a definitely related Government procurement operation, the United States Government thereby incurs no responsibility nor any obligation whatsoever; and the fact that the Government may have formulated, furnished, or in any way supplied the said drawings, specifications, or other data, is not to be regarded by implication or otherwise as in any manner licensing the holder or any other person or corporation, or conveying any rights or permission to manufacture, use, or sell any patented invention that may in any way be related thereto.

Qualified requesters may obtain copies of this report from the Defense Documentation Center (DDC), (formerly ASTIA), Cameron Station, Bldg. 5, 5010 Duke Street, Alexandria, Virginia, 22314.

This report has been released to the Office of Technical Services, U.S. Department of Commerce, Washington 25, D. C., for sale to the general public.

Copies of this report should not be returned to the Research and Technology Division, Wright-Patterson Air Force Base, Ohio. unless return is required by security considerations, contractual obligations, or notice on a specific document.

C

FOREWORD

The work described in this report, designated AiResearch Report L-9443, was supported by the Atomic Energy Commission and the Research and Technology Division of the United States Air Force Systems Command through Contract AF 33(615)-1551, BPSN 4 6399-675A). The program was under the direction of C. H. Armbruster at RTD and J. A. Boppart and K. O. Parker at AiResearch.

Among the members of the AiResearch program staff, acknowledgment is due the following R. A. Stone for constructive suggestions during all phases of the program; R. W. Susag and W. Ziegler for the detailed design of the test loop and supervision of the subsequent construction, R. A. Fick and G. L. Schroyer for construction, maintenance, and operation of the equipment used in the experimental research; L. B. Meek for the photographs of two-phase flow; and J. Aranguren and A. M. Shah for assistance with the data processing.

ABSTRACT

This report describes work undertaken to resolve the SNAP-50/SPUR liquid-metal boiler two-phase flow stability problems. A review is presented of existing literature pertaining to forced-convection vaporization heat transfer and two-phase flow stability. Dimensionless simulation criteria are defined on the basis of the significant parameters determined from the survey. The test program, in which Freon 113 was used as the test fluid and the values of the dimensionless two-phase flow stability parameters applicable to the SNAP-50/SPUR boiler were simulated, is presented. The design of the transparent closed test loop, which incorporates a five-tube boiler, is described. Conclusions and discussions are presented, based on the measured data and the high speed photographs of two-phase flow in both plain tubes and tubes with twisted tape inserts, which indicate that stable flow can be achieved in the SNAP-50/SPUR boiler by inserting at the entrance of each boiler tube an orifice which has a pressure drop between 100 and 200 percent of the two-phase pressure drop.

TABLE OF CONTENTS

ILLUSTRATIONS

ILLUSTRATIONS

TABLES

NOMENCLATURE

C_p	Specific heat, Btu/lb-°F
D	Tube diameter, ft
f	Frequency, cps
G	Mass velocity, lb/hr-sq ft
h	Heat transfer coefficient, Btu/hr-sq ft-°F
h_{fg}	Heat of vaporization, Btu/lb
L	Tube length, ft
P	Pressure, psi
Q/A	Heat flux, Btu/hr-sq ft
ρ	Density, lb/cu ft
T	Temperature, °F
U	Overall coefficient of heat transfer, Btu/hr-sq ft-°F
W	Flow rate, lb/hr
X	Quality

Subscripts

a	air
b	boiler
c	critical
f	freon
in	in
ℓ	liquid
out	out
sat	saturation
TP	two-phase
tube	tube
v	vapor

SECTION I

INTRODUCTION

The SNAP-50/SPUR power-conversion system requires a boiler that converts subcooled liquid potassium into dry potassium vapor using liquid lithium, heated in a nuclear reactor, as the heat source. The boiler is a shell-and-tube design, with the potassium vaporizing inside parallel tubes which contain twisted tape inserts. This report describes work undertaken to resolve the SNAP-50/SPUR liquid-metal boiler two-phase flow problems by simulating flow conditions with conventional fluids. Two-phase flow problems may arise due to flow stability phenomena, multichannel flow distribution effects, or high quality dry-wall transition effects, as described below.

- Flow Stability. Flow stability is a problem inherent in forced-convection boilers of the SNAP-50/SPUR type, in which subcooled liquid is passed into parallel passages and vaporized to high quality. Small local changes in pressure drop or heat transfer rate can cause rapid and substantial shifts in flow rate through individual tubes. One reason for this is that, in the two-phase region, the curve of pressure drop vs flow rate can have a negative slope owing to the phase change. That is, a decrease in flow leads to an increase in vapor quality and, since the pressure drop associated with vapor flow is much greater than that for liquid, a greater pressure drop is required. The imposed pressure drop, however, tends to remain constant; therefore, a decrease in flow, which requires an increased pressure drop, in turn leads to a further decrease in flow.

- Multichannel Flow Distribution. Flow distribution is another problem existing in any heat exchanger with multichannels. Poor flow distribution causes different rates of temperature or quality increase in each tube, so that the required exit condition is not attained at an equal distance from the inlet in every tube. The effect of unequal distribution is to require that every tube be lengthened so that each tube will produce a satisfactory exit condition; this increases the boiler weight. Good flow distribution normally is promoted by the design of the inlet manifold.

- High Quality Dry-Wall Transition. At high quality in forced convection vaporization, there is a transition from a liquid covered wall to a partially dry wall, with a corresponding decrease in heat transfer rate. The quality at which this occurs cannot be predicted, and the factors affecting this transition and the flow patterns are uncertain. It is not known, for example, whether the small volume of liquid present covers one percent of the wall, or none of the wall. The use of whirlers to centrifuge the liquid to the wall may increase the amount of wall covered by liquid. Observation of the flow pattern for various whirlers with high speed motion pictures is a very valuable tool for clarifying this important area. Essentially every advancement in the field of boiling heat transfer and two-phase flow has been the result of visual observations.

Manuscript released by author October 1964 for publication as an RTD Technical Documentary Report.

Since liquid thermal conductivity, which is the only property of liquid metals that varies greatly from the value for common fluids, does not directly influence the two-phase flow processes, it is possible to simulate liquid-metal flow processes with conventional fluids. This approach allows the use of simple flow visualization techniques, which provide a more complete understanding of the major problem areas, and considerably reduces test complexity during initial evaluation and solution of the two-phase flow problem areas.

The objective of this investigation was to proceed as far as possible toward the solution of the SNAP 50/SPUR boiler two-phase flow problems using information available in the literature and conventional fluid testing. This approach minimized the amount of liquid-metal testing required to obtain the final solution to these problems, and thus resulted in a significant cost saving.

This report contains a brief literature review that produced information on the important parameters which were then used to formulate flow simulation criteria. The test program resulting from the application of these simulation criteria and the transparent test loop designed to measure the effect of the controlling parameters are described. Finally, the results of the test program are presented and discussed.

SECTION 2

TECHNICAL DISCUSSION

GENERAL

Flow instability may occur under an unknown combination of heat exchanger boundary conditions, flow rate vs pressure drop relationships (functions of fluid properties), and external disturbances, and has been detected by many investigators. It is clear from the experimental evidence that destablized flow conditions, both with and without heat addition. For example, Prandtl showed that, in the transition region, single-phase flow in a pipe could destabilize and oscillate between laminar and turbulent flow. Of greater concern in this program, however, are the flow instabilities associated with two-phase flow; only these cases will be discussed in succeeding sections.

Understanding and analysis of the flow instability problem requires a knowledge of many related technical specialties. Some of the instabilities are the result of flow or heat transfer regime transitions, and many can be qualitatively explained by more than one mechanism. A thorough understanding of all heat transfer mechanisms and flow regimes possible with forced-convection vaporization heat transfer and two-phase flow is required to preclude erroneous conclusions. Therefore, a brief discussion of the state of the art in forced-convection vaporization heat transfer, including research results from an earlier phase of this investigation, is presented below, prior to a review of the literature containing information on two-phase flow stability.

FORCED-CONVECTION VAPORIZATION HEAT TRANSFER

A large number of both experimental and analytical investigations of forced-convection vaporization heat transfer have been performed during the past 20 years. Reference 1* contains an excellent review of the state of the art up to 1957. The process depends upon a great number of variables and is made more difficult by the complexity of the various two-phase flow patterns which occur as the quality increases along the tube.

Because of the large differences in the various flow patterns which occur as the volume fraction of the vapor increases along the tube, a separate correlation is required for each flow pattern. Therefore, familiarity with the characteristics of each flow pattern is required before an analytical model can be formulated to yield correlations for the heat transfer coefficient in each regime, and the quality at which flow regime transitions occur.

Visual studies of adiabatic two-phase, two-component flow have provided information on the flow patterns. Attempts have been made to develop flow regime maps, which would make it possible to predict the boundaries between the observed flow patterns[2,3]. While the

*Numbers refer to references at the end of this report.

flow regimes depend to some extent upon whether the flow is vertical or horizontal, the flow regimes shown in Figure 1 appear to be most common for both orientations. The flow patterns shown are as follows:

a. Bubbly Flow--This pattern occurs at very low quality and consists of individual bubbles of vapor entrained in the liquid flow. The bubbles are formed at nucleation sites on the wall.

b. Plug or Slug Flow--As the quality increases, the individual bubbles agglomerate and grow to form plugs or slugs of vapor, which periodically pass a given point on the wall.

c. Annular Flow--At higher quality, the vapor flows in a high-velocity core in the center of the pipe, and a thin film of liquid covers the pipe wall. Liquid droplets are generally dispersed in the vapor core.

d. Mist Flow--At moderate to high quality, the liquid film on the wall disappears and all the liquid is dispersed throughout the vapor as droplets.

Forced-convection vaporization heat transfer data have shown that the heat transfer coefficient for a fixed geometry and flow rate increases with increasing quality[4,5]. At a critical quality, which varied considerably with fluid, geometry, and heat flux, there is a sharp decrease in the heat transfer coefficient toward the value characteristic of vapor flow, as shown in Figure 2. When the quality reaches 100 percent, the coefficient equals the vapor heat transfer coefficient. Numerous heat transfer correlations have been recommended [1,4,6,7] for the various flow regimes.

It is often of great importance to be able to predict the quality at which the sharp decrease in heat transfer coefficient occurs, for, if the heat flux is the imposed condition, burnout may occur beyond this point. It has been suggested[4] that this quality corresponds to the point at which the transition from annular flow to mist flow occurs. This is very likely, since this is a transition from a liquid covered wall to a gas blanketed wall, which is similar to the pool boiling burnout condition that occurs in changing from nucleate to film boiling. Many reasons have been suggested for the transition from annular to mist flow, and numerous correlations of the forced-convection vaporization burnout condition have been attempted.

Most of the visual studies of forced-convection vaporization have been performed under adiabatic conditions because of the relative ease of this type of experiment. In addition, most of the heat transfer tests have used electrical heating, thereby imposing the heat flux boundary condition. An experiment[8] performed at AiResearch during an earlier phase of this program used high speed motion pictures to study the forced-convection vaporization process, when the overall temperature difference was the imposed boundary condition. Motion pictures were obtained of all the significant flow patterns; the resulting film may be borrowed from the writer.

Figure 1. Two-Phase Flow Patterns

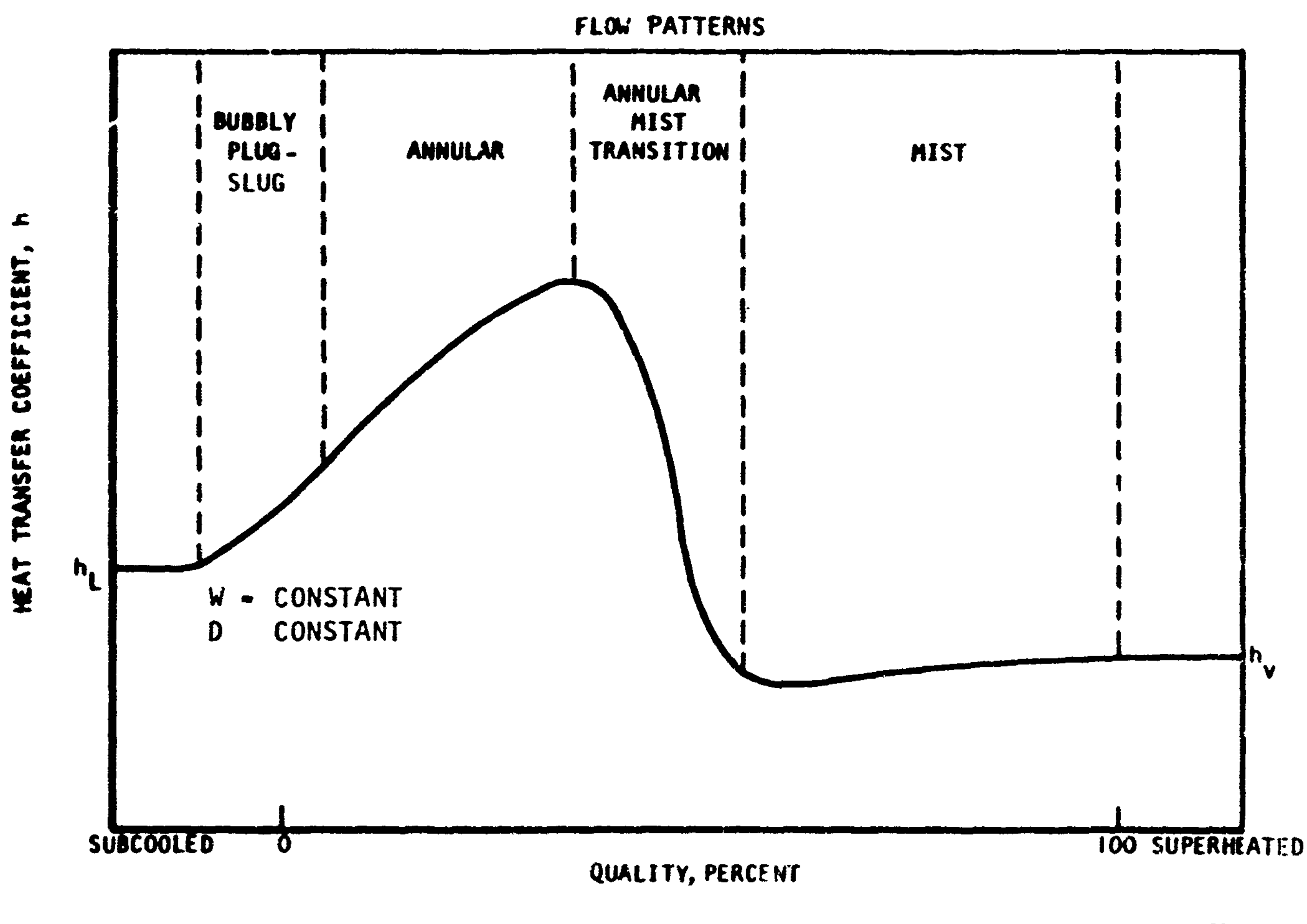

Figure 2. Characteristic Forced-Convection Vaporization Heat Transfer Coefficient

The following conclusions were based on results of an earlier phase of this program, which is reported in Reference 8 (included as an appendix to this report).

Bubbly Flow

Because of the high ratio of liquid to vapor density for most fluids of interest, the vapor mass fraction (quality) in the bubbly flow regime is generally much less than 1 percent. The bubbly flow regime can occur in a subcooled liquid, since the bubbles nucleating at the wall may depart from the wall because of the inertia caused by their growth rates. Thermal equilibrium does not exist, as there is insufficient time for the bubbles to condense before the surrounding liquid is heated to the saturation temperature as it flows along the tube.

In the bubbly flow regime, the volume fraction of the vapor is very small. so that it has little effect on the liquid velocity. Bubbles grow and depart from nucleation sites on the wall much as they do in nucleate pool boiling. Depending upon the wall and fluid temperatures and the nucleation characteristics of the wall, the nucleate pool boiling heat transfer mechanism may or may not dominate the forced-convection heat transfer to the liquid occurring between the bubble nucleation sites In the very narrow quality range over which bubbly flow exists, it seems reasonable to assume that the heat transfer can be predicted by superimposing liquid forced convection and nucleate pool boiling, provided the superheat temperature difference is not great enough to produce film boiling.

Plug Flow

As the vapor volume fraction or the tube length-to-diameter ratio increases, the individual bubbles grow and agglomerate to form plugs or slugs of vapor, which occur periodically along the tube. Even though the vapor volume fraction has increased, the corresponding quality is still very low. However, the presence of the larger volume fraction of vapor begins to cause a significant increase in the liquid velocity in the plug flow regime.

Bubbles may nucleate and depart from the wall at numerous sites inside the tube in the plug flow regime. The heat transfer mechanism is probably the same as that in the bubbly flow regime, a superposition of forced convection to a liquid and nucleate pool boiling.

The plugs of vapor are compressible volumes which make possible flow oscillations within the tube even though the flow entering the tube is steady. Actual flow reversal was observed in the motion picture study. It is possible that the periodic nature of plug flow, combined with the compressible volume it provides, is the source of many of the exit flow oscillations that occur in forced-convection vaporization, inasmuch as all other flow regimes are steady.

Annular Flow

Theoretical stability analysis of a liquid film[9] predicts that a liqui film is stable for sufficiently small Reynolds numbers, independent of the vapor velocity. Since the liquid-film Reynolds number decreases as the quality increases in a forced-convection vaporizer, the liquid annulus will be stable at sufficiently high quality, independent of the value of the vapor velocity.

While annular two-phase flow is sometimes idealized so that all the liquid is in the annular film and all the vapor in the high velocity core, observations generally have shown that droplets of liquid exist in the vapor core. This is consistent with the stability analysis which predicts that a high-Reynolds-number liquid film, such as exists at low quality, may be unstable and produce droplets. These droplets may or may not rejoin the liquid annulus, depending upon the magnitude of the turbulent vapor fluctuations, the transit time of the droplets through the vaporizer and the passage length-to-diameter ratio.

The liquid vapor interface between the continuous liquid film on the wall and the high-velocity vapor core is wavy. Although there are active bubble nucleation sites, these probably have a negligible effect on the rate of vapor generation. The vapor is generated primarily by vaporization from the liquid vapor-core interface inside the tube, and not by the formation of bubbles at the wall. The heat transfer in annular flow is very similar to that for condensation inside a tube; heat is transferred through the liquid film to the interface with the vapor core.

Annular-Mist Flow Regime Transition

A description of the transition from annular to mist flow is of great interest, since this is presumably the point at which the vaporizer heat transfer coefficient experiences a sharp decrease and causes the forced-convection vaporization burnout condition.

The following significant observations of the wall drying process were made. A small dry spot forms and grows in all directions, as the liquid vaporizes, because of conduction heat transfer through the liquid. The small strips of liquid on the wall remain almost stationary relative to the high-velocity vapor and the liquid droplets flowing in the tube. The dominant heat transfer mechanism is conduction through the liquid. Nucleation may produce the initial dry spot on the wall, but has a small effect on heat transfer. This is the same drying process that would occur with a thin film of liquid in a hot pan whose temperature is not great enough to cause nucleate boiling.

As a result of the visual observations of the transition process, it was concluded that the transition is due simply to vaporizing of the liquid film on the wall as a result of conduction heat transfer through the liquid, while the vapor core still contains a dispersion of liquid droplets formed upstream at lower quality and carried along by the vapor. While the volume-fraction of these droplets is very small, they account for a substantial mass fraction because of the high liquid-to-vapor density ratio.

In summary, the liquid droplets dispersed throughout the vapor core are produced as a result of a film instability at low quality. The transition from annular to mist flow occurs when the liquid annulus vaporizes as a result of conduction through the thin liquid film, while liquid droplets remain dispersed throughout the vapor core. The quality at the transition is determined by the mass of liquid contained in the droplets when the transition occurs.

Mist Flow

In mist flow, the wall is dry except when the liquid droplets in the vapor core impinge upon the wall and vaporize. Most of the heat transfer is from the wall to the vapor. After the heat is transferred to the vapor, it is then transferred to the liquid droplets; the mist flow vaporization process actually takes place in the interior of the pipe and not at the wall. For this reason, the temperature of the vapor in the mist flow regime is greater than the saturation temperature; thermal equilibrium does not exist in the tube. The mechanism of heat transfer in mist flow is, therefore, forced convection to a gas.

Flow Stability

For low values of pressure drop across the throttle valve at the entrance to the heated tube, flow instability was observed. The flow rate fluctuations apparently were due to the interaction of the two-phase flow pressure drop characteristics with the compressible volumes in the system[10]. At all heat fluxes and flow rates investigated, the inlet flow rate could be made steady with a sufficiently great pressure drop across the inlet throttle valve. Even though there was steady flow into the tube, the flow rate and temperature at the exit were seen to fluctuate. This apparently was due to the periodic nature of plug flow, the compressible volume of the plugs, and the fact that thermal equilibrium does not exist in mist flow.

TWO-PHASE FLOW STABILITY LITERATURE REVIEW

Causes of Flow Instability

The relative influence of a given design parameter on the stability of fluid flow systems depends quite strongly on the particular type of instability to which a system is subject. Nonetheless, where catastrophic power excursions are not involved, the literature dealing with two-phase flow instability indicates that the following parameters are influential: (a) fluid inlet subcooling, (b) heat flux, (c) pressure, (d) inlet velocity, (e) orifices, and (f) acceleration fields.

1. Subcooling

A primary cause of instability in boiling water reactors has been inlet subcooling, and this has been particularly evident where large void fractions were present. Beckjord[11] attributed the flow instabilities he observed in a boiling water reactor to inlet subcooling. It has also been noted that, in nonreactor circulation tests with heat addition, the condition for the onset of oscillation is strongly dependent upon the inlet temperature, and that the observed instabilities increase in severity with increases in the amount of subcooling. This is in agreement with formal calculations of density changes in coolants, which lead to the conclusion that subcooling increases unstable density changes. It also is in agreement with other calculations which demonstrate that increasing subcooling enlarges regions of operation in which the slope of the curve for pressure drop vs flow rate is negative, and hence unstable [12]

On the other hand, in tests conducted of boiling burnout with water in vortex or swirl flow [13], where degree of subcooling was treated as a variable, excellent stability was exhibited up to the burnout point. This would suggest that subcooling perhaps does not influence the stability of swirl flow, or that the influence is extremely weak; more definitive investigations are required to confirm or refute this conjecture.

Recent results of Gouse[14] from a forced-flow, parallel-channel system showed that there was a range of subcooling within which the flow would oscillate. If the inlet subcooling was either greater or less than this range, the flow was steady.

2. Heat Flux

There is considerable disagreement regarding the effect of heat flux on stability. This probably is because heat flux should not be considered an independent variable; it can be determined from inlet velocity, subcooling, exit quality, and geometry. Some experimental workers find that instabilities have a tendency to be strongly damped and reduced in amplitude when design heat inputs are raised sufficiently. Although not clearly understood, the phenomena seem to be connected with the possibility that damping forces may increase more rapidly than forces driving the instabilities. On the other hand, Gouse[14], Quandt[15], and Meyer[16] have observed that oscillatory instabilities can be induced by increasing the heat flux.

Investigators apparently have not considered the effect on stability of a constant wall temperature boundary condition instead of a uniform wall heat flux.

3. Pressure

Oscillations are strongly damped and relatively low in amplitude at elevated pressures. Blubaugh and Quandt[17] noted that conditions for the onset of oscillation were primarily a function of the channel inlet temperature and the pressure. Quandt's[15] theoretical analysis showed that flow oscillations become less prevalent at higher pressures. Mendler, et al[18] also observed that flow fluctuations in natural circulation tests increased with the reduction of pressure and inlet temperature.

While this subject requires more study, the influence of pressure seems to be connected with the fact that, at higher pressures, the ratio of liquid to vapor densities is reduced and, in a sense, the two phases are more similar. Stenning[19] has shown in his analysis that oscillatory flow will exist for a variety of configurations, provided that the density ratio across the system exceeds a critical value, which depends on the geometry and the flow relationships. Calculations performed by Wright[20] also indicate that flow stability exists if the specific volume ratio is below a critical value.

4. Inlet Velocity

Inlet velocity, mass velocity, and flow rate, which are discussed by various investigators, are different names for the same variable, and all will be grouped under the above heading. Approximate calculations indicate that an increase in the design inlet velocity has a stabilizing influence in once-through high quality boilers. Jones[21] has shown that the tendency toward instability varies inversely with the square of the subcooled fluid velocity. Gouse[14] observed that increasing the flow rate, with other variables held constant, tends to stabilize the system. At the present time, however, the sparseness of the literature does not lend itself to definitive statements.

5. Orifice Pressure Drop

Several investigators have considered the effects of orifices at the inlet on flow stability. Fraas[12] has shown that, in low pressure subcooled water, orificing has a pronounced stabilizing influence; moreover, the effect increases with the ratio of the orifice pressure drop to the pressure drop for the rest of the passage. Stenning[19] considered analytically the time-varying flow of a boiling liquid through a series of ducts and heaters for the case in which the flow rate is controlled by a downstream orifice. He showed that oscillatory flow will exist, provided that the density ratio across the system exceeds a certain critical value. He concluded that upstream orificing will help to damp out these oscillations.

A one-pass boiler also has been studied by Jones[21] for the case in which there is significant subcooling. He found that, while an orifice can be a stabilizing influence, it also can destabilize the system. From his conclusions regarding the stabilizing influence of high subcooled velocities, it is by no means clear that orificing would be effective in high performance systems where there is turbulent flow and vigorous subcooled boiling with a relatively high friction factor.

Wallis and Heasley[22] have discussed a natural circulation loop with a constriction at the top of the heated section. They assert that their results have wide application because many systems without outlet orifices have most of the pressure drop at the exit where velocities and shear stresses are high. They observed instability in a pentane loop when the heater exit was constricted.

Several investigators have demonstrated that the stability of coolant flow during boiling is influenced by the pump and system flow characteristics. Stability is improved as the test-section pressure drop becomes a smaller part of the total system pressure drop. The change in pressure drop caused by a phase change of the coolant, then, has less influence on the flow rate, since this pressure drop is a smaller part of the total pump head.

Lowdermilk[23] found that it always was possible to stabilize the flow in a single tube with a great enough inlet-restriction pressure drop. The required pressure drop was concluded to be a function of L/D ratio and mass velocity.

6. Acceleration Field

Depending upon the direction of the field, acceleration can be extremely important, either in stabilizing or in destabilizing a fluid flow system. At one extreme is the well known catastrophic Taylor instability, resulting when the field is in the "wrong direction" across the interface between liquid or gaseous media of different densities (24). At the other extreme is the case of the highly stable interface that exists in high-velocity separated two-phase flow in a tight spiral. Because of the extreme difficulties involved in carrying out both theoretical and experimental work in reduced gravity fields, very little work has been reported in this area beyond the fact that the tendencies toward instability seem to increase as the conditions for free fall are approached.

Classes of Flow Instabilities

Although authors have not formally categorized the hydrodynamic instabilities in two-phase fluid flow systems, those not involving actual burnout may be divided approximately into the following four classes:

- Flow regime transitions
- Negative derivative of pressure drop with respect to flow rate
- Compressibility
- Parallel channel coupling

A fifth, the amplification of a "maldistribution," has been reported by Adorni, et al (23), but with neither a description nor discussion adequate for review at this time. Also, Quandt (15), on the basis of an analytical and experimental investigation of flow oscillations, concludes that another type of flow instability, "stable flow oscillations," associated with definite frequency and reproducibility from cycle to cycle, should be recognized.

Systems subject to different classes of instabilities may exhibit quite similar performance. For example, oscillations may be associated with flow regime transitions and parallel channel coupling as well as with compressibility. Flow excursions may be associated with all classes. In spite of these similarities, it is necessary to treat each class separately because of basic differences in the phenomena believed to be responsible in each case. In addition, the type of instability is a function of the imposed boundary conditions on the heat exchanger. Typical boundary conditions are constant pressure drop, constant inlet pressure, and constant inlet flow rate. The boundary condition selected in the analysis or imposed in the experiment will determine the different types of instabilities that will be possible.

1. Flow Regime Transitions

The recognized types of flow regime transitions that can give rise to unstable operation are nucleate-to-film boiling, bubble flow-to-slug flow-to-annular flow and laminar-to-turbulent flow. These transitions give rise to such instabilities as pressure variations, transient pressure drop (and recovery), and sustained oscillations.

Isbin, et al[26] has noted that large pressure variations are usually associated with a flow regime transition. In their work, the instabilities were associated with transitions from bubble-to-plug flow and annular-to-slug flow. In regard to the general concept that flow transitions may have an important influence on stability, Isbin[27], discussing a paper by Mendler, et al, suggested that, if one provides step changes in flow regimes corresponding to specified conditions, sustained oscillations may be generated.

The change in effective head that occurs at the onset of bulk boiling can be serious enough to generate sustained oscillations[28]. Bergles and Rohsenow[24] observed sustained oscillations where a transition takes place between nucleate and film boiling. In the latter case, film boiling begins in a restricted area and moves upstream, followed by a surge of water which cools the tube. The temperature again rises and the fluid flow decreases until a transition is made from nucleate to film boiling at a point downstream. In tubes of small diameter (less than 1/4 in.ID), the cycle is complete in seconds. Matzner[30] also reports on instability that could be due to a transition from nucleate to film boiling. In this case, the instability took the form of a sudden transient pressure drop with an immediate recovery.

While annular flow, mist flow, and fully developed slug flow are all stable, both bubble flow and "developing" slug flow are transient regimes and could be expected to lead to flow instabilities under certain conditions. An instability in a subcooled water flow system under conditions of zero gravity has been reported by Papell[31], which he attributes to transitions between bubble and slug-flow regimes. Extremely severe flow perturbations were required, however, to initiate the instability. Under normal gravity conditions, the instability could not be produced, even with large perturbations. This has some similarity to a phenomenon reported by Radovcich and Moissis[32]. In a normal-gravity adiabatic system of air and water, they observed a mode in which Taylor bubbles some 50 to 70 tube diameters in length would leave the tube in what would appear to have been "developing" slug flow. This would be followed by a return to bubble flow and a buildup of large bubbles to complete the cycle. In contrast to Papell's interpretation, they attribute this cycle to some instability limitation which was not discussed.

In view of the earlier work of Isbin, et al[26,27], the question is not definitely settled, and the possibility that this form of instability may appear cannot be definitely ruled out.

Another unstable mode of operation that could arise from a flow regime transition involves the transition from laminar to turbulent flow. A similar situation may be encountered in two-phase flow in the neighborhood of incipient boiling where bubbles first form on the walls. Such a transition also could take place near burnout in the case of highly subcooled fluids. Tripping of the boundary layer from laminar to turbulent flow in the neighborhood of incipient boiling has been reported by Bergles and Rohsenow[29]. Depending upon the geometry, this could reduce the flow enough to cool the tube to the point where the flow would become laminar and provide the mechanism for sustained oscillations. Descriptions of this mode of instability were not found in the literature. There may be a relationship to the flow oscillations in subcooled fluids that are associated with the sudden increase in pressure drop taking place in the neighborhood of burnout.

2. Negative Pressure Drop vs Flow Rate Derivative

It has been known for a number of years that, under a wide range of operating conditions, the pressure drop plotted against flow rate has a smooth hump in an otherwise monotonically increasing curve. As illustrated in Figure 3, then, there are three possible flow rates for a given pressure drop. If the system should operate at the intermediate point, it may be seen from the curve that flow will increase with decreasing pressure drop. This is a very unstable situation, and the system may experience a very rapid increase in flow rate until it is operating at the high flow rate. On the other hand, the operating point may shift rapidly to the low flow rate and lead to burnout[29]. Since both high and low flow rates are stable, the instability consists of a simple flow excursion. This form of instability has recently been s' ~'ied by Fraas[12,33], who calculated pressure drop vs flow rates in channe' for the purpose of establishing stability criteria which, as seen in Figure 3 is assured if operating parameters are chosen to force the system to a point where the slope is definitely positive. His calculations reveal that the negative slope region increases with the amount of subcooling and decreases with the system pressure (see Figure 4), confirming experimentally observed trends. Of particular interest is that the instability is impossible for high pressure systems (in the neighborhood of 600 psia for water). Although it is not practical to have saturation conditions at the inlet, it nonetheless is of interest to note that such an operating point is stable relative to negative pressure drops.

Recent experimental results of Collier[34] have shown that, while operation within the negative slope region may be impossible, a negative slope is not a necessary condition of oscillatory instability in parallel heated channels.

3. Compressibility

For a number of years authors have recognized that compressibility effects can lead to both transient and sustained oscillations in fluid flow systems. This is quite evident for two-phase flow systems where the design results in impedance of the vapor phase exhaust. It also may be serious in single-phase flow systems, as was demonstrated by the theoretical work of Poppendiek and Rickard[35], in which they showed that the observed excursions and oscillations accompanying reactor power surges could be accounted for by considering compressibility and thermal expansion. More recently, Lowdermilk, et al[23] have called attention to the fact that systems have a strong tendency to instability when designed in such a way that noncondensible gases can become entrained and trapped. This was demonstrated by the introduction of a compressible volume containing a noncondensible gas in the flow system between a throttling valve and the test section. Here the velocity of the gas was essentially zero, so that frictional losses were extremely small relative to

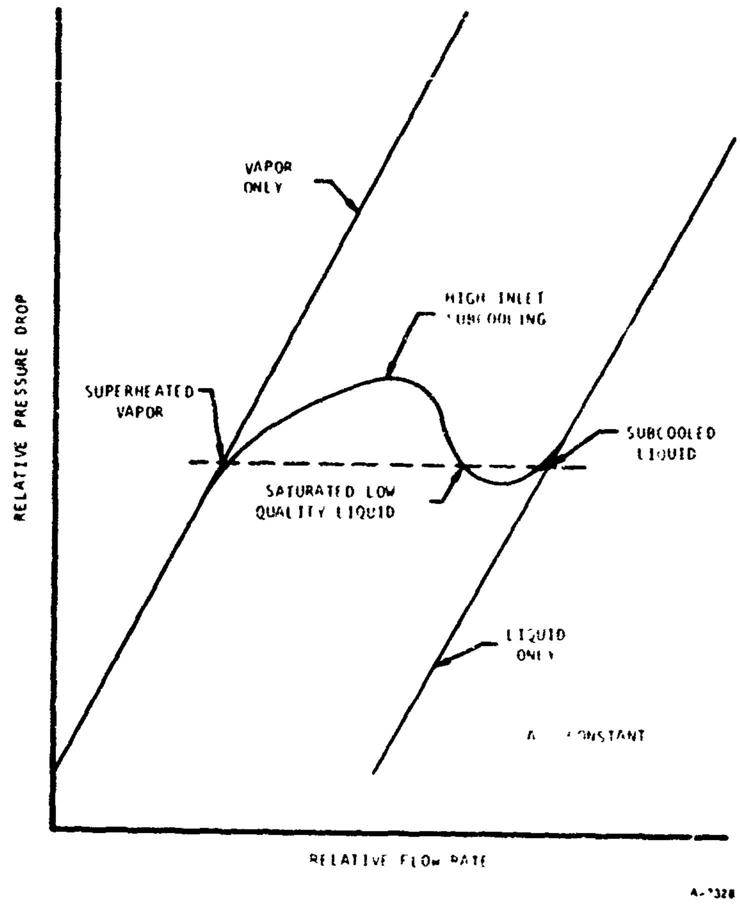

Figure 3. Dependence of Negative Pressure Drop Region on Subcooling

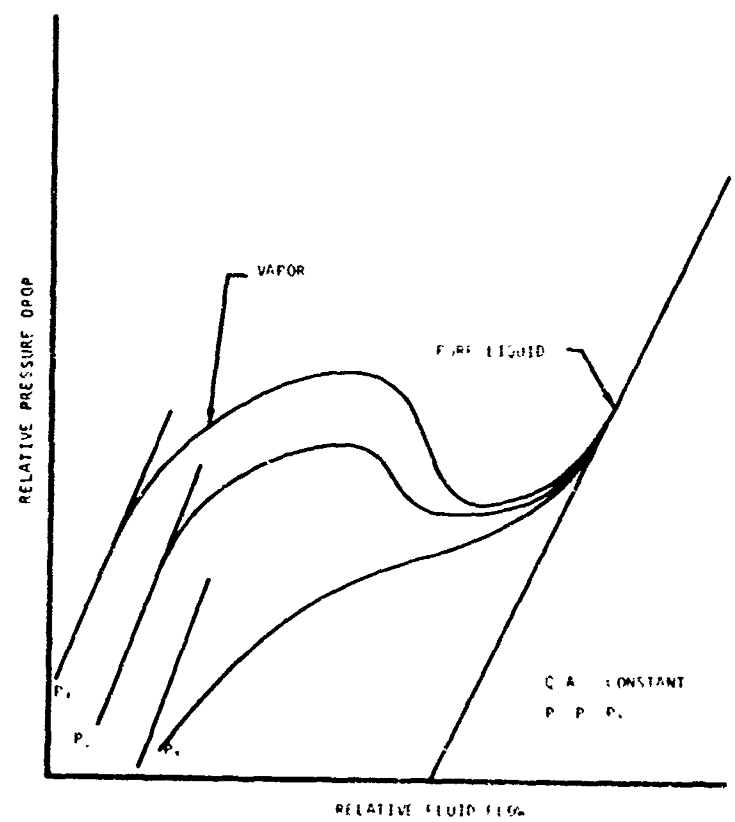

Figure 4. Effect of System Pressure Variation on the Negative Pressure Drop Regions at Constant Subcooling

those of the vapor in two-phase flow. During burnout they observed flow fluctuations which occurred at lower heat transfer rates as the static compressible volume was increased.

Bergles and Rohsenow[29], in a recent study of burnout in tubes of small diameter, concluded that flow oscillations caused by system compressibility can greatly reduce the burnout heat flux in the subcooled region, and that this instability is particularly difficult to avoid with small-diameter tubes.

4. Parallel Channel Coupling

Because the technical literature concerning instabilities in parallel channel flow systems is extremely sparse, no definitive statements on this subject are possible. However, Fraas[12] analysis on multichannel stability concludes that several possibilities exist for flow instability in parallel channels if the individual channels operate in a region that may give rise to flow instability. He notes that coupled oscillations may develop between parallel channels, inducing flow rate to increase in one channel and diminish in another.

The experimental program reported by Matzner[30] is of some interest in connection with the parallel channel instability problem. Forced convection was maintained through a bundle of 19 parallel electrical heaters which were packed close enough to very roughly approximate a number of parallel channels. At high pressures, only slight pressure fluctuations were observed. On approach to burnout, pressure transients were attributable to possible flow regime transitions as discussed above. The inside rod did not undergo any temperature instability, while the adjacent six inner rods showed worse performance than the outer 12 rods. Of particular interest was the fact that the pressure transient took the form of a pressure drop that did not exceed 4 to 12 psi at an operating pressure of 1000 psi. This was followed by an immediate recovery to slightly over the initial pressure.

Discussion

The literature review summarized above revealed far more problems than it solved and led to the obvious conclusion that the two-phase flow stability problem is extremely complex. There are many different types of instabilities; each may exhibit more than one behavior and is affected by numerous parameters, including fluid properties, geometry, and imposed boundary conditions. Instabilities may exist with steady imposed conditions, or may be caused by a change in the nominal operating condition of the heat exchanger.

It does not appear possible to derive one equation covering all possible instabilities; each type of instability and set of boundary conditions generally must be analyzed separately. While most types have been observed empirically, usually by unfortunate accident, few have been correlated analytically. Most of the analyses, while predicting qualitatively the effect of some of the variables, have been unsuccessful in predicting the quantitative results which were experimentally observed. In addition, none of the analyses has been verified thoroughly enough by experiment to warrant its application without subsequent experimental confirmation.

It is felt that, in a once-through, high exit quality vaporizer, the most prevalent class of instability is that resulting from negative derivative of pressure drop with respect to flow rate. The analysis of this instability by Fraas (33) has much to recommend it since it is simple, reveals the physical importance of the variables, and has predicted the effect of pressure, subcooling, and heat flux on flow stability which has been observed in practice.

In summary, the state of the art is not far advanced; there is lack of agreement about the effect of many variables; most conclusions about two-phase flow stability are qualitative (e.g., high pressure is good) and there is no general analytical approach which shows promise of describing flow stability behavior.

SIMULATION CRITERIA

Because of the complexity of the two-phase flow stability problem and the lack of an available, dependable, general analysis of the problem, the decision was made to resolve the SNAP-50/SPUR boiler flow stability problem experimentally. A through investigation of the effect of all the important parameters, using potassium as the test fluid, was not economically feasible. Also, it was judged very desirable to use a fluid which would allow the construction of a transparent boiler so that visual observations would be possible; potassium does not satisfy this requirement. It was therefore necessary to develop simulation criteria which would provide a rational basis for: selecting a test fluid, designing a test loop, and planning a test program whose results would be applicable to the SNAP-50/SPUR potassium boiler.

The literature review revealed a large number of parameters affecting the two-phase flow stability problem. Those discussed by various investigators are:

1. Entrance subcooling
2. Subcooled liquid pressure drop
3. Pressure level
4. Liquid-to-vapor density ratio
5. Exit quality
6. Heat flux
7. Pressure drop
8. Flow rate
9. Inlet velocity
10. Mass velocity
11. Passage length-to-diameter ratio

The expense of experimentally investigating a range of values of each of the above parameters is prohibitive, even with a conventional fluid. Because of this, and the necessity for applying the experimental results to potassium, it was judged necessary to reduce the important physical variables to a complete set of independent, dimensionless, similarity parameters.

The application of dimensional analysis to heat transfer and fluid mechanics problems is very common. It serves two very important functions in experimental investigations: (1) the number of independent variables is reduced because there are fewer independent dimensionless groups than physical variables, and (2) simulation of the actual problem is possible with more convenient geometry and test fluids. The theory and methods of dimensional analysis are discussed by McAdams (39) and other authors of heat transfer textbooks. The method used here to define dimensionless groups was to combine (1) nondimensionalizing of the controlling fundamental equations, (2) past experience with the same physical variables, (3) and intuition. The nondimensionalizing procedure was simplified because Fraas (12) presented his results in dimensionless form.

In calculating the pressure drop-vs-flow rate relations, it becomes apparent that the importance of subcooling is determined by the ratio of (1) the heat added to raise the fluid to the saturation temperature to (2) the heat required for vaporization. Therefore, the dimensionless parameter that measures the effect of subcooling is $C_p \Delta T / h_{fg}$. This same parameter appears if the energy balance for a boiler is expressed in dimensionless form. It also has been revealed in analysis of boiling heat transfer; and in some places is called the Boiling Number.

As discussed above in the literature review, pressure level is important primarily because of its effect on density ratio. For a constant friction factor, the ratio of liquid to vapor pressure drop is proportional to the density ratio, which is therefore a measure of potential pressure drop fluctuation. For these reasons, and because previous investigators have used liquid-to-vapor density ratio as an independent variable, it was selected as one of the dimensionless similarity parameters.

Pressure drop, flow rate, inlet velocity, and mass velocity were chosen separately for emphasis by various investigators. However, they are all a function of the dimensionless pressure-drop ratio, (pressure drop divided by pressure level,) which is proportional to Mach number and L/D. The system geometry is defined by the length-to-diameter ratio.

The heat balance on a boiler, expressed in dimensionless form, shows that the dimensionless heat flux, $\frac{Q/A}{G\, h_{fg}}$, is a function of the dimensionless subcooling parameter, exit quality, and L/D. Therefore, exit quality was chosen as the final independent variable.

Subcooled liquid pressure drop, expressed in dimensionless form by dividing it by the two-phase pressure drop, was selected as the dependent dimensionless parameter. The results of Fraas (12), Lowdermilk (10), and others showed that two-phase flow always could be stabilized with a great enough pressure drop in the subcooled liquid region. As a result, the decision was made to solve the two-phase flow stability problem in the SNAP-50/SPUR boiler by inserting orifices at the entrance of each boiler tube. The test program described in the following section was designed to provide specific information pertaining to the magnitude of the pressure drop in the subcooled liquid region required to provide stable flow.

In summary, the physical variables were reduced to a complete set of six independent, dimensionless parameters, which can be expressed as follows

$$\Delta P_{\ell}/\Delta P_{TP} = f(C_p \Delta T/h_{fg}, \rho_{\ell}/\rho_v, \Delta P_{TP}/P, X, L/D)$$

The purpose of the test program was to determine experimentally the liquid pressure drop ratio required to produce stable flow for values of the five independent parameters on the right-hand side of the above equation covering a range around SNAP-50/SPUR boiler test and operating conditions

SECTION 3

TEST PROGRAM

OBJECTIVE

The primary objective of this program was to obtain sufficient information to design the SNAP 50/SPUR boiler so that stable two-phase flow will occur. The boiler is a tube-and-shell unit with twisted tapes inserted in the tubes to produce swirl which will centrifuge entrained droplets to the tube wall. The design approach was to place an orifice in the subcooled liquid region at the entrance to each boiler tube. The liquid pressure drop across the orifice must be made high enough to dominate the possible variations in two-phase flow rate that are possible with a constant header-to-header pressure drop. The ratio of orifice pressure drop to boiling two-phase pressure drop is considered to be the controlling dimensionless parameter and must be maintained above a critical value to provide stable flow. Since the problem was too complex to analyze, this test program was developed to determine the pressure-drop ratio required.

A major objective for later work with the test loop described below is a study of the condensing process in parallel tubes. Since the same loop, type of instrumentation, and observations will be utilized in the condensing studies as in the boiling studies, the objectives and requirements of this later work necessarily affected loop design.

Due to the complexity of the two-phase flow process, more than one plausible, but contradictory, explanation often can be found to rationalize unexpected experimental results. For this reason, it is essential that research on two-phase flow include visual observations whenever possible. The following partial list gives examples of the type of information that only visual observations can provide.

1. Determine the flow patterns that occur during forced-convection vaporization, with and without tube inserts.

2. Determine if a substantial amount of liquid flows along the twisted tape after the wall is dry, and how the liquid breaks off the end of the tape.

3. Determine the length beyond the end of a twisted tape that the swirl which was induced by the tape persists.

4. Establish the mechanisms for the various flow regime transitions.

5. Establish the flow patterns and flow maldistribution that occurs in parallel condensing tubes

6. Study the fluid dynamics at the condenser liquid-vapor interface.

7. Establish the visual characteristics of boiler and condenser flow instabilities.

The test program was designed to achieve the general objectives described above for values of the controlling dimensionless parameters developed in the preceding section, including the range of importance to the SNAP 50/SPUR boiler. Table 1 presents the current values of the five dimensionless similarity parameters in the design-point boiler and in a 19-tube prototype test boiler.

TABLE 1

VALUE OF DIMENSIONLESS SIMILARITY PARAMETERS IN SNAP 50/SPUR BOILER

	Design Point Boiler	19-Tube Test Boiler
$C_p \Delta T/h_{fg}$	0.18	Variable
ρ_ℓ/ρ_v	200	400
$\Delta P_{TP}/P$	0.1	0.4
Exit Quality, percent	100	Variable
L/D	150	200

In summary, the test program and test loop were designed to determine the pressure drop in the subcooled liquid region of the boiler required to provide stable two-phase flow for a range of conditions including those presented in Table 1; it was necessary that this be done with a transparent test loop.

FLUID SELECTION

A survey of the compatibility of the characteristics of common fluids with the test objectives of this program led to selection of Freon 113 as the test-loop working fluid. This inexpensive, easily available fluid is relatively nonhazardous and has well established physical properties.

To decrease the hazards involved in visually observing the two-phase flow processes at close range, it was desirable to run the tests near atmospheric pressure and temperature. The saturation temperatures of Freon 113 are 80°F and 120°F, respectively for liquid-to-vapor density ratios of 400 and 200. The saturation pressures at these conditions are 7 and 15 psia, as shown in Figure 5. While both saturation pressure and temperature are somewhat lower than the most desirable values, they are compatible with the anticipated test program and the requirement for maintaining the boiling temperature sufficiently above that of common cooling fluids to ease the design of the condensing side of the test loop.

Another advantage of Freons in general, and Freon 113 in particular, is the relatively low value of 60 to 70 Btu per lb for the heat of vaporization.

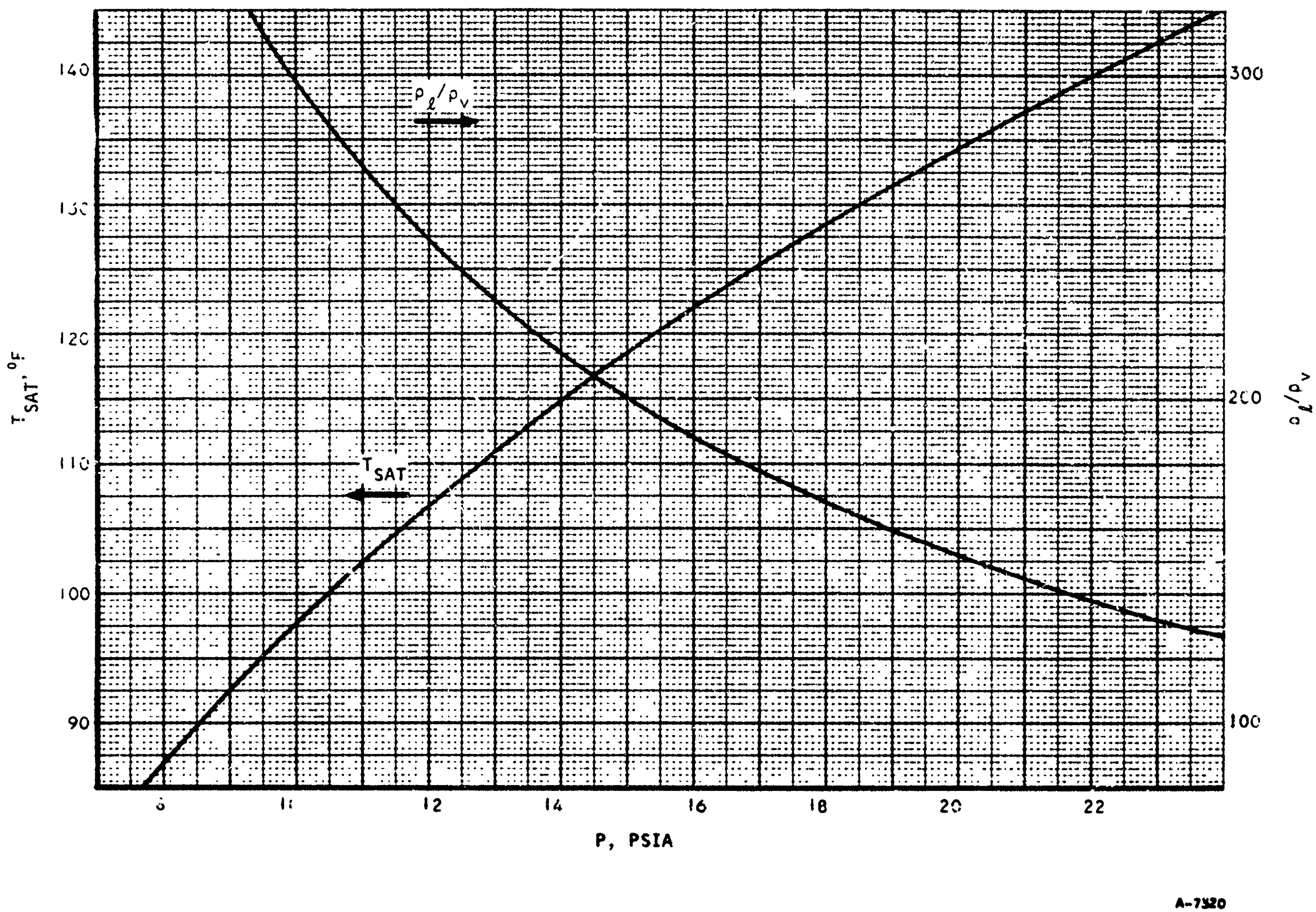

Figure 5. Freon 113 Properties

This makes it much easier to simulate and investigate a range of values of the dimensionless subcooling parameter, since only small changes in entrance temperature are required. In addition, both the heat flux and the total quantity of heat required to vaporize the fluid completely are proportional to the heat of vaporization, low values for these parameters ease the test loop design problem

Finally, Freon systems are common at AiResearch; therefore, a great deal of experience existed for the design and proper instrumentation of a reliable, leakproof Freon test loop.

RUN SPECIFICATION

Of the five parameters given in Table 1, it was necessary to test a range of values of only the first three, since the exit quality was kept near 100 percent in all runs, and the test boiler was designed with a constant L/D ratio of 160.

The dimensionless subcooling parameter has the required value of 0.18 with Freon 113 when the entrance subcooling is 50°F. To determine the effect of variations in subcooling, values of 25°F, 50°F, and 100°F were tested.

Pressures of 10, 15, and 20 psia, corresponding to density ratios of 300, 200, and 150, respectively were tested. At each of these pressures, pressure drops of 1, 2, and 3 psi were run, yielding a normalized pressure drop range of 0.05 to 0.3 The lowest pressure of 10 psia is higher than the value of 7 psia, which corresponds to the 19-tube boiler density ratio, however, it was the minimum pressure that allowed substantial subcooling to be tested, in the loop described below, due to the difficulty of cooling the boiler inlet to much below 50°F. The pressure range provides a 2 to 1 variation in density ratio, and the middle pressure simulates the design-point boiler.

The individual test conditions run for each type of tube insert, as listed in Table 2, include most combinations of the following properties.

P_{out} = 10, 15, and 20 psia

$T_{sat} - T_{in}$ = 100, 50, and 25°F

ΔP_{TP} = 1, 2, and 3 psia

TABLE 2

BOILER TEST PROGRAM

RUN	P_{out} (psia)	ΔP_{TP} (psia)	$T_{sat}-T_{in}$ (°F)	T_{out} (°F)	T_{in} (°F)
1	20	1	100	135	40
2	20	1	50	135	90
3	20	1	25	135	115
4	20	2	100	135	40
5	20	2	50	135	90
6	20	2	25	135	115
7	20	3	100	135	45
8	20	3	50	135	95
9	20	3	25	135	120
11	15	1	100	120	20
12	15	1	50	120	70
13	15	1	25	120	95
14	15	2	100	120	25
15	15	2	50	120	75
16	15	2	25	120	100
17	15	3	100	120	30
18	15	3	50	120	80
19	15	3	25	120	105
24	10	1	25	100	75
25	10	1	50	100	50
26	10	2	25	100	80
27	10	2	50	100	55
28	10	3	25	100	35
29	10	3	50	100	60

SECTION 4

APPARATUS

TEST LOOP

A schematic of the Freon flow-stability test loop is shown in Figure 6. Figures 7, 8, and 9 are photographs of the loop, showing the boiler, test condenser, auxiliary equipment, and instrumentation panel. The two components studied were boiler and test condenser, both of these were made from transparent materials, as was much of the rest of the loop. As mentioned previously, the primary parameter for this study was the liquid-to-two-phase pressure-drop ratio.

A variable orifice (Hoke 280 series metering valve), as shown in Figure 9, was installed near the entrance of each boiler tube. The Freon, after leaving the boiler, passed through a glass water-cooled heat exchanger. The main use of this heat exchanger was in conjunction with condensing tests, the quality to the condenser could be adjusted at the cooler while maintaining constant boiler conditions.

The main condenser was capable of condensing all the Freon vaporized in the boiler. The cooling medium was air, passing counterflow to the Freon. Liquid coolants also may be used.

A versatile mounting for the high-speed camera was fabricated above the boiler as shown in Figure 9. The mounting was such that the camera could film any tube and any position along the tube.

Liquid Freon, leaving the condensing section of the loop, passed through a subcooler (chilled by water or trichloroethylene) before entering the pump. The pump was an explosion-proof, seal-less, centrifugal Series G Chempump. A wraparound water-cooling jacket was incorporated for pump cooling.

A bypass loop and control valve were incorporated around the pump. All tests were conducted with the bypass control valve in a closed position. A Greer bladder accumulator, pressurized with water, was utilized for system makeup and pressure level control. Most of the tests were conducted at pressure levels that allow the solenoid valve to be in a closed position.

COMPONENTS AND INSTRUMENTATION

The boiler which is shown in Figure 10, consists of five quartz tubes (6-mm ID, 8-mm OD, and 53-in. length). A 0.63 in. by 3.57 in. rectangular cross-section pyrex duct, 42-1/2 in. in length, was built to surround the tubes so that hot air would flow outside the tubes and counterflow to the Freon. The air flow rate was limited to 18 lb per min, with a maximum inlet temperature of 800°F. Figure 11 is a schematic of the boiler showing those quantities that were measured.

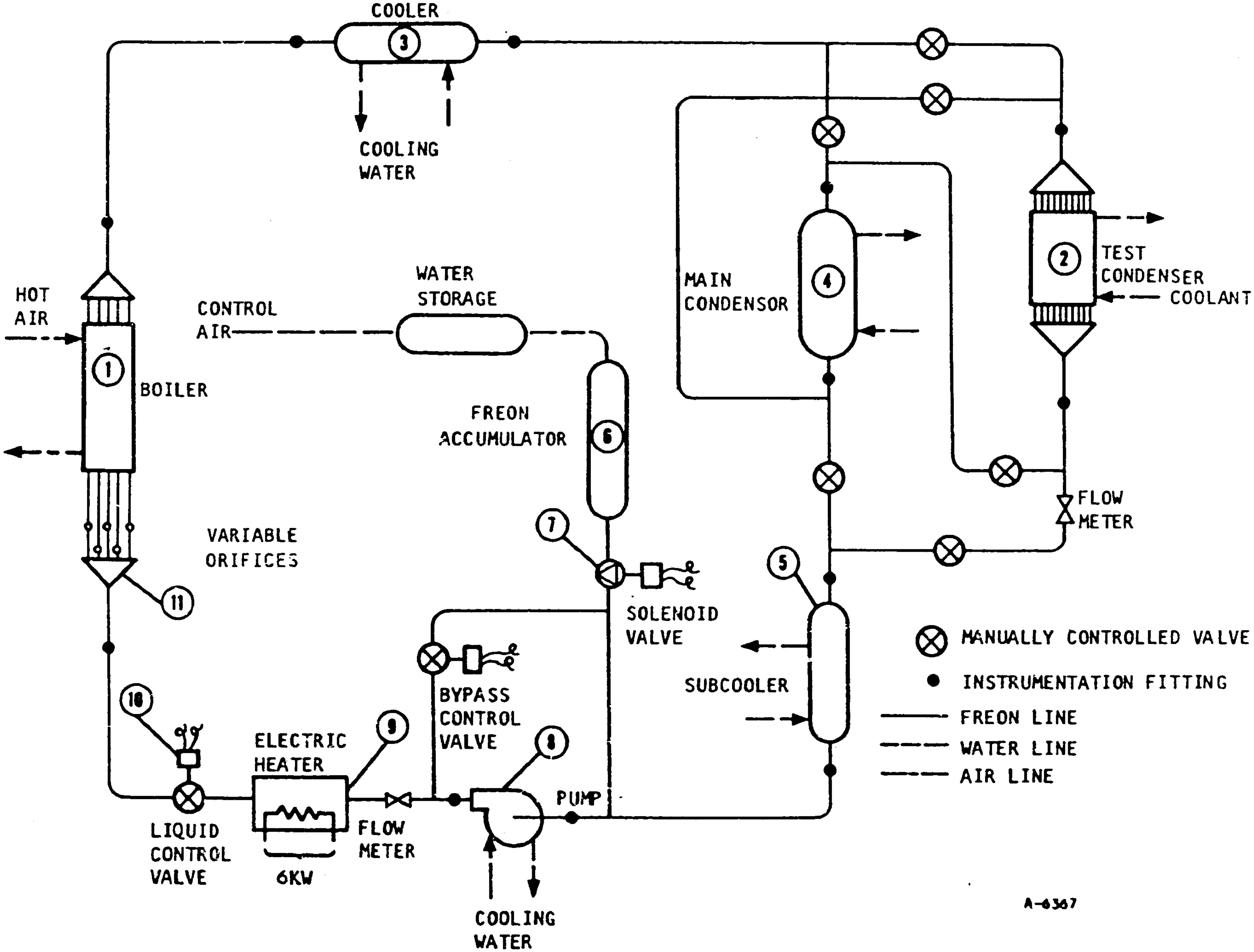

Figure 6   Freon Flow Stability Loop Schematic

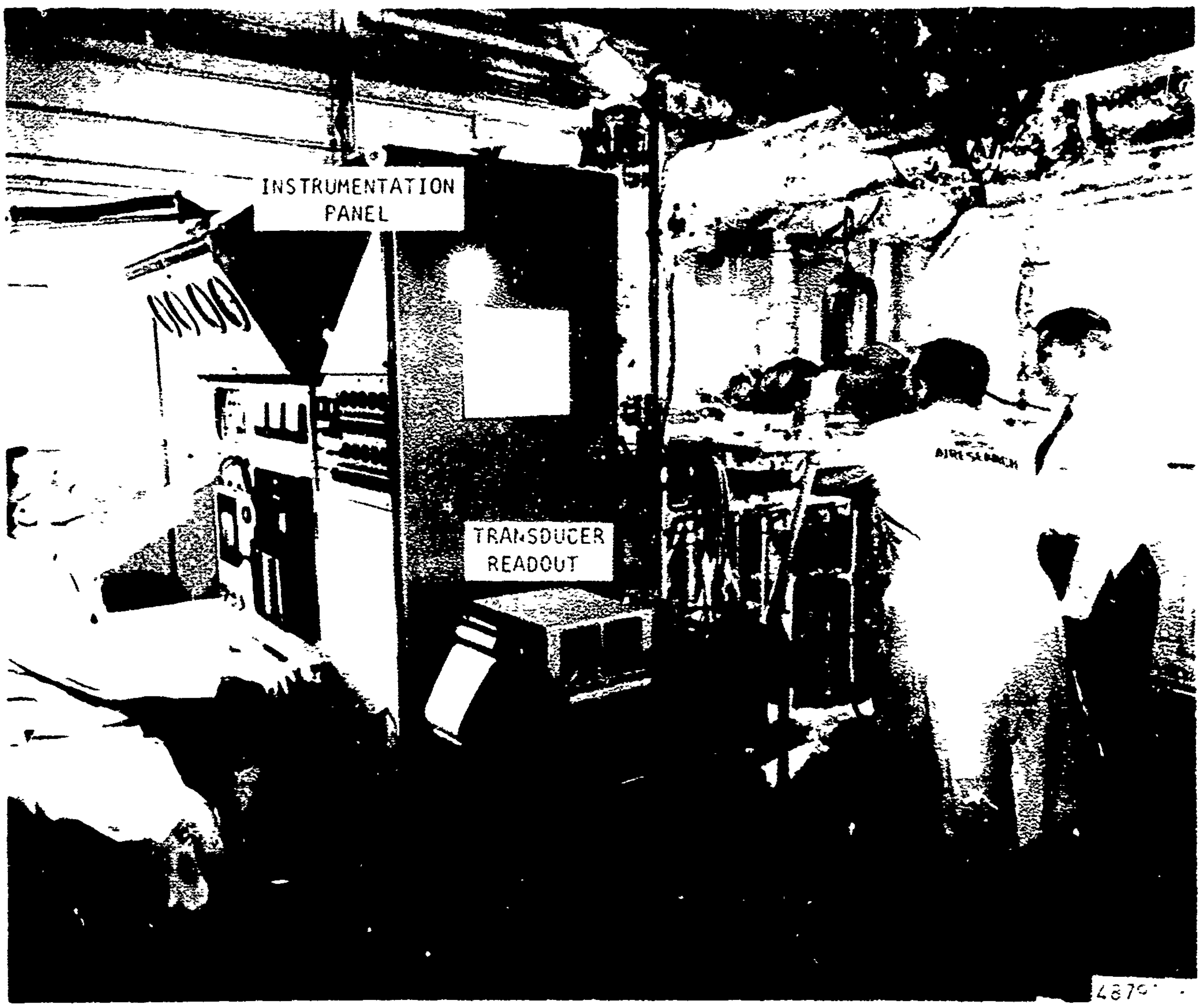

Figure 7. Freon Flow Stability Loop

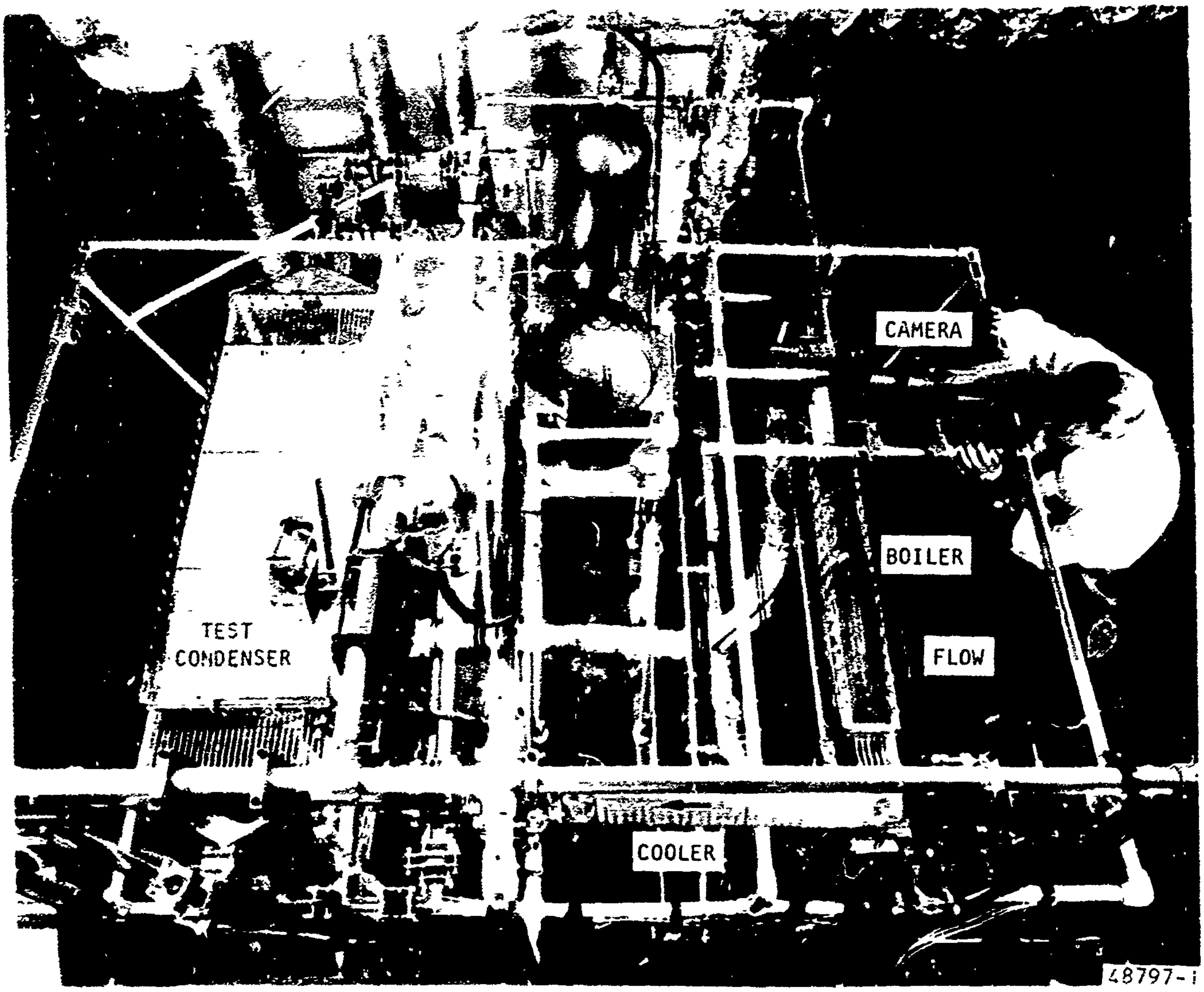

Figure 8. Freon Flow Stability Loop

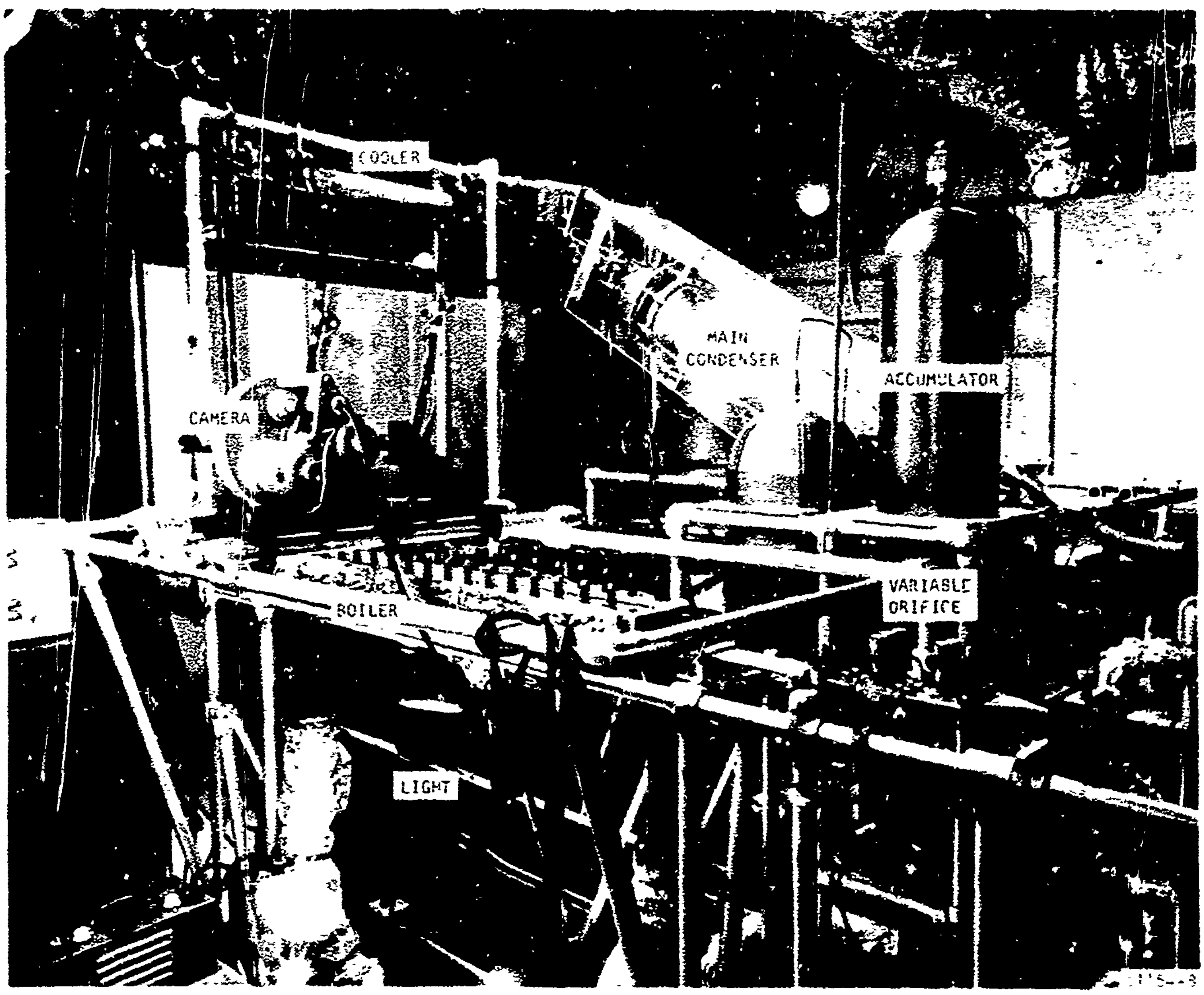

F-835

Figure 9 Freon Flow Stability Loop

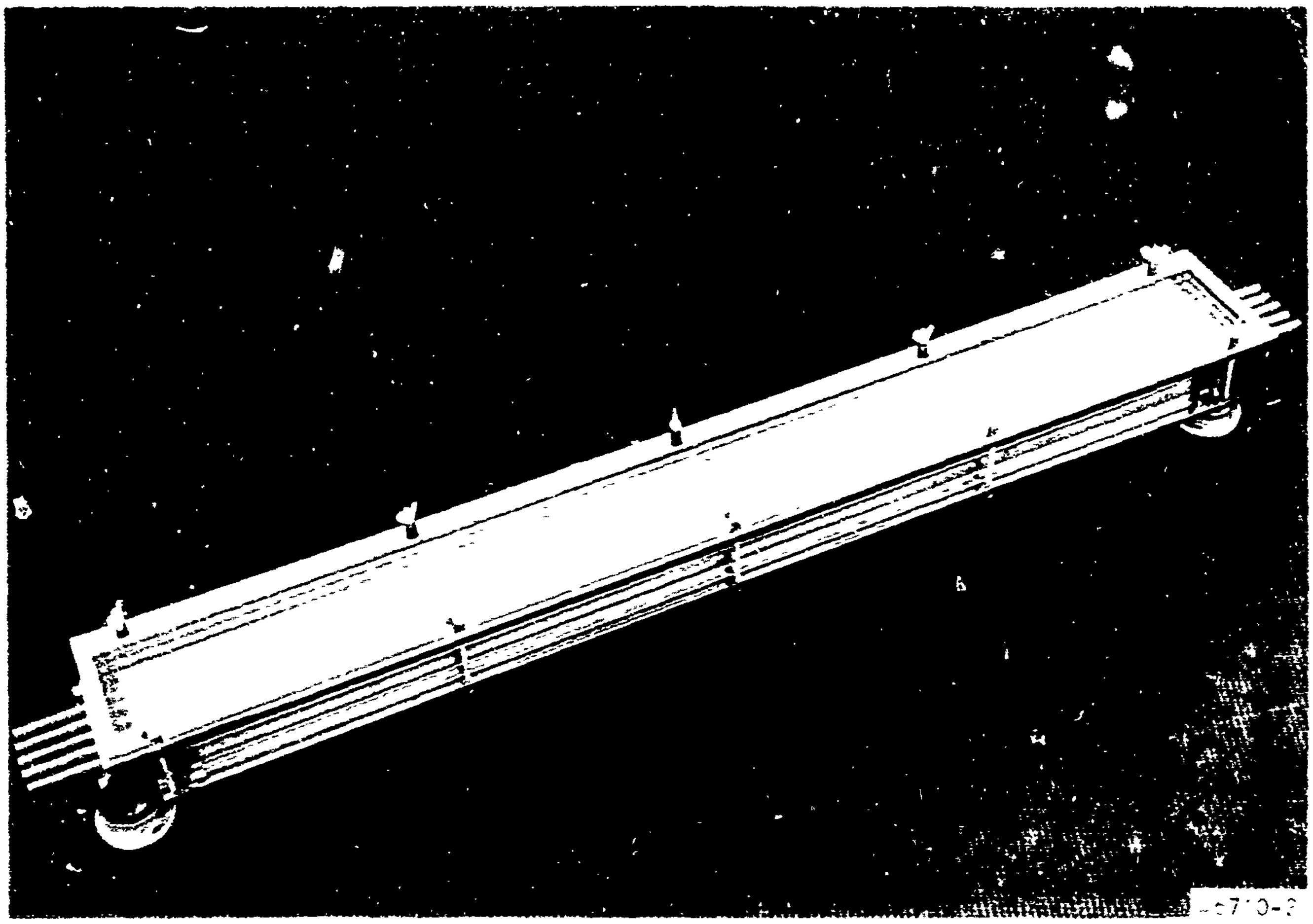

Figure 10. Freon Boiler

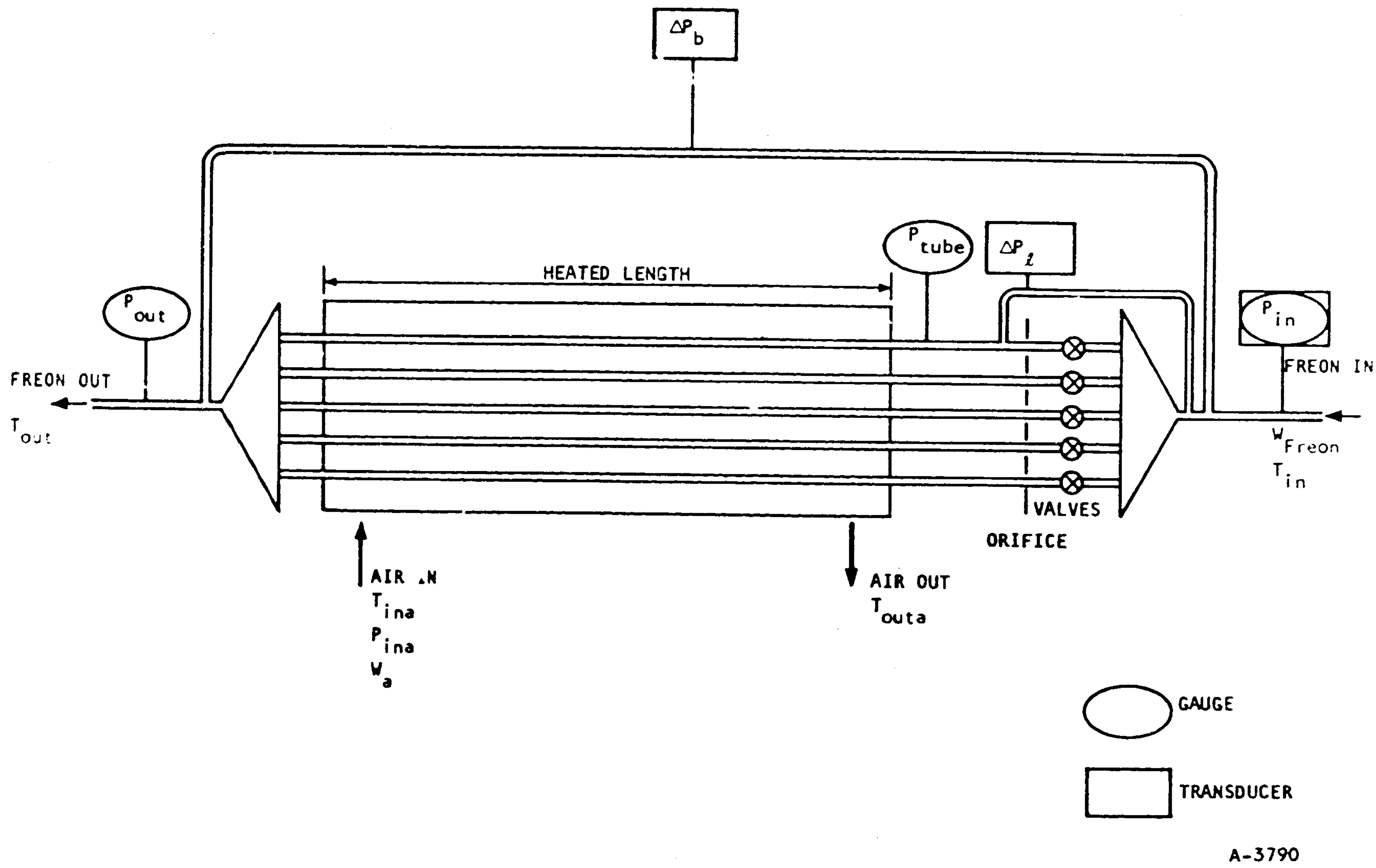

Figure 11 Freon Boiler Schematic

The test condenser consisted of 30 quartz tubes the same dimensions as the boiler tubes. A rectangular cross-section Pyrex glass duct, 42-1/2 in. in length was constructed around the tubes to serve as the coolant flow passage.

An electric heater (6-kw capacity) was provided to control the Freon inlet temperature to the boiler. An electrically operated Series 715 Flow-Ball Valve was used to control the liquid flow rate to the boiler, which was measured with a turbine-type Cox flowmeter.

Ashcroft Laboratory test gauges were used to measure pressures in the Freon loop. Transducers (Pace Engineering Model PID and Model PIG, respectively) were used to record the liquid (orifice) pressure drop and the total boiler pressure drop. A standard calibrated orifice was used for air-flow measurements. Inlet and outlet temperatures on all heat exchangers were measured with iron-constantan thermocouples and recorded on a Brown 48-point temperature indicator. Toggle-action Dahl valves were used throughout the loop to control the Freon flow rate to the various heat exchangers. Figures 12 and 13 are photographs of the instrumentation and control panel.

Table 3 lists components used in the loop. Glass piping and fittings were used when convenient.

PHOTOGRAPHIC EQUIPMENT

A WF-3 Fastax camera, mounted horizontally above the test section as shown in Figure 14, obtained vertical shots by use of a 2 by 2 prism Single-tube closeups were shot with a 152-mm lens in the camera and a supplementary 6-in. Aero Ektar lens mounted horizontally below the prism.

Shots of all five tubes were taken with a 50-mm lens in the Fastax. Additional five-tube shots were obtained by using a Cine Kodak Special camera with either a 25-mm or 50-mm lens.

Ektachrome ERB (ASA 125) film was used in the Fastax camera and Ektachrome Commercial Type 72S5 (ASA 25) film was used in the Kodak camera.

Lighting was provided by two Colortran Quartz lite 1000-w, 110-v lamps located below the boiler, which gave 50,000 to 100,000 ft-candles of light. The cameras were stopped down to provide the maximum depth of field possible with the above lighting. When the Fastax camera was operating at its maximum film speed of 8000 frames per sec in the single-tube shots, the resulting depth of field was approximately 0 10 in.

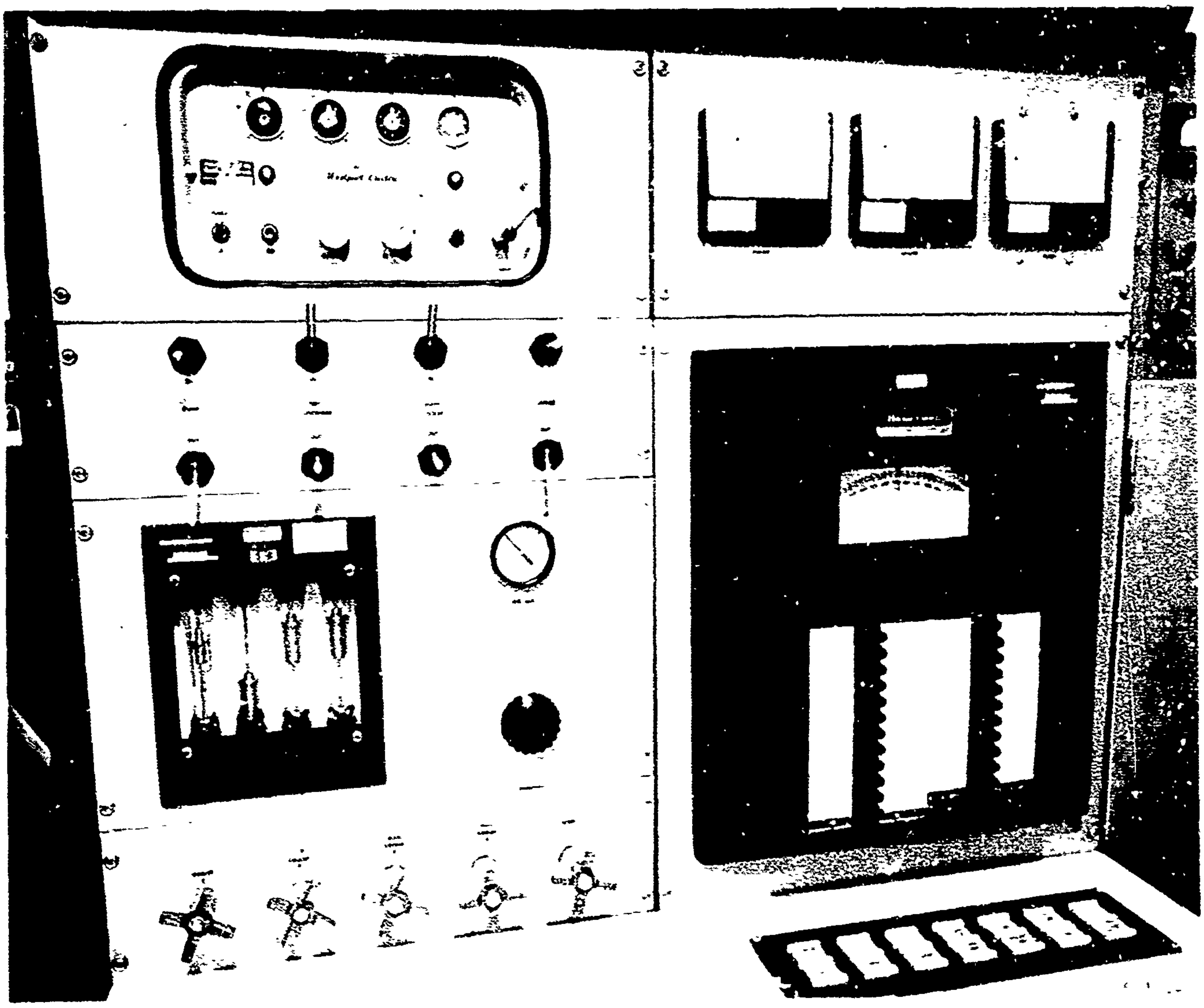

Figure 12. Instrumentation and Control Panel

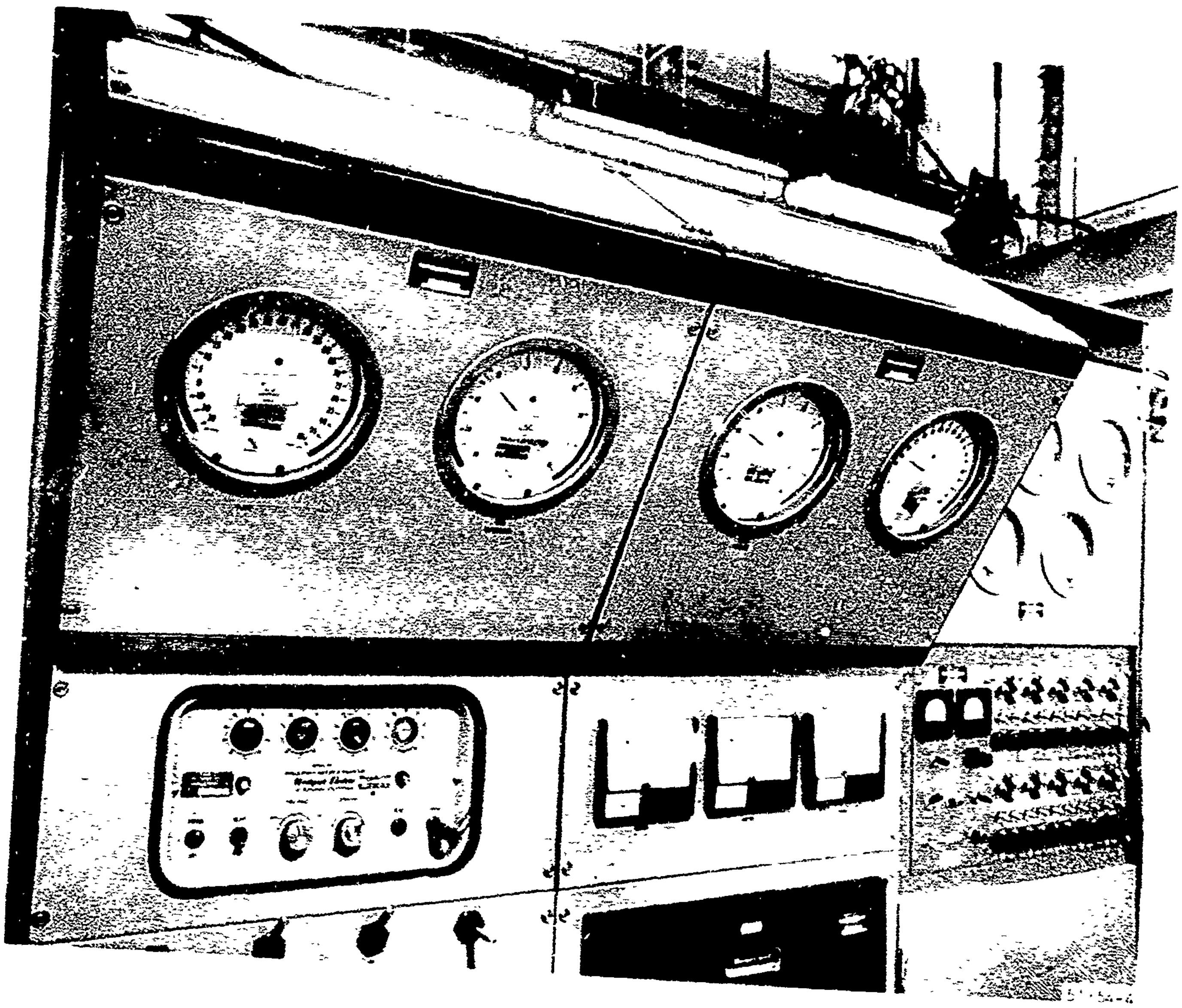

Figure 13. Instrumentation and Control Panel

TABLE 3

FREON LOOP COMPONENTS

Item Number on Figure 6	Component	Description
1	Boiler	5 quartz tubes, 53-in. length, 6-mm ID, 8-mm OD; Pyrex duct built over tubes for air flow
2	Test Condenser	30 quartz tubes, 53-in. length, 6-mm ID, 8-mm OD; Pyrex duct built over tubes for air flow
3	Cooler	QVF 2/3½ glass condenser
4	Main Condenser	QVF 6/15 glass condenser
5	Sub-Cooler	QVF 2.3½ glass condenser
6	Accumulator	10-gal Greer transfer barrier accumulator with a neoprene bladder, coated shell (phenolic resin sprayed and baked), 300-series stainless steel fittings.
7	Solenoid Valve	Sporlan solenoid valve, 1-in. FPT, direct-acting, 24-v d-c coil
8	Pump	Series G Chempump, Model GA 1 1/2
9	Electric Heater	Thermolab duct assembly preheater, 115-v, 60-cycle
10	Liquid Control Valve	Series 715 flow-ball valve, electrically operated.
11	Variable Orifices	Hoke 230 series metering valve, globe pattern, 316SS valve, 1/8-in. orifice
	Water Flow Meters	Sho rate "50" flow meter, Model 1350, size 8, chrome plated, brass constructed
	Freon Control Valves	Dahl valves; panel mounting; toggle action; Teflon seat
	Pressure Gauge	Ashcroft Laboratory test gauge, 60 psi to 30-in. vacuum
	Temperature Indicator	Brown temperature indicator, 48-point, IC thermocouple, 115-v 60-cycle, 100°F to 1000°F scale. Minneapolis-Honeywell

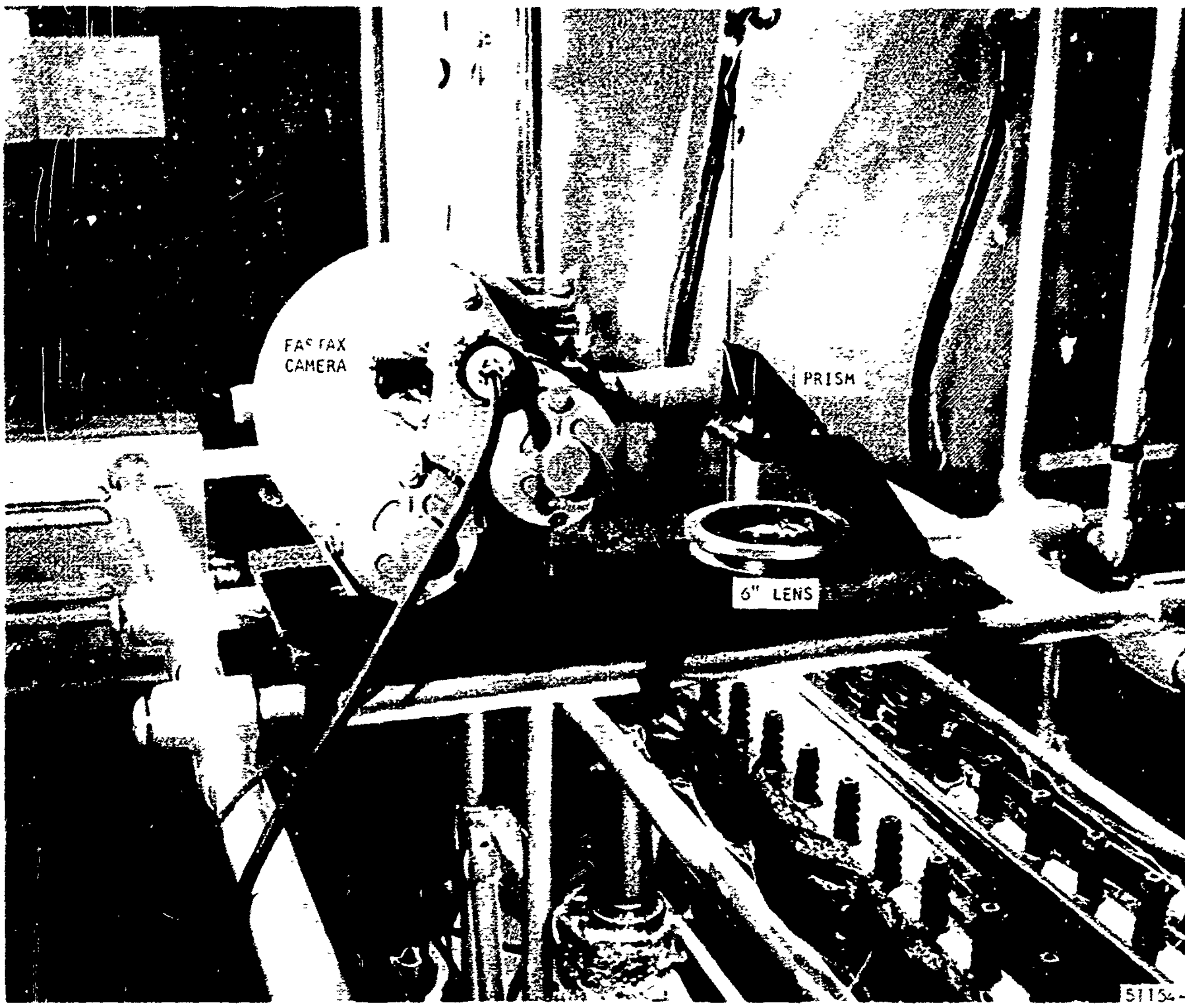

Figure 14. Camera and Mounting
F-884

SECTION 5

TEST PROCEDURE

RUN CRITERIA

The tolerances allowed on the nominal test conditions for each run presented in Table 2 were ±0.5 psia on P_{out}, ±5°F on T_{in}, and ±0.2 psi on ΔP_{TP}. Each run (set of test conditions) consisted of obtaining data at nominal valve settings of 2,3,4,5,8, and 15 (pressure drop across the valve is a function of the valve setting, with 0 the full closed position). The runs were started with the valve setting of two, which always gave stable flow. The air and Freon flow rates were adjusted to yield the specified boiling pressure drop (P_{tube} - P_{out}) and an exit quality close to 1.0.

The valve settings on the five tubes were adjusted so that the average value of the tube pressure read from each gauge was the same within ±0.2 psi. This provided uniform flow in each tube. Other checks on the uniformity of conditions in the five tubes were the visual appearance of the flow in the Freon tubes on either end of the boiler, and the uniformity of the transducer traces from the five tubes.

Air at temperatures up to 600°F was used to vaporize the Freon. The air flow rate and temperature were adjusted so that the temperature of the Freon at the boiler exit was approximately 30°F higher than the saturation temperature corresponding to the boiler exit pressure. The boiler was operated at the highest exit quality possible within the preceding restriction on boiler exit temperature.

The data points at valve settings greater than two were taken after changing only the valve settings. This sometimes tended to cause changes in Freon exit quality; this was controlled by adjusting the air temperature. Tolerances on the primary variables for any set of six points were as follows:

Freon flowmeter, ±4 cps

Freon exit pressure, ±0.1 psi

Freon tube pressure, ±0.1 psi

Freon inlet temperature, ±3°F

The boiler pressure drop was within ±0.2 psi of the specified value and was held as constant as possible during each set of six points, which make up a run.

A typical set of data, which corresponds to Run 26, is presented in Figure 15. The data processing procedure described below uses these data as the example.

Date 4-30-64 Test Engr. Schroyer Data Engineer Paul Bergman

Barometer 29.86 Log Book Page No. 74 (25)

Run Number Series #1 Run #26 (Transistor Tape)

Run Time Run Condition # 1 2 3 4 5 6

	1	2	3	4	5	6		
FREON								
Pressures, [illegible] PSIG								
Boiler in PSIA	14.9	13.0±.1	12.9±.3	12.5±.2	12.3±.2	12.1±.3		
Boiler out	10.0	10.0	10.0±.1	10.0±.1	10.0±.2	10.0±.1		
Boiler Tubes N 1	11.9±.2	12.0±.2	11.9±1.7	12.0±1.8	12.0±1.8	12.0±1.6		
N 2	12.0±.2	12.1±.2	12.2±1.8	12.1±1.7	12.2±1.8	12.2±1.6		
N 3	11.9±.1	12.0±.2	12.0±1.6	12.0±1.8	12.1±1.8	12.2±1.6		
N 4	12.0±.3	12.1±.2	12.2±1.8	12.9±1.9	12.8±1.7	12.4±1.8		
N 5 PSIA	11.9±.3	11.9±.2	12.0±1.7	12.0±1.9	12.1±1.9	12.1±1.9		
Test Condenser in								
Test Condenser out								
Auxil. Condenser in	-16.0	-15.2	-15.0	-14.8	-14.6	-14.4		
Auxil. Condenser out	-15.0	-15.2	-15.0	-14.8	-14.6	-14.4		
Pump in	-15.5	-15.5	-15.5	-15.5	-15.0±.5	-15.5±.5		
Pump out	47.5±20	42.5±20	47.0±20	46.5±20	47.5±20	42.5±20		
Flow Rates, cps/lbs/min								
Boiler	85/2.48	84/2.50	85/2.53	86/2.55	84/2.50	85/2.53		
Condenser								
Valve Setting	App 2	App 3	App 4	App 5	App 8	App 15		
Exit Quality	.940	.950	.890	.860	.940	.900		
Temperatures, °F								
Pump in	41	43	49	55	35	37		
Pump out	61	66	72	77	58	60		
Boiler in	80	80	80	80	80	79		
Boiler out	130	129	130±1	128±1	130±2	130±1		
~~Test Condenser~~ in Cooler	129	128	126	126	123	124		
~~Test Condenser~~ out Cooler	104	104	104	104	104	104		
Auxil. Condenser in	78	88	88	88	88	88		
Auxil. Condenser out	64	73	73	73	74	74		
Subcooler in	74	73	73	73	74	74		
Subcooler out	33	36	41	47	28	30		
AIR								
Pressures								
Boiler Orifice, in HgA	34.6	34.4	34.05	34.05	34.55	34.3		
Boiler Orifice ΔP in H_2O	2.85	2.95	2.10	2.10	2.4	2.2		
Condenser Orifice, in HgA								
Condenser Orifice ΔP in H_2O								
Boiler in, in Hg	3.8	3.75	3.45	3.45	3.85	3.7		
Boiler out, in Hg	.6	.6	.55	.55	.60	.55		
Condenser in, in Hg								
Condenser out, in Hg								
Flow Rates, lb/min								
Boiler	7.7	7.65	7.2	7.25	7.75	7.4		
Condenser								
Temperatures °F								
Boiler Orifice	460	468	473	458	460	462		
Boiler Orifice	460	468	473	458	460	462		
Condenser Orifice								
Condenser Orifice								
Boiler in	435	440	445	436	435	438		
Boiler out	326	329	331	326	326	328		
Test Condenser in								
Test Condenser out								
WATER								
Flow Rates, gpm								
Cooler	.80	.76	.71	.75	.84	.82		
Subcooler No Meter	—	—	—	—	—	—		
Auxiliary Condenser	3.75	3.75	3.75	3.75	3.75	3.75		
Auxiliary Condenser	3.75	3.75	3.75	3.75	3.75	3.75		
Temperatures, °F								
Cooler in	67	66	66	66	67	67		
Cooler out	84	85	86	85	84	84		
Auxiliary Condenser in	66	66	66	66	66	67		
Auxiliary Condenser out	66	67	67	67	66	67		
Subcooler in	26	27	34	41	17	20		
Subcooler out	40	42	47	51	36	39		

Test Condenser out of System

CALCULATED BY		SNAP 50/SPUR FREON FLOW LOOP	
TRACED BY			
CHECKED BY		Aeronautical Manufacturing Division	
APPROVED BY			
SHEET NO.			

Figure 5 Data Sheet

HEAT LOSS CALIBRATION

A heat loss calibration was performed immediately before and after each series of runs by obtaining the following data with no Freon in the boiler; for air inlet temperatures of 800°F, 600°F, and 400°F, the air exit temperature was measured for air flow rates of 9, 12, 15, and 18 lb per min. These data were taken very carefully, allowing sufficient time (15 to 30 min) for the exit temperature to reach steady state after each change in conditions.

The results of the heat loss calibration indicated that a significant part of the energy loss was due to air leakage. An energy balance on the boiler, assuming that the air leakage was proportional to the air pressure, revealed that the energy loss due to leakage was proportional to the product of the air pressure and the air temperature change in the boiler. This loss was added to the heat leak itself, which was proportional to the temperature difference between the hot air and the atmosphere. An equation for the energy loss, consisting of the two terms defined above, was developed from the heat loss calibration data which correlated all the results within ±10 percent. This equation remained valid even after the boiler was taken apart and reassembled during the test program.

SECTION 6

DATA PROCESSING

The data obtained for each run included the information recorded on the data sheet for the six valve settings and the corresponding transducer strip charts. A typical complete set of data for Run 26 with full-length twisted tape inserts is presented in Figures 15 to 21 and will be used to illustrate the data processing procedure. The transducer strip chart calibration information is presented in Table 4.

The data from the data sheet shown in Figure 15 were entered on the data processing sheet as shown in Figure 22.

TABLE 4

TRANSDUCER STRIP CHART CALIBRATION

Trace Break No.	Measurement	Range (psi)	Reference Point (in.)	Calibration (psi/in.)
3	Reference			
4	ΔP_{ℓ}, tube 1	-2 to +10	1.5	8
5	ΔP_{ℓ}, tube 2	-2 to +10	2.0	8
6	ΔP_{ℓ}, tube 3	-2 to +10	2.5	8
7	ΔP_{ℓ}, tube 4	-2 to +10	3.0	8
8	ΔP_{ℓ}, tube 5	-2 to +10	3.5	8
9	Boiler P_b	-2 to +10	4.0	4
10	Condenser P	-2 to +10	4.5	4
16	Boiler inlet P_{in}	0 to 50	6.5	10
18	Reference		6.5	

The exit quality was calculated on a computer. The net heat input was obtained by subtracting the calibrated energy loss from the energy decrease of the air as it flowed through the boiler. The Freon exit quality was then calculated from an energy balance using the net heat input.

Figure 16 Transducer Strip Chart Data, Full Tape, Run No. 26, Condition No. 1

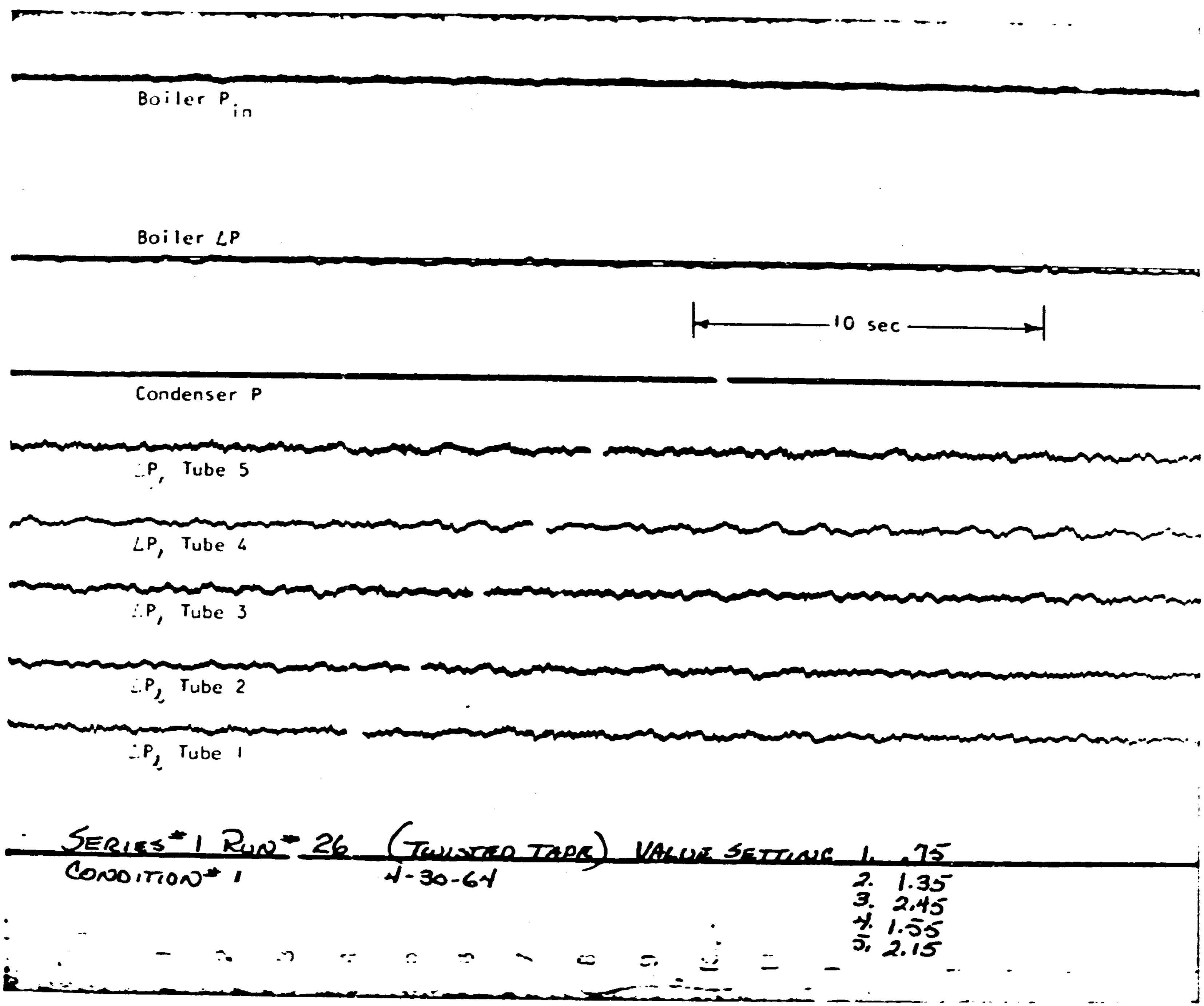

Figure 16 Transducer Strip Chart Data. Full Tape, Run No. 26, Condition No. 1

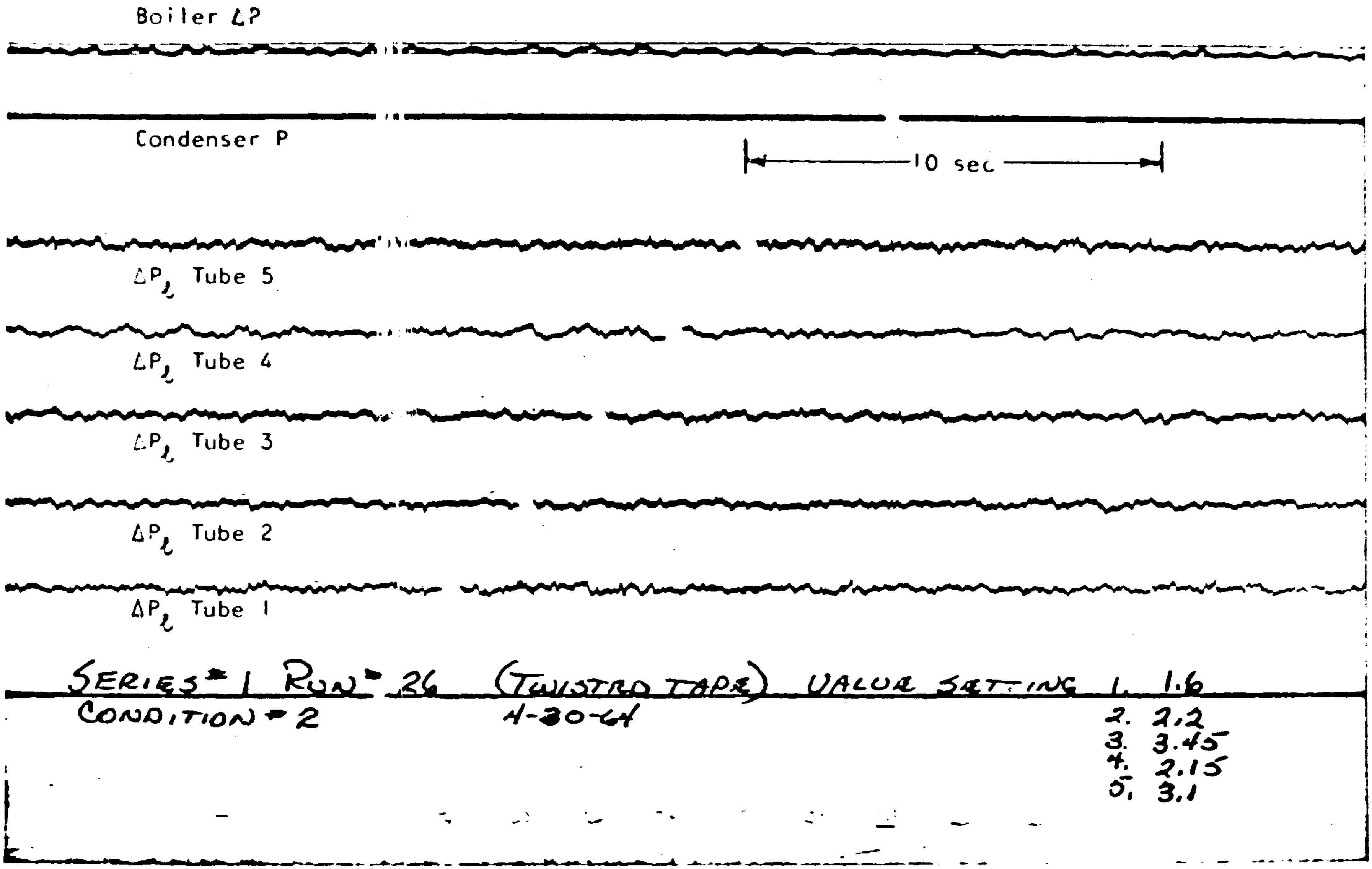

Figure 17. Transducer Strip Chart Data. Full Tape, Run No 26, Condition No. 2

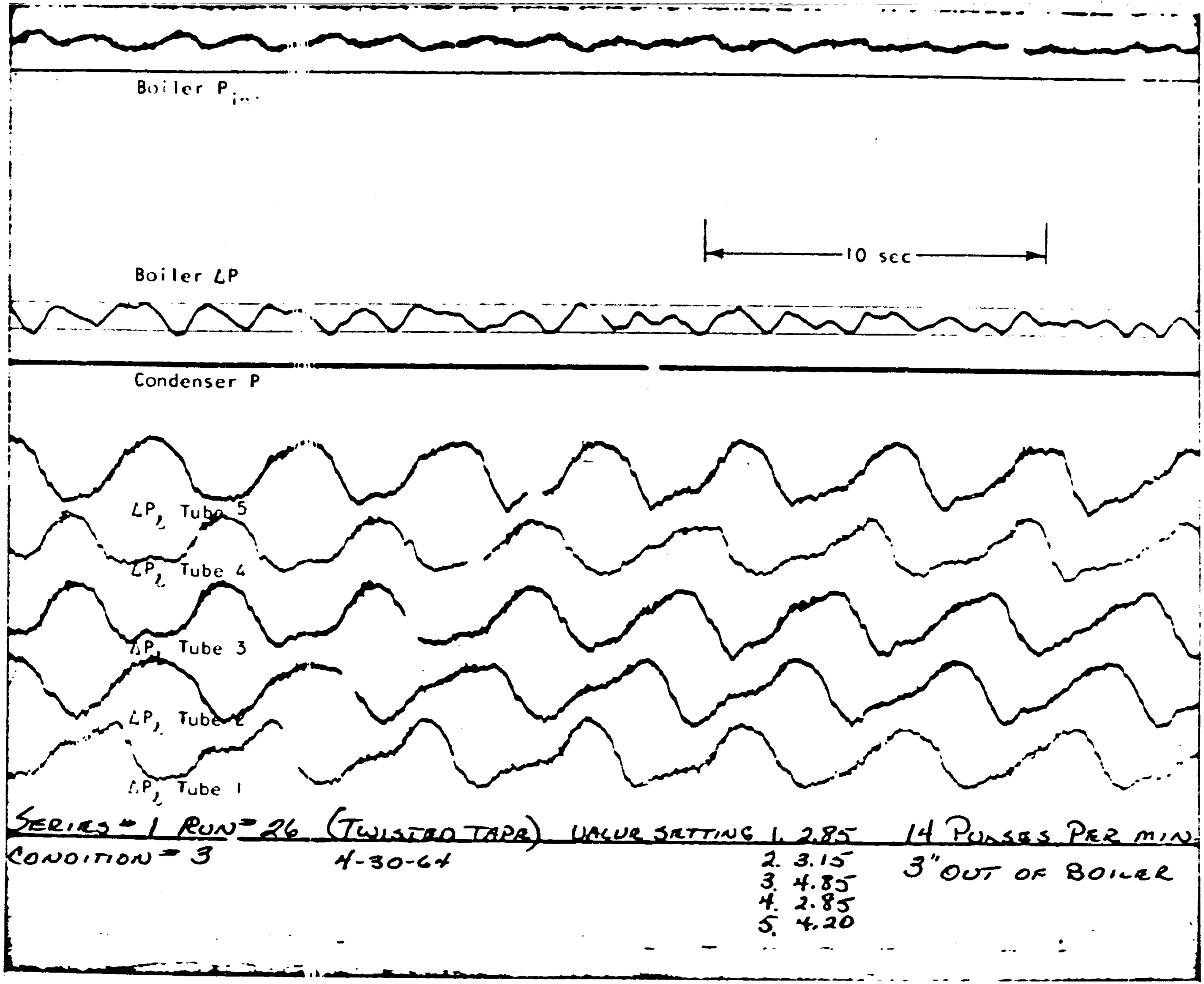

Figure 18. Transducer Strip Chart Data. Full Tape. Run No 26, Condition No 3

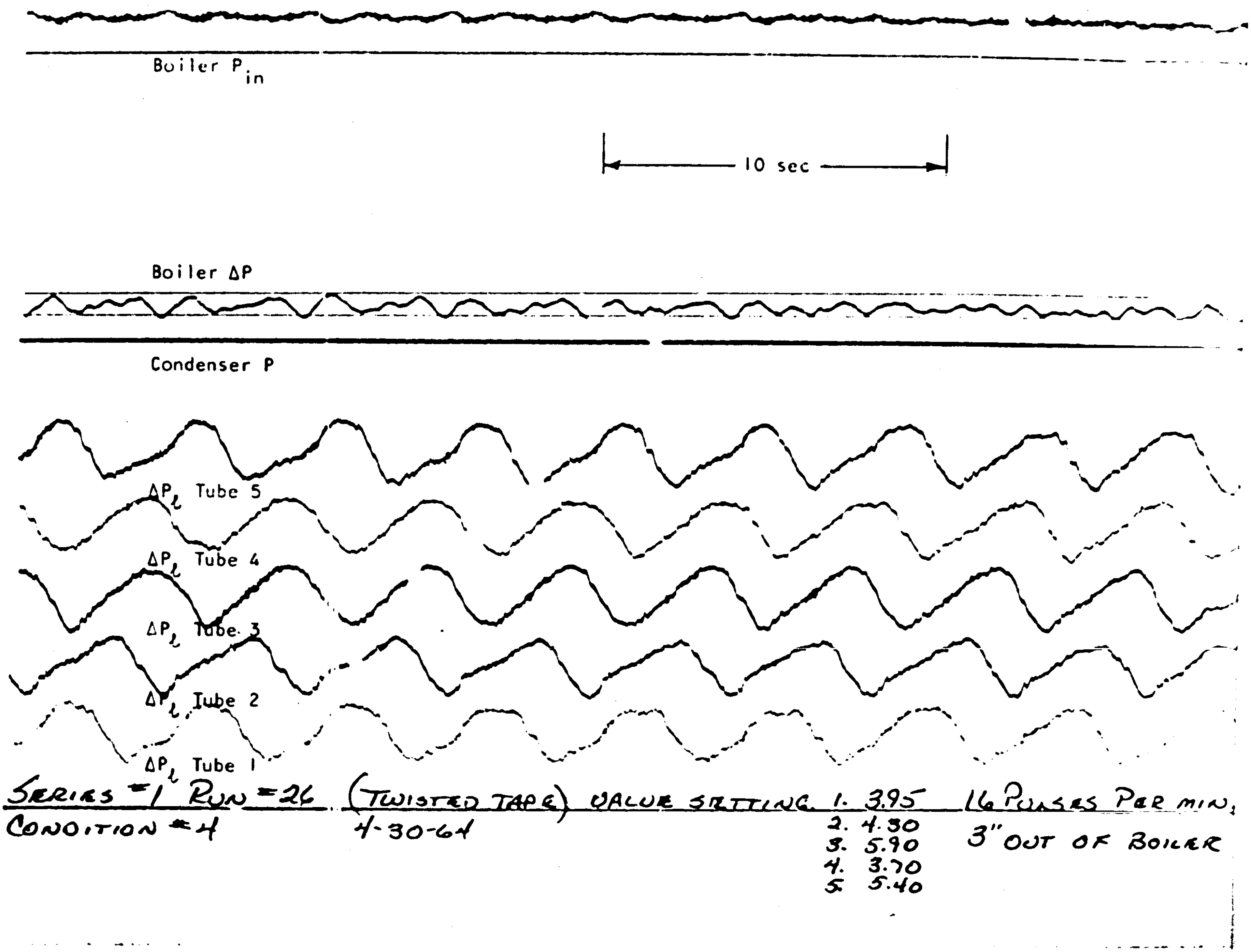

Figure 19. Transducer Strip Chart Data, Full Tape, Run No. 26, Condition No. 4

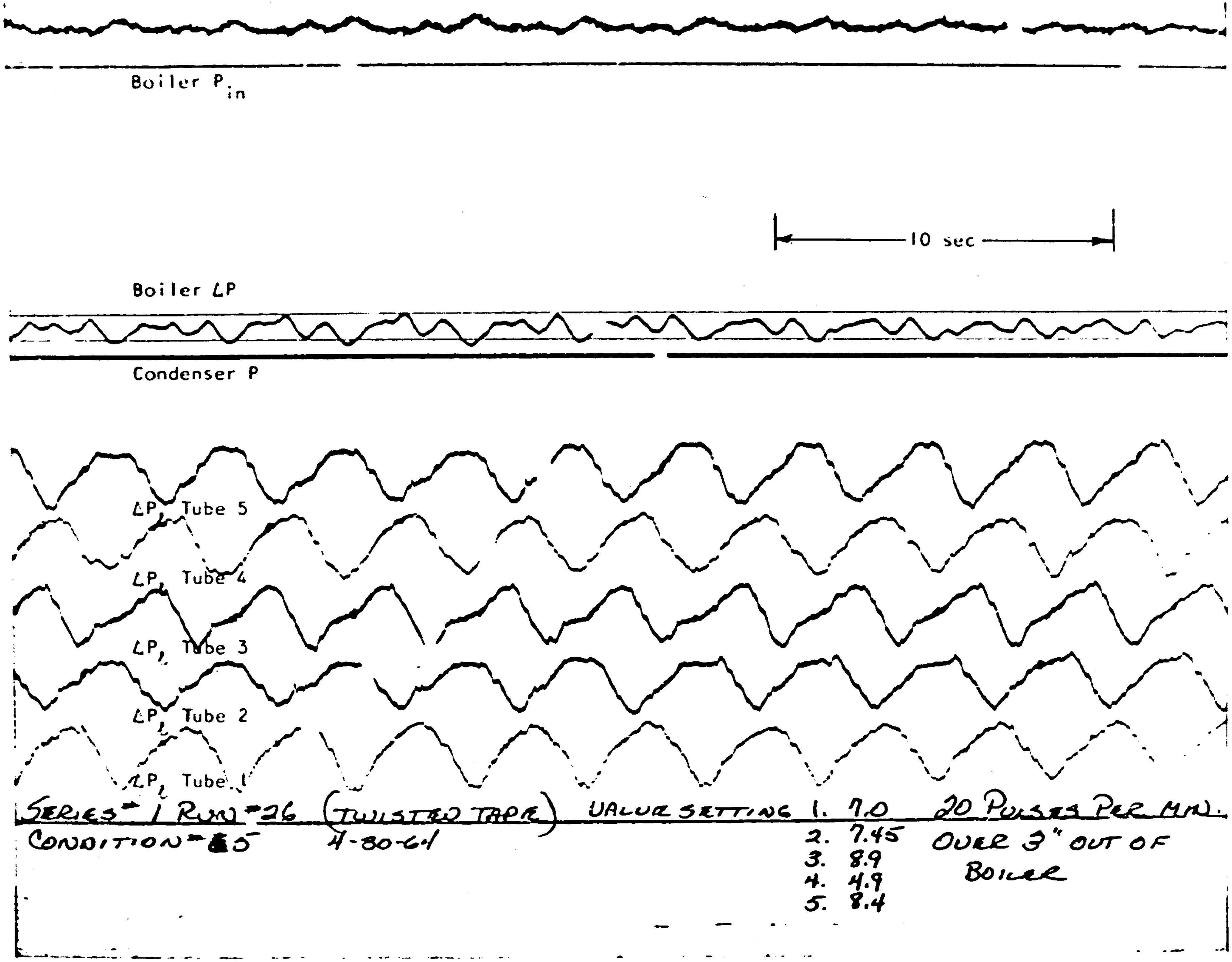

Figure 20. Transducer Strip Chart Data. Full Tape, Run No 26, Condition No. 5

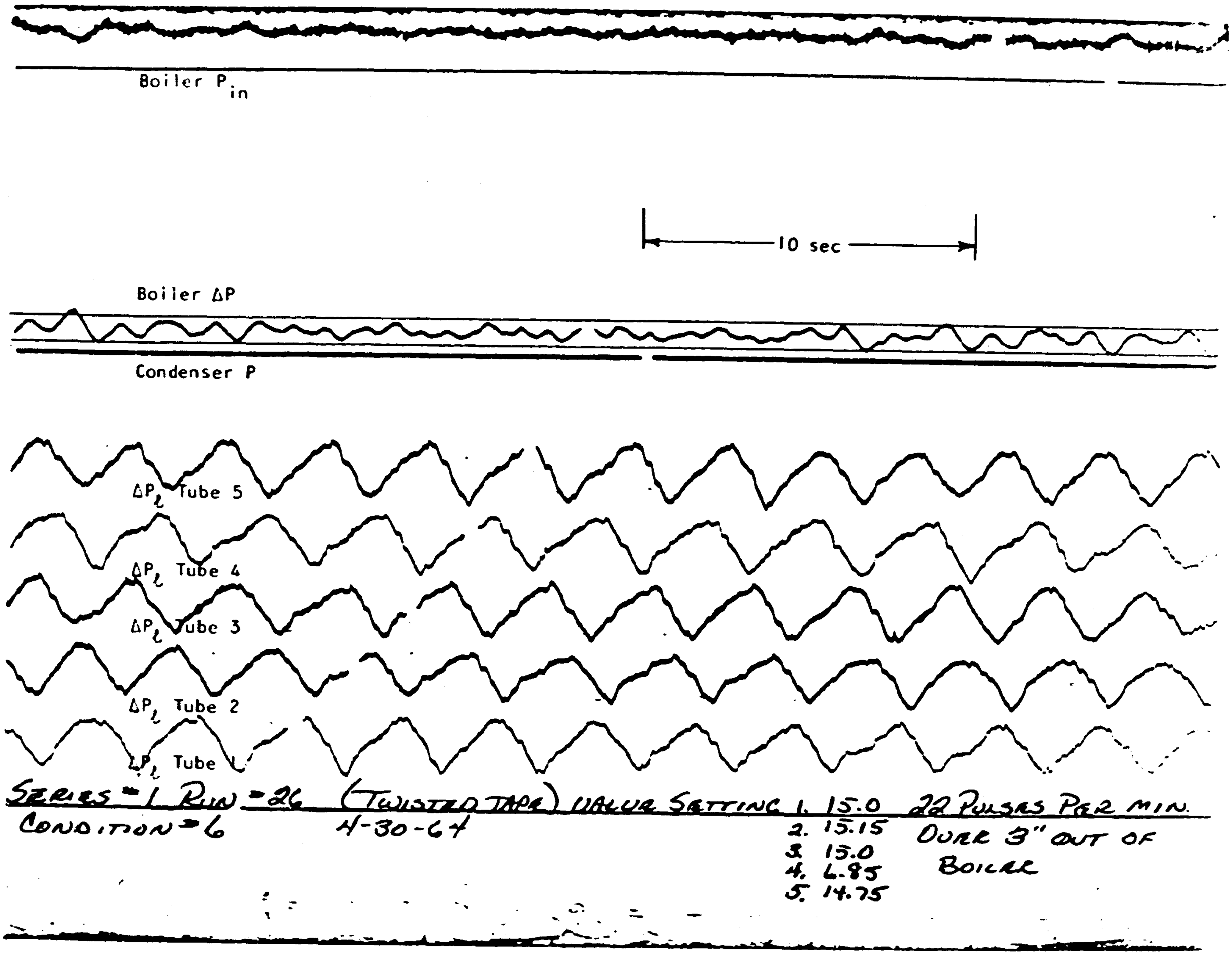

Figure 21. Transducer Strip Chart Data. Full Tape, Run No 26, Condition No.6

5-TUBE FREON BOILER FLOW STABILITY DATA

RUN NO. 26 Date 4/30/64

Tube Full-Length Twisted Tape Log Sheet No. 74

$C_p (T_{sat} - T_{in})/h_{fg}$ = 0.09 ; ρ_ℓ/ρ_v = 300 ; $\Delta P_{TP}/P_{out}$ = 0.20

Point	1	2	3	4	5	6
Flow Rate, lb/min	2.43	2.50	2.53	2.55	2.50	2.53
Exit Quality	0.828	0.833	0.792	0.762	0.826	0.781
T_{in} °F	80	80	80	80	80	79
T_{out} °F	130	129	130	128	130	130
P_{in} psia	14.9	13.0	12.9	12.5	12.3	12.1
P_{tube} psia	11.9	12.0	12.1	12.1	12.1	12.1
P_{out} psia	10.0	10.0	10.0	10.0	10.0	10.0
ΔP_ℓ psi	3.0	1.0	0.8	0.4	0.2	0.0
ΔP_{TP} psi	1.9	2.0	2.1	2.1	2.1	2.1
$\Delta P_\ell/\Delta P_{TP}$	1.6	0.5	0.38	0.19	0.10	0.0
Frequency, cps	--	--	0.22	0.25	0.30	0.33
Amplitude, in.	0.01	0.02	0.10	0.03	0.09	0.10
$\Delta (\Delta P_b)$ psi	0.04	0.08	0.40	0.32	0.36	0.40
$\Delta (\Delta P_b)/\Delta P_{TP}$	0.02	0.04	0.19	0.15	0.17	0.19

Figure 22. Data Processing Sheet for 5-Tube Boiler Flow Stability Data

The frequency and amplitude of the flow oscillations were measured on the transducer strip charts and entered at the bottom of Figure 22; the overall boiler pressure drop trace, break No. 9, was used for the amplitude measurement. The amplitude in psi was obtained by multiplying the measured amplitude by the 4-psi-per-in. scale factor. After the amplitude was normalized by dividing it by the boiler two-phase pressure drop, the results were plotted as shown in Figure 23. The critical liquid pressure drop is located by the knee of the curve.

The dividing line between stable and unstable conditions was much sharper than expected. It was actually possible to pick out the critical liquid pressure drop by simply surveying the transducer strip charts. In the example given, the flow clearly becomes unstable between conditions 2 and 3. This is confirmed by the uncertainty in the tube pressure measurements recorded by the technician, which exhibit a factor-of-ten increase between these two points. It was possible, therefore, to pick out the critical liquid pressure drop directly, without going through the steps represented by Figures 22 and 23. In this case, the liquid pressure drop of condition two was selected as that required to provide stable flow for the conditions of run 26.

The oscillation amplitude of the overall boiler pressure drop was about half the amplitude in the individual tubes, indicating a damping effect in the manifolds where the oscillations of the individual tubes were superimposed upon one another. The oscillation frequency was greatest when the valves were wide open at a nominal setting of 15. It is this maximum frequency that is reported for each run in the following section.

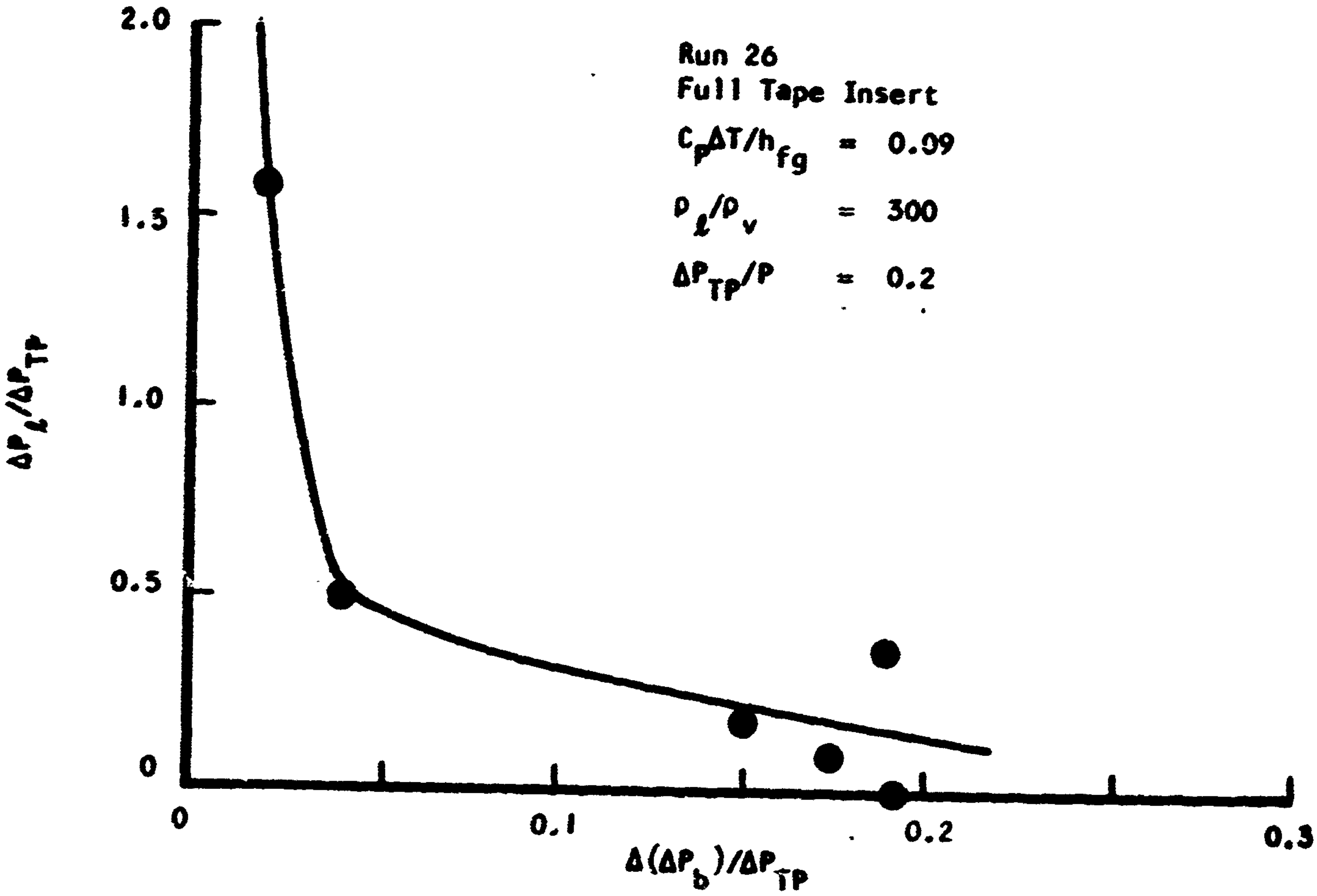

Figure 23. Freon Boiler Flow Stability Data A-7315

SECTION 7

RESULTS

The experimental results are presented on the following pages in Tables 5 and 6. Table 5 includes the results with twisted tape inserts running the entire length of the tubes. The results presented in Table 6 were obtained with twisted tape inserts which extended only three-quarters of the boiler heated length; they stopped approximately 10 in. from the end of the heated length. A tape-twist ratio of 3 (180-degree twist in a length equal to three tube diameters) was used in all tests. The tapes were relatively loose fitting and could be pulled or pushed through the tubes by hand.

No plain-tube results are presented because these earlier tests were run with valve settings of 2, 5, 8, 10, and 15. This did not provide close enough definition of the critical liquid pressure drop since, in most cases, a valve setting of 3 or 4 corresponded to the critical condition. If the plain tube tests are completed by obtaining results at these valve settings, the results will be reported separately.

The results presented in the tables include those measurements required to define the state of the two fluids at the highest valve setting which gave stable flow. The transducer measurements corresponding to a valve setting of 15 also are presented. The amplitude given is that for the overall boiler pressure drop, which generally is half the amplitude of the individual tube oscillations. The frequency was obtained from the transducer traces of the individual tubes such as shown in Figure 21.

The value of the quality calculated from the boiler energy balance is considered to be about 20 percent lower than actually existed. The reason for this disagreement is not known, since the heat loss calibration was reproduced five times. However, the fact that the temperature at the entrance to the cooler, which was located 3 ft and two 90-degree turns beyond the boiler exit (a condition which tends to produce equilibrium), remained greater than the saturation temperature indicates that the exit quality was close to 100 percent.

The overall coefficient of heat transfer was calculated from the net heat input to the Freon, the Freon saturation temperature, and the measured air temperatures. The heat transfer resistance was approximately equally distributed between the two fluids.

The data could be reproduced without difficulty, indicating that all the important variables were under control. The resulting values of the controlling dimensionless parameters were calculated from the measurements and are presented in Tables 5 and 6.

The data for each run corresponding to Figures 15 to 21 will be retained at AiResearch by the author.

TABLE 5

FREON BOILER STABILITY DATA (FULL-LENGTH TWISTED TAPE)

Measurements													Dimensionless Parameters					Transducer (with valve fully open)		
RUN	DATE	W_f (lb/min)	T_{in} (°F)	T_{out} (°F)	T_{cooler} (°F)	P_{out} (psia)	W_a (lb/min)	T_{ina} (°F)	T_{outa} (°F)	ΔP_{TP} (psi)	$\Delta P_{\ell c}$ (psi)	U (Btu/hr ft² °F)	x	ρ_ℓ/ρ_v	$\Delta P_{TP}/P_{out}$	$C_p\Delta T/h_{fg}$	$\Delta P_{\ell c}/\Delta P_{TP}$	$\Delta\Delta P_b$ (psi)	$\Delta\Delta P_b/\Delta P_{TP}$	f (cps)
1	4-15-64	2.1	43	154	148	20	9.5	430	339	1	0.2	26	0.79	150	0.05	0.34	0.2	0.16	0.16	0.40
2	4-16-64	2.2	90	150	145	20	9.8	396	316	1	0.4	26	0.79	150	0.05	0.17	0.4	0.16	0.16	0.30
3	4-17-64	2.1	115	153	142	20	9.2	358	290	1	0.4	26	0.70	150	0.05	0.08	0.4	0.20	0.20	0.30
4	4-8-64	3.0	40	146	-	20	17.6	412	344	2	1.6	30	0.55	150	0.10	0.37	0.8	0.48	0.24	0.45
5	4-7-64	2.9	90	140	-	20	16.5	374	315	2	1.2	30	0.60	150	0.10	0.18	0.6	0.40	0.20	0.35
6	3-23-64	2.95	115	142	-	20	16.2	400	333	2	2.4	30	0.75	150	0.10	0.09	1.2	0.48	0.24	0.40
7	4-9-64	3.8	45	151	150	20	17.5	471	385	3	0.9	31	0.56	150	0.15	0.36	0.3	0.72	0.24	0.50
8	5-6-64	3.9	96	148	148	20	15.4	457	371	3	3.0	39	0.82	150	0.15	0.165	1.0	0.60	0.20	0.40
9	3-25-64	3.9	120	150	0	20	16.5	432	356	3	2.1	31	0.66	150	0.15	0.08	[illegible]	0.90	0.30	0.45
11	5-5-64	2.05	29	169	140	15	8.6	435	336	1	0.4	24	0.75	200	0.07	0.32	0.4	0.24	0.24	0.30
12	4-24-64	2.0	70	142	131	15	8.3	371	294	1	0.6	23	0.70	200	0.07	0.17	0.6	0.24	0.24	0.30
13	4-27-64	2.03	94	150	134	15	9.2	360	290	1	1.0	24	0.72	200	0.07	0.09	1.0	0.24	0.24	0.30
14	4-23-64	3.0	35	150	140	15	10.5	489	377	2	0.4	27	0.70	200	0.13	0.33	0.2	0.44	0.22	0.35
15	4-22-64	3.0	75	134	136	15	7.4	538	386	2	1.4	26	0.87	200	0.13	0.18	0.7	0.40	0.20	0.35
15	4-21-64	2.9	75	143	139	15	10.2	449	349	2	1.8	27	0.71	200	0.13	0.18	0.9	[illegible]	0.22	0.35
16	4-20-64	2.9	100	134	134	15	10.2	421	330	2	2.0	27	0.74	200	0.13	0.09	1.0	0.44	0.22	0.40
17	4-28-64	3.68	34	150	150	15	10.2	571	427	3	0.6	28	0.68	200	0.20	0.33	0.2	0.60	0.20	0.40
18	4-13-64	3.4	81	137	137	15	17.0	409	338	3	1.5	31	0.64	200	0.20	0.165	0.5	0.52	0.17	0.40
19	4-14-64	3.3	105	140	143	15	12.2	437	347	3	1.2	28	0.75	200	0.20	0.08	0.4	0.48	0.16	0.40
24	4-29-64	1.55	75	130	115	10	7.4	312	248	1	1.0	22	0.75	300	0.10	[illegible]	1.0	0.24	0.24	0.25
25	4-28-64	1.55	50	132	115	10	7.5	344	268	1	0.9	22	0.80	300	0.10	0.17	0.9	0.24	0.24	0.25
26	4-30-64	2.5	80	129	128	10	7.65	440	329	2	1.0	24	0.83	300	0.20	0.09	0.5	0.40	0.20	0.35
27	4-23-64	2.5	55	130	122	10	9.2	427	328	2	1.4	25	0.78	300	0.20	0.17	0.7	0.32	0.16	0.35
28	4-30-64	3.07	85	127	127	10	9.05	454	346	3	1.5	26	0.78	300	0.30	0.08	0.5	0.56	0.19	0.38
29	5-1-64	3.05	61	129	129	10	9.4	467	354	3	1.5	26	0.75	300	0.30	0.17	0.5	0.52	0.17	0.35

TABLE 6

FREON BOILER FLOW STABILITY DATA (3/4-LENGTH TWISTED TAPE)

	Measurements												Dimensionless Parameters					Transducer with valve full open		
RUN	DATE	W_f (lb/min)	T_{in} (°F)	T_{out} (°F)	T_{cooler} (°F)	P_{out} (psia)	W_a (lb/min)	T_{ina} (°F)	T_{outa} (°F)	ΔP_{TP} (psi)	$\Delta P_{\ell c}$ (psi)	U (Btu/hr ft² °F)	x	ρ_ℓ/ρ_v	$\Delta P_{TP}/P_{out}$	$C_p\Delta T/h_{fg}$	$\Delta P_{\ell c}/\Delta P_{TP}$	ΔP_b (psi)	$\Delta P_b/\Delta P_{TP}$	f cps
1	5-27-64	2.9	39	160	160	20	11.8	485	385	1.0	0.8	22	0.65	150	0.05	0.35	0.8	0.36	0.36	0.50
2	5-26-64	2.85	91	165	165	20	9.9	473	370	1.0	1.0	28	0.67	150	0.05	0.17	1.0	0.30	0.30	0.35
3	5-26-64	3.1	115	160	155	20	11.7	442	352	1.0	1.2	28	0.72	150	0.05	0.077	1.2	0.32	0.32	0.40
4	5-27-64	4.2	41	160	170	20	11.1	622	470	2.0	1.0	28	0.63	150	0.10	0.35	0.5	0.60	0.30	0.50
5	5-19-64	3.83	90	160	161	20	11.1	530	412	2.0	1.2	27	0.69	150	0.10	0.18	0.6	0.68	0.34	0.35
6	5-19-64	3.78	115	160	170	20	11.3	514	406	2.0	1.8	29	0.74	150	0.10	0.09	0.9	0.64	0.32	0.40
7	5-21-64	4.9	47	160	170	20	16.1	584	465	3.0	0.9	29	0.50	150	0.15	0.35	0.3	1.05	0.35	0.35
8	5-21-64	4.7	96	168	170	20	13	567	441	3.0	2.1	39	0.82	150	0.15	0.17	0.7	0.81	0.27	0.45
9	5-21-64	4.52	120	154	155	20	12.1	542	423	3.0	1.5	25	0.71	150	0.15	0.08	0.5	0.72	0.24	0.50
11	5-28-64	2.5	26	132	148	15	10.8	445	350	1.0	0.5	27	0.70	200	0.07	0.33	0.5	0.36	0.36	0.35
12	5-23-64	2.5	75	155	155	13	11.4	409	330	1.0	1.1	26	0.72	200	0.07	0.15	1.1	0.35	0.35	0.35
13	5-25-64	2.55	100	150	145	15	9.96	412	324	1.0	1.6	27	0.81	200	0.07	0.077	1.6	0.40	0.40	0.40
14	5-28-64	3.8	25	150	160	15	11.0	590	445	2.0	0.8	23	0.71	200	0.13	0.35	0.4	0.72	0.36	0.45
15	5-15-64	3.7	75	140	155	15	9.7	551	415	2.0	1.0	26	0.72	200	0.13	0.175	0.5	0.80	0.40	0.40
16	5-16-64	3.58	100	126	152	15	8.55	547	406	2.0	1.6	25	0.79	200	0.13	0.087	0.8	0.80	0.40	0.45
17	5-28-64	4.5	30	135	155	15	12.8	615	470	3.0	1.0	29	0.60	200	0.20	0.33	0.33	0.90	0.30	0.35
18	5-16-64	4.28	80	151	160	15	15.2	503	403	3.0	2.1	29	0.62	200	0.20	0.175	0.7	1.0	0.33	0.45
19	5-18-64	4.6	105	153	156	15	15.5	496	397	3.0	2.7	29	0.65	200	0.20	0.047	0.9	1.0	0.33	0.55
24	5-22-64	2.1	74	120	149	10	7.7	410	315	1.0	1.0	23	0.81	300	0.10	0.063	1.0	0.20	0.20	0.30
25	5-23-64	2.1	50	130	150	10	10.8	399	321	1.0	1.2	24	0.80	300	0.10	[illegible]	1.2	0.32	0.32	[illegible]
26	5-18-64	3.8	80	122	133	10.4	11.7	480	375	2.0	2.8	27	0.72	290	0.20	[illegible]	1.4	0.58	0.34	[illegible]
27	5-19-64	3.05	55	126	137	10	11.7	450	355	2.0	2.2	28	0.73	300	0.20	[illegible]	1.1	0.40	0.30	0.45
28	5-20-64	4.15	85	150	135	10	12.5	487	379	3.0	2.7	26	0.72	300	0.30	0.083	0.9	0.84	0.28	0.45
29	5-20-64	4.3	60	130	137	10	13.9	510	405	3.0	2.4	29	0.66	300	0.30	0.156	0.8	0.64	0.21	0.40

After the data acquisition runs were completed, 10,000 ft of high-speed motion pictures were obtained of both stable and unstable flow, in plain tubes and tubes with twisted tape inserts. The motion pictures include sequences covering a wide range in quality and showing one and five tubes. It is intended to edit this film to approximately those 1000 ft which most clearly show each phenomenon, and to produce a finished motion picture which will be available on load from the author in approximately one year.

SECTION 8

DISCUSSION AND CONCLUSIONS

FLOW STABILITY MEASUREMENTS

The measured values of $\Delta P_{\ell c} / \Delta P_{TP}$ range from 0.2 to 1.6, with 85 percent of the results falling below a value of 1.0. This is almost exactly the same range of this parameter that was obtained when Lowdermilk's (10) results with water were presented in terms of this parameter. Although the range of values of the other dimensionless parameters in Lowdermilk's experiment are not available, this agreement gives added confidence for the use of Freon flow stability data in the design of the SNAP 50/SPUR boiler, since the heat of vaporization of water, like that of potassium, is an order of magnitude greater than that of Freon.

To clarify the relationship between the liquid pressure drop ratio and the other dimensionless parameters, the results tabulated in Tables 5 and 6 are presented graphically in Figures 24 to 27. While lines have been drawn through the data points presented in the figures, the location and, in some cases, even the direction of the slope, is very uncertain, since only three points are available to define each line. Nonetheless, certain trends seem to exist.

Figures 24 and 25 reveal that the liquid orifice pressure drop required to produce stable flow decreases as the fractional pressure drop increases. This is consistent with the results disclosed by the literature review, and discussed in the paragraphs on Inlet Velocity earlier in this report, which conclude that increasing inlet velocity or flow rate tends to stabilize the system. This conclusion is somewhat weakened by the reverse slope shown in Figure 25b for a density ratio of 150, and by the scatter in Figure 25a for the same density ratio. The experimental results of this study, however, when combined with the opinions of others, leads to the conclusion that an increase in fractional pressure drop tends to stabilize the flow in a forced-convection boiler.

Figures 26 and 27 show a tendency for increased stability with an increase in subcooling; this is inconsistent with the results of most previous investigators. However, Gouse (14) observed in his recent experiments that there was a range of subcooling which produced instability and that increasing subcooling beyond this range tends to stabilize the system. The results of the present experiment tend to confirm the conclusion that increased subcooling may stabilize as well as destabilize.

The effect of density ratio (pressure level) is best displayed in Figures 24 and 25. For the range of density ratio investigated, the scatter in the data almost disguises the effect; however, increased density ratio appears to require a greater orifice pressure drop. This conclusion is considered to be well established by previous work; the fact that the present experimental results do not show a reverse trend is considered sufficient confirmation.

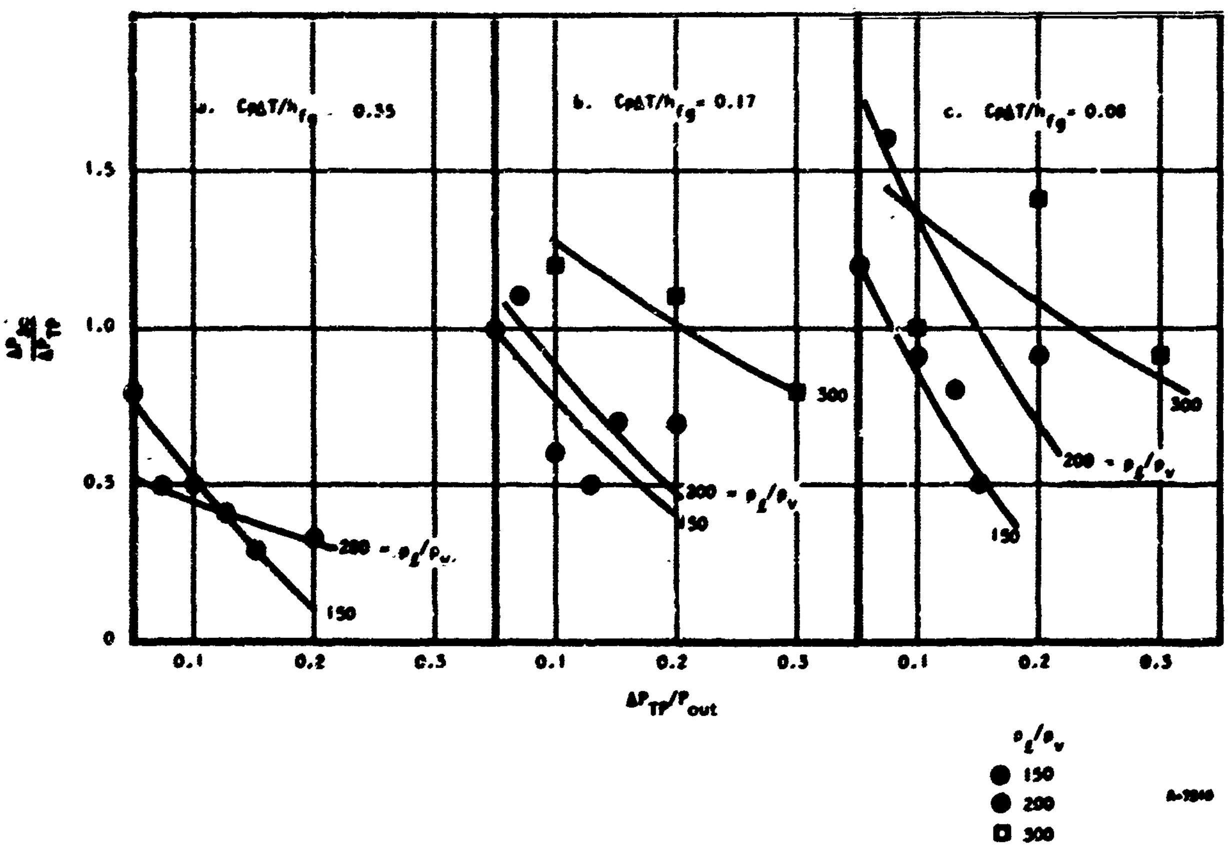

Figure 24. Effect of Fractional Pressure Drop with 3/4 Tape

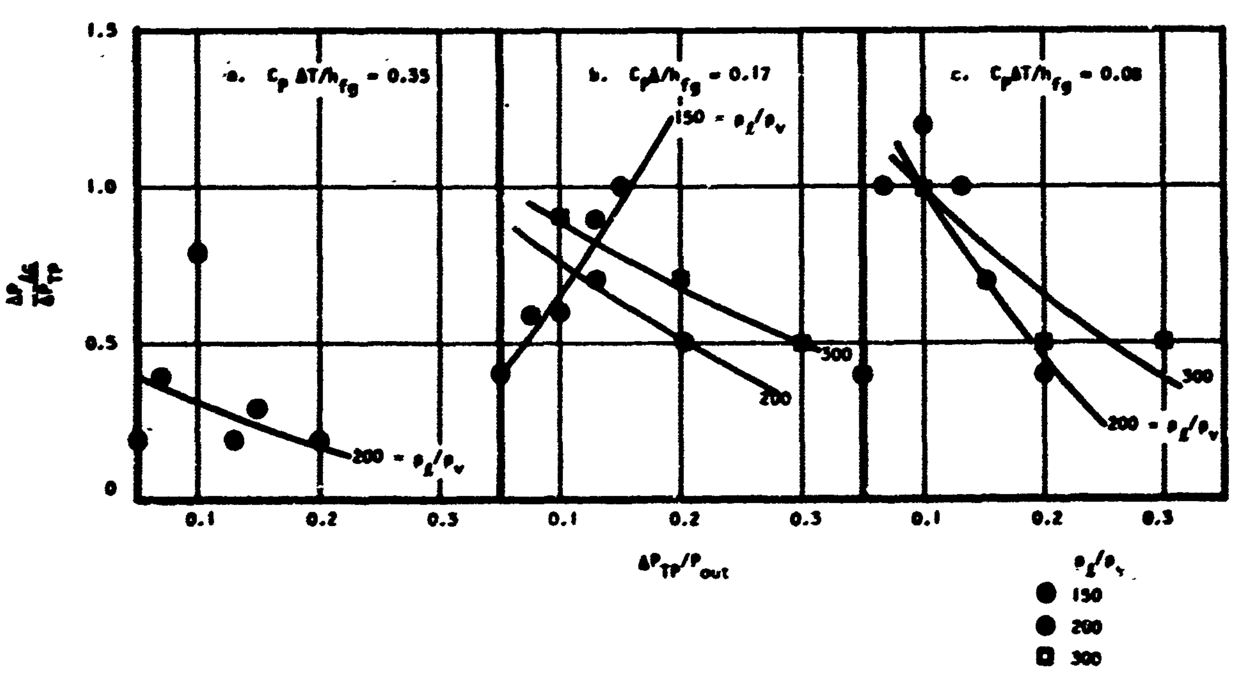

Figure 25. Effect of Fractional Pressure Drop with Full Tape

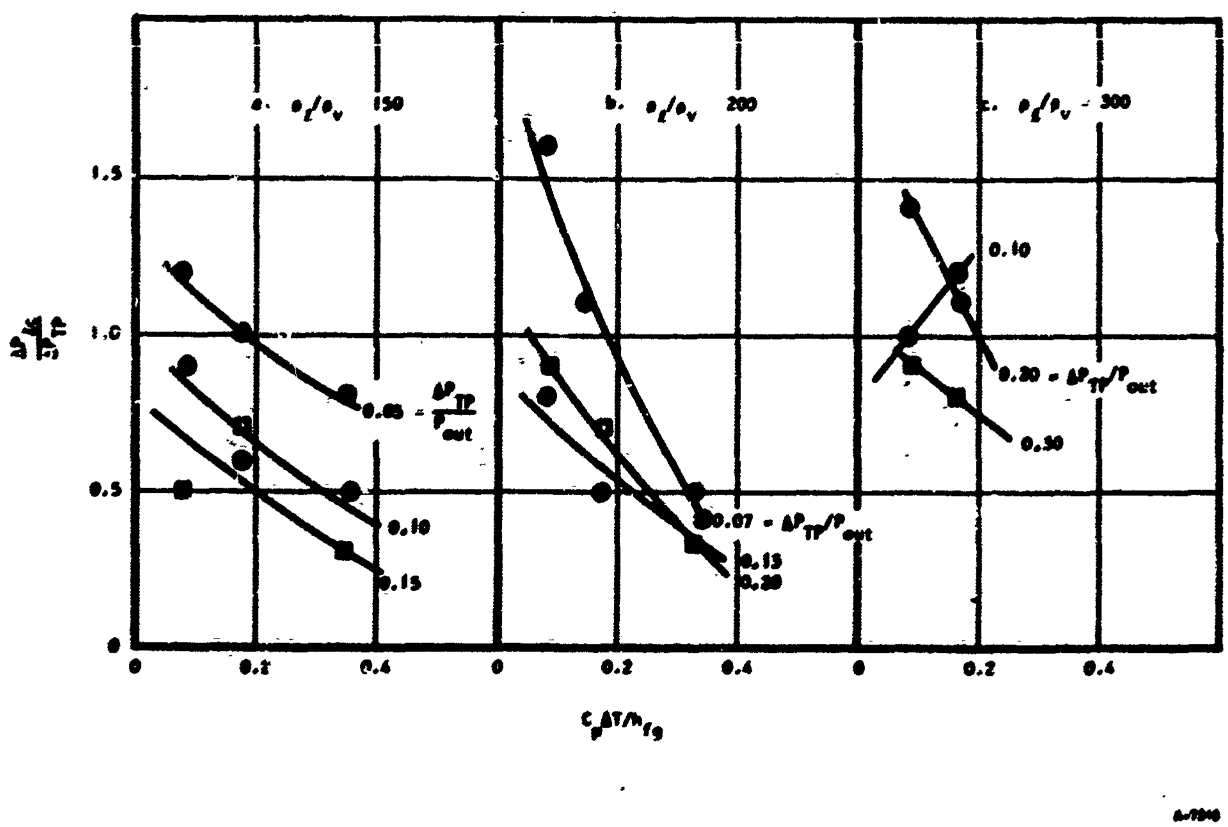

Figure 26. Effect of Subcooling with 3/4 Length Tape

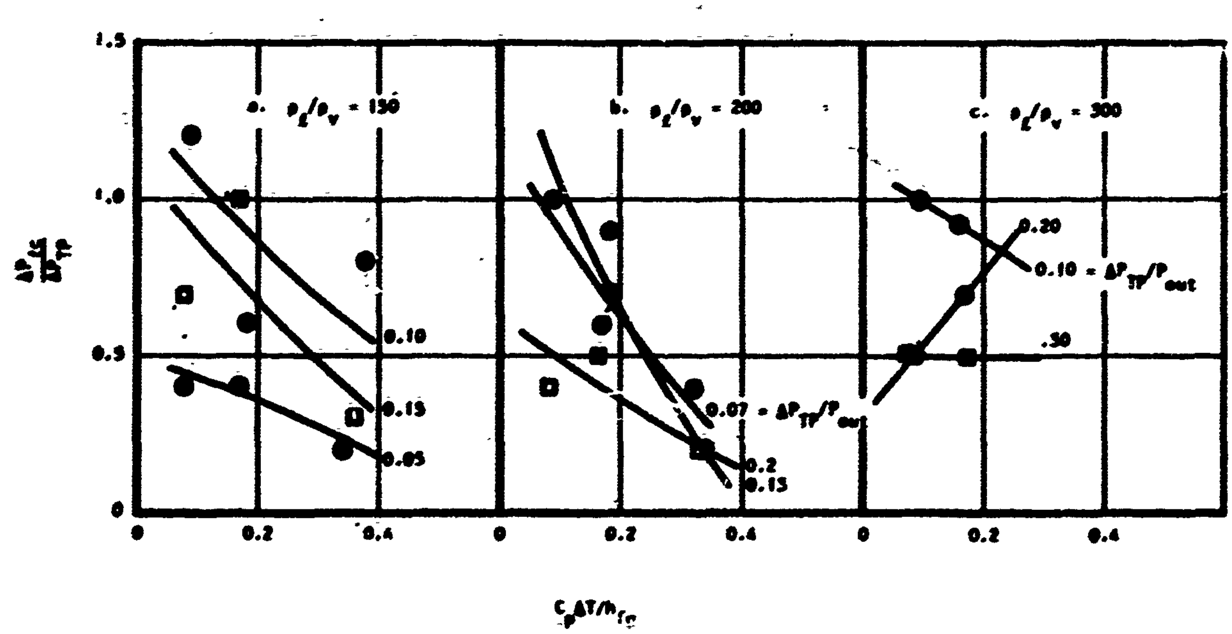

Figure 27. Effect of Subcooling with Full Length Tape

The effect of exit quality was not intentionally investigated in this experiment. However, the 30-percent variation in exit quality which exists in the results is probably one reason for the scatter in the data exhibited in the figures, since the accuracy of the data is well within the scatter that is evident.

No consistent difference is discernible between the results for the full-length or 3/4-length twisted tape insert. Any effect may be overcome by variations produced by different exit qualities at corresponding points

The temperature into the cooler, shown as component 3 in Figure 6, is included in the data recorded in Tables 5 and 6 since it illustrates the complexity and uncertainty of the forced-convection vaporization process. This temperature generally differed from the boiler exit temperature, which was typically 30°F greater than the saturation temperature; in some cases, it was greater and in other cases less. All of these observations can be explained by the fact that the vapor in high quality mist flow can be greatly superheated, even while liquid exis[illegible] the flow. The heat first is transferred from the wall to the vapor, [illegible]en vaporization occurs in the interior of the tube due to heat transfer fr[illegible]e vapor to the liquid. Depending upon the location of the thermocouple and the way in which the superheated vapor and saturated liquid impinge upon the thermocouple, a range of temperatures between the extreme values existing in the tube can be recorded. Also, as vaporization occurs in the unheated length between the boiler and the cooler due to heat transfer between the vapor and the liquid, the temperature of the vapor tends to decrease. The multiplicity of nonequilibrium temperatures which it is possible to measure in high quality, two-phase flow gives rise to the curious combinations of data recorded in these experiments.

PHOTOGRAPHIC OBSERVATIONS

The high-speed motion pictures provided the following qualitative information about two-phase flow in a tube with twisted tape inserts. Beyond the point at which the tube wall becomes dry, a significant quantity of liquid continues to flow along the center of the tape. This quantity of liquid appears to resist the tendency to centrifuge to the tube wall, and much of it persists to the end of the tape. Interruptions in the tape, which would serve to shatter this liquid film, would probably cause much of the liquid in the film to centrifuge to the wall where it would vaporize.

The photographs also confirmed the earlier results (with plain tubes) that, even when the flow into each tube was steady, the exit flow, and therefore quality, always fluctuated. This was true even though the transducer traces of the overall boiler pressure drop and individual tube pressure drop exhibited no fluctuations. It was evident from the visual observations that these stable flow, exit quality oscillations were the result of the plug-annular flow regime transition. The plugs, which exist at low quality, grow very rapidly as they flow along the tube and additional vapor is generated. Even after the vapor plugs join, due to their growth, to produce annular flow, a disproportionate amount of liquid continues to exist where two plugs have joined. This liquid is pushed along the tube by the vapor, and probably much of it ends up as dispersed droplets in the vapor core. The disproportionate amount of liquid which exists between two vapor plugs is not distributed uniformly along the tube after annular flow occurs. Consequently, exit flow and quality fluctuations from individual tubes, which manifest themselves visually as periodic surges of mist at the end of the heated length, occur even in stable two-phase flow.

The distance from the end of the 3/4-length twisted tape to the end of the heated length was approximately 10 in, which is an L/D ratio of 40. In spite of this, the swirl flow produced by the tape persisted to the end of the tube in all runs. There was a visible decrease in the angle between the flow direction and the tube axis as the end of the tube was reached, but an effective amount of swirl remained at the end of the tube.

The motion pictures provided some very interesting sequences of subcooled, forced-convection boiling. Bubbles nucleated on the wall, grew to about 0.020 in. in diameter, and then broke away from the wall due to the inertia caused by their growth rate. After breaking away from the wall and penetrating the subcooled liquid core in the interior of the pipe, the bubbles very rapidly decreased in size as they condensed, until only a small spot was visible where the bubble had been located. When this small spot moved downstream and reached the point where the liquid exceeded the saturation temperature, it again grew into a bubble in the interior of the tube. Other forms of subcooled boiling were observed in which the bubble collapsed while it was still attached to the wall, but the process described above was particularly dramatic and interesting.

SUMMARY OF CONCLUSIONS

The following conclusions appear to be valid for the conditions investigated in this experiment.

1. The ratio of liquid orifice pressure drop to two-phase pressure drop required to produce stable flow for SNAP-50/SPUR boiler conditions is 0.2 to 1.6. To be conservative, a value between 1 and 2 should be used.

2. The flow tends to become more stable as: (a) fractional pressure drop is increased, (b) entrance subcooling is increased, and (c) density ratio is decreased.

3. The vapor in mist flow is always superheated, which makes temperature measurements very hard to interpret.

4. Exit flow and quality oscillations from individual tubes exist due to the plug-annular flow regime transition, even when the flow into the tube is steady.

5. Swirl flow persists for a length equal to more than 40 diameters after the end of the twisted tape in high quality two-phase flow.

6. A significant quantity of liquid continues to flow along the center of a plain, twisted tape after the tube wall becomes dry.

REFERENCES

1. J. G. Collier, "A Review of Two-Phase Heat Transfer 1935-1957," AERE Report CE/R 2496, Harwell, Berkshire, England, 1958.

2. Peter Griffith, "Two-Phase Flow in Pipes," Massachusetts Institute of Technology, Course 2.529 Lecture Notes, July 1958.

3. Earl Quandt, "Analysis of Gas-Liquid Flow Patterns," A.I.Ch.E. Preprint No. 47, Sixth National Heat Transfer Conference, August 1963.

4. C. E. Dengler, and J. N. Addoms, "Heat Transfer Mechanism for Vaporization of Water in a Vertical Tube," Chemical Engineering Progress Symposium Series, No. 18, Vol 52, 1956.

5. H. Groothius and W. P. Hendal, "Heat Transfer in Two-Phase Flow," Chemical Engineering Science, Vol 11, pp 212 to 220, 1959.

6. P. Sachs and R.A.K. Long, "A Correlation for Heat Transfer in Stratified Two-Phase Flow with Vaporization," Int. J. of Heat and Mass Transfer, Vol 2, pp 222-230, 1961.

7. John C. Chen, "A Correlation for Boiling Heat Transfer to Saturated Fluids in Convective Flow," A.S.M.E. Paper 63-HT-34, August 1963.

8. P. J. Berenson and R. A. Stone, "A Photographic Study of the Mechansim of Forced Convection Vaporization," A.I.Ch.E., Paper No. 21, Fifty-First National Meeting, 1963, to be published in 1964 A.I.Ch.E. Heat Transfer Symposium.

9. J. W. Miles, "The Hydrodynamic Stability of a Thin Film of Liquid in Uniform Shearing Motion," J. of Fluid Mechanics, Vol 8, 1961, pp 592-610.

10. W. H. Lowdermilk, C. D. Lanzo and B. L. Siegel, "Investigation of Boiling Burnout and Flow Stability for Water Flowing in Tubes," NACA TN 4382, September 1958.

11. E. S. Beckjord, "The Stability of Two-Phase Loops and Response to Ships Motion," GEAP 3493 (Rev. 1), September 1960.

12. A. P. Fraas, "Flow Stability in Heat Transfer Matrices Under Boiling Conditions," Addendum No. 1, ORNL 59-11-1, Oak Ridge, Tennessee March 22, 1961

13. W. R. Gambill and N. D. Greene, "Boiling Burnout with Water in Vortex Flow," Chemical Engineering Progress, Vol 54, No. 10, October 1958 pp 68-76

14. S. W. Gouse, Jr., and C. C. Andrysiak, "Flow Oscillations in a Closed Loop with Transparent, Parallel, Vertical, Heated Channels," Report No. 8973-2, Dept. of Mech. Eng., MIT, Cambridge, Mass. June 1963.

REFERENCES (Continued)

15. E. R. Quandt, "Analysis and Measurement of Flow Oscillations," Chemical Engineering Progress Symposium Series No. 32, Vol 57, 1961, pp 111-126.

16. J. E. Meyer and R. P. Rose, "Application of a Momentum Integral Model to the Study of Parallel Channel Boiling Flow Oscillations," ASME Paper No. 62-HT-41, August 1962.

17. A. L. Blubaugh and E. R. Quandt, "Analysis and Measurement of Flow Oscillations," (Westinghouse-Bettis Atomic Power Lab) WAPD-AD-TH 538, p 72, November 1960.

18. O. J. Mendler, A. S. Rathbun, N. E. Van Huff, and A. Weiss, "Natural Circulation Tests with Water at 800 to 2000 psia Under Nonboiling, Local Boiling, and Bulk Boiling Conditions," Journal of Heat Transfer 83 C p 261, August 1961.

19. A. H. Stenning, "Instabilities in the Flow of a Boiling Liquid," ASME Paper 62-WA-155, November 1962.

20. H. R. Wright and H. F. Poppendiek, "Unsteady State Flow in Boiling Heat Transfer Systems," Technical Progress Report No. 2, GLM-15, Geoscience Ltd., Solana Beach, Calif., October 1962.

21. A. B. Jones, "Hydrodynamic Stability of a Boiling Channel," Knolls Atomic Power Laboratory Report KAPL - 2178, October 1961.

22. G. B. Wallis and J. H. Heasley, "Oscillations in Two-Phase Flow," The American Society of Mechanical Engineers, 83, C. No. 3, August 1961.

23. W. H. Lowdermilk, C. D. Lanzo and B. L. Siegel, "Investigation of Boiling Burnout and Flow Stability For Water Flowing in Tubes," NACA TN 4382, September 1958.

24. S. Ostrach, and A. Koester, "Film Instabilities in Two-Phase Flows," A.I.Ch.E. Preprint No. 45, Sixth National Heat Transfer Conference, August 1963.

25. N. Adorni, I. Casagrande, L. Cravarolo, A. Hassid, and M. Silvestri, "Experimental Data on Two-Phase Adiabatic Flow: Liquid Film Thickness, Phase and Velocity Distribution, Pressure Drops in Vertical Gas-Liquid Flow," CISE R35 (Euroatom), March 1961.

26. H. S. Isbin, R. H. Moen, and O. R. Mosher, "Two-Phase Pressure Drops," Univ. of Minn., Tech. Info. Services, Oak Ridge, Tenn., AECU 2994, November 1954.

27. H. S. Isbin, "Comments on a Paper by Mendler, et al.," Journal of Heat Transfer, 83 C, p 261, August 1961.

28. R. Delagre and J. P. Saunier, "D'Acoulement Du Fluide Dans Un Canal Chauffant Refroidi a L'Eau--R," Commissariat A L'Energie Atomique, Centre D Etudes Nucleaires, Saclay, France, pp 55 (1961).

29. A. E. Bergles and W. M. Rohsenow, "Forced Convection Surface Boiling Heat Transfer and Burnout in Tubes of Small Diameter," Tech. Report No. 8767-21, Dept. of Mech. Eng., MIT

30. B. Matzner, "Basic Experimental Studies on Boiling Fluid Flow and Heat Transfer at Elevated Pressures," Columbia Univ., Chem. Eng. MPR 1161, November 30, 1961.

31. S. Stephen Papell, "An Instability Effect in Two-Phase Heat Transfer for Subcooled Water Flowing Under Conditions of Zero G ty," ARS, Space Power Systems Conference, Santa Monica, Calif., September 25-28, 1962.

32. N. A. Radovcich and R. Moissis, "The Transistion from Two-Phase Bubble Flow to Slug Flow," MIT Tech. Report No. 7-7673-22, June, 1962.

33. A. P. Fraas, "Flow Stability in Heat Transfer Matrices Under Boiling Conditions," ORNL 59-11-1, Oak Ridge, Tennessee, November 1, 1959

34. J. G. Collier and D. J. Pulling, "Instabilities in Two-Phase Flow," A.E.R.E. Report M1105, Atomic Energy Research Establishment, Harwell, Berkshire, England, 1963.

35. H F. Poppendiek, and C. L. Rickard, "Remarks on Transient Pressures Within the Core of the Research Reactor Under Power Excursions," GAMD 176, General Atomics, San Diego, Calif., July 1957.

36. E. H. Wissler, H. S. Isbin, and N. R. Amundson, "Oscillatory Behavior of a Two-Phase Natural Circulation Loop," The American Institute of Chemical Engineer's Journal No. 2, pp 157-162, 1956.

37. A. R. Gruber, and S. C. Hyman, "Flow Distribution Among Parallel Heated Channels," The American Institute of Chemical Engineer's Journal No. 2, p 199, 1956.

38. F. Schroeder, S. G. Forbes, W. E. Nyer, F. L. Bentzen, and G. O. Bright, "Experimental Study of Transient Behavior in a Subcooled Water-Moderated Reactor," Nuclear Science and Engineering 2, No. 1, pp 96-115, February 1957.

39. W. H. McAdams, Heat Transmission, McGraw-Hill Book Co., Inc., New York 1954, Chapter 5.

APPENDIX

A PHOTOGRAPHIC STUDY OF THE MECHANISM OF FORCED CONVECTION VAPORIZATION

by

P. J. Berenson
R. A. Stone

AiResearch Manufacturing Company
Los Angeles 9, California

ABSTRACT

The vaporization of Freon 113 flowing inside a horizontal pyrex tube was studied with the aid of 7000 frame per second motion pictures. Heat fluxes up to 40,000 Btu/hr-ft^2 were obtained using 800°F air flowing in the space between the glass tube and a rectangular quartz duct as the heat source. The Freon entered the tube subcooled and the exit condition varied from moderate quality to superheated vapor. The two phase flow patterns and heat transfer mechanisms revealed in the photographs are discussed. The photographs lead to the conclusion that the annular-mist flow transition (forced convection vaporization burnout condition) results simply from the vaporization of the liquid annulus while liquid droplets remain dispersed throughout the vapor core.

I INTRODUCTION

The ability to accurately predict the heat transfer and pressure drop characteristics of the forced convection vaporization process has become increasingly important in recent years. Boiling nuclear reactors, Rankine cycle space power systems, environmental control systems for spacecraft, and other advanced systems depend upon this process.

A large number of both experimental and analytical investigations of forced convection vaporization have been performed during the past twenty years. Reference 1 contains an excellent review of the state-of-the-art up to 1957. Considering the amount of work that has been done, relatively little progress has been made toward predicting the characteristics of forced convection vaporization. This is due to the great number of variables upon which the process depends, compounded by the complexity of the various two-phase flow patterns which occur as the quality increases along the tube.

Because of the large differences in the various flow patterns which occur as the volume fraction of the vapor increases along the tube, it is unlikely that a single correlation can adequately predict the heat transfer characteristics of forced convection vaporization from 0 to 100 percent quality. It is probable that a separate correlation will have to be developed for each flow pattern. To do this requires a familiarity with the characteristics of each flow pattern so that an analytical model can be formulated to yield correlations for the heat transfer coefficient in each regime and the quality at which flow regime transitions occur.

Visual studies of adiabatic, two-phase, two-component flow have provided information on the flow patterns. Attempts have been made to develop flow regime maps which would make it possible to predict the transition conditions (2). While the flow regimes depend to some extent on whether the flow is vertical or horizontal, for both orientations the flow regimes shown in Figure 2 appear to be that most important for relatively high flow rates. The flow patterns shown are as follows:

1. <u>Bubbly Flow</u>--This pattern occurs at very low quality and consists of individual bubbles of vapor entrained in the liquid flow. The bubbles are formed at nucleation sites on the wall.

2. <u>Plug or Slug Flow</u>--As the quality increases, the individual bubbles agglomerate to form plugs or slugs of vapor which periodically pass a given point on the wall.

3. <u>Annular Flow</u>--At higher quality, the vapor flows in a high velocity core in the center of the pipe and a thin film of liquid covers the pipe wall. Liquid droplets are generally dispersed in the vapor core.

4. <u>Mist Flow</u>--At high quality, the liquid film on the wall disappears and all the liquid is dispersed throughout the vapor as droplets.

Forced convection vaporization heat transfer data have shown that the heat transfer coefficient increases as the quality increases (3, 4). At a critical quality, which varies considerably with fluid, geometry, and heat flux, there is a sharp decrease in the heat transfer coefficient toward the value characteristic of vapor flow, as shown in Figure 29. When the quality reaches 100 percent, the coefficient equals the vapor heat transfer coefficient.

It is often of great importance to be able to predict the quality at which the sharp decrease in heat transfer coefficient occurs, for, if the heat flux is the imposed condition, burnout occurs beyond this point. It has been suggested (3) that this quality corresponds to the point at which the transition from annular flow to mist flow occurs. This is very likely, since this is a transition from a liquid-covered wall to a gas-blanketed wall, which is similar to the pool boiling burnout condition that occurs in changing from nucleate to film boiling. There have been many suggestions as to the reason for the transition from annular to mist flow, and numerous correlations of the forced convection burnout condition have been attempted. No general correlation is presently available, and there is considerable confusion regarding the transition mechanism.

Most of the visual studies of forced convection vaporization have been performed under adiabatic conditions because of the relative ease of this type of experiment. In addition, most of the heat transfer tests have used electrical heating, thereby imposing the heat flux as the boundary condition (5). The purpose of the experiment described below was to study the forced convection vaporization process with high-speed motion pictures when the overall temperature difference is the imposed boundary condition. In addition, it was desired to obtain motion pictures of all the significant flow patterns, since insufficient emphasis has previously been placed on annular and mist flow.

The motion picture supplement to this paper, showing the various flow regimes, is available on loan from the American Institute of Chemical Engineers and the AiResearch Manufacturing Company.

II APPARATUS AND PROCEDURE

The schematic of the test setup is shown in Figure 30 and the test section geometry in Figure 31. The test section consists of an inner Pyrex tube 6 mm ID, 8 mm OD, and 40 inches long, in which Freon flows. Air flows outside this tube, inside a 20-inch-long rectangular quartz duct whose inside dimensions are 3/8 inch by 1-3/4 inch. The air flow is counter to the Freon flow. The heated length of the test section is approximately 24 inches, consisting of the 20 inches of quartz tube plus approximately 2 inches on each end inside the flange connection. The Freon tube is insulated from contact with the air until it reaches the 24-inch test section. The air is heated in a gas furnace to approximately 800°F and metered in an insulated section before it passes into the test section.

Manometer pressure taps were located at the flanges of a 1-1/2 inch orifice inside a 2-inch pipe on the inlet air line and on both sides of the test section. These permitted measurement of the air flow rate through the orifice and later provided a means of estimating the air leakage from the test section. Air inlet and outlet temperatures were measured by means of thermocouples in the air stream. Freon inlet and outlet temperatures were measured by thermocouples located in mixing sections inside the Freon tube. The Freon inlet line was instrumented with an expansion and contraction chamber, with transducer taps on the chamber inlet and outlet lines and also in the central stagnant chamber. Forward flow rate was indicated as an entrance loss in the latter two taps in the expansion chamber, while reverse flow was indicated by entrance pressure loss in the first two taps of the test section. The forward and reverse pressure drops across the Freon inlet flow section were recorded on a Sanborn recorder. Freon flow rate was measured by using a stop watch to measure the time required for collection of one pound of Freon from the condenser.

A WF-3 Fastax camera with a 6-inch f4.5 lens was mounted approximately 8 inches from the quartz tube, shooting horizontally at the test section through a 6-inch Aero Ektar supplementary lens. Ektachrome ERB (ASA 50) film was used with the shutter of the camera wide open. At this lens opening, the depth of field over which the camera was in focus was approximately one millimeter. The test section was backlighted to 40,000 ft-candles by two 1000-watt quartz iodine lamps reflecting from white cardboard. The film speed was approximately 7000 pictures per second; each motion picture run took approximately 1-1/2 seconds, and approximately half of this time was required for the camera to attain full speed.

The first motion pictures obtained showed poor resolution between Freon liquid and vapor. As a result, Trace, a bright red Freon-coloring agent used in detecting leaks in Freon air conditioning systems, was added to the Freon supply in a concentration of approximately one weight percent. Subsequent pictures showed excellent resolution and detail of the vaporization process.

Heat input to the Freon was determined by measuring the heat lost by the air when no Freon was flowing, and subtracting that quantity from the total enthalpy change of the air during a run. It was later learned that there was a leak of hot air through the flange connections, varying from about 15 percent to 25 percent of the total air flow. The steady-state heat loss from the test section was approximately equal to the heat input into the Freon; as a result, the quality at the test section was later estimated to be accurate only to ±30 percent.

At the start of each run, the air flow through the unit was adjusted by means of a valve in the inlet air line to the desired value. The Freon tank was then pressurized to 40 psig, and the position of the Freon throttle valve was adjusted until the proper flow rate was observed leaving the condenser. The following quantities were recorded: air inlet temperature, air outlet temperature, Freon inlet temperature, Freon outlet temperature, test section air static pressure, test section air ΔP, air line orifice static pressure, air line orifice ΔP, and Freon flow rate (the time it took for 1 pound of Freon to be collected at the condenser). Motion pictures were taken at the same spot throughout; approximately 6 inches from the Freon inlet to the heated section and approximately 14 inches from the pyrex tube entrance.

III DISCUSSION OF RESULTS

A. FLOW STABILITY

For low values of pressure drop across the throttle valve at the entrance to the heated tube, flow instability (i.e., oscillations of the orifice pressure drop) was observed. This is consistent with the results of other investigators (6). Figure 32 is a typical pressure transducer trace under these conditions. The magnitude of the pressure and, therefore, flow fluctuations decreased as the pressure drop across the inlet throttle valve was increased as shown in Figure 32. The flow rate fluctuations were apparently due to the interaction of the two-phase-flow pressure drop characteristics with the compressible volumes in the system (6). When the inlet throttle valve is choked, the flow downstream of the throttle valve is insensitive to conditions upstream; the presence of the compressible volume provided by the pressurizing gas on top of the Freon no longer has any effect. It is of interest to note that the elimination of some flexible connections between the throttle valve and the heated tube, which were observed to be periodically expanding, yielded increased flow stability. At all heat fluxes and flow rates investigated, the inlet flow rate could be made steady with a great enough pressure drop across the inlet throttle valve. Even though there was steady flow into the tube, the flow rate and temperature at the exit fluctuated. This is apparently due to the periodic nature of plug flow, the compressible volume of the plugs, and the fact that thermal equilibrium does not exist in mist flow.

B. FLOW REGIMES

A summary of the characteristics of the flow regimes shown in the motion picture and discussed below is presented in Table 7.

TABLE 7

MOTION PICTURE SUMMARY

Film Strip Flow Regime	1 Bubbly	2 Plug	3 Annular (Slug)	4 Annular	5 Annular-Mist Transition
Freon Flow Rate, lb/min ±2%	3.4	1.0	1.0	1.0	0.50
Air Flow Rate, lb/min	3.5 ±0.2	3.5 ±0.2	3.3 ±0.2	8 ±2	8 ±2
Heat Flux BTU/hr ft^2 ±10%	20,000	20,000	20,000	27,000	35,000
Quality ±30%	60° subcooled	0.1%	1%	5%	30%

1. <u>Bubbly Flow</u>

A photograph typical of the bubbly flow regime shown in the first film strip is presented in Figure 33. In order for this flow pattern to exist, the vapor volume fraction must be low. Because of the high ratio of liquid-to-vapor density for most fluids of interest, the corresponding mass fraction (quality) in the bubbly flow regime is extremely small, for example, much less than 1 percent. The bubbly flow regime can occur in a subcooled liquid since the bubbles nucleating at the wall may move into the liquid core because of the inertia caused by their growth rates. Thermal equilibrium does not exist as there is insufficient time for the bubbles to condense before the surrounding liquid is heated to the saturation temperature as it flows along the tube.

In the bubbly flow regime, the vapor volume fraction is so small that it has little effect on the liquid velocity. Bubbles grow and depart from nucleation sites on the wall the same as in nucleate pool boiling. Depending upon the wall and fluid temperatures and the nucleation characteristics of the wall, the nucleate pool boiling heat transfer mechanism may or may not dominate the forced convection heat transfer to the liquid occurring between the bubble nucleation sites. In the very narrow quality range over which bubbly flow exists, it seems reasonable to assume that the heat transfer can be predicted by superimposing liquid forced convection and nucleate pool boiling, provided the superheat temperature difference is not great enough to produce film boiling (7).

2. <u>Plug Flow</u>

As the vapor volume fraction or the L/D ratio increases, the individual bubbles begin to agglomerate and form plugs or slugs of vapor, as shown in Figure 34 and the second film strip. These large volumes of vapor occur periodically along the tube. Even though the volume quality has increased to approximately 15 percent in the film strip, the corresponding mass fraction, or quality, is approximately 0.1 percent. The presence of the larger volume fraction of vapor begins to cause a significant increase in the liquid velocity in the plug flow regime.

The plugs of vapor are compressible volumes which make possible the flow oscillations within the tube that are observed in the film strip even though the flow entering the tube is steady. Actual flow reversal is shown in the movie. It is possible that the periodic nature of plug flow, combined with the compressible volume it provides, is the source of many of the exit flow oscillations which occur in forced convection vaporization inasmuch as all other flow regimes are steady.

The film strip shows that, for the conditions prevailing in this experiment, bubbles nucleate and depart from the wall at numerous sites inside the tube in the plug flow regime. The heat transfer mechanism in the plug flow regime is probably the same as in the bubbly flow regime: a superposition of forced convection to a liquid and nucleate pool boiling.

While both the bubbly and plug flow regimes are very interesting, it must be emphasized that, for the density ratios of general interest in forced convection evaporators, they occur up to only very low quality, so that, if one is vaporizing to high quality, these flow regimes have a relatively small effect on the heat transfer process. They only become important if the temperature difference is great enough to cause film boiling or because of the flow oscillations produced in the plug flow regime.

3. Annular Flow

The two film strips showing annular flow were taken without moving the camera. A typical photograph of annular flow is presented in Figure 35. The waves present on the liquid-vapor interface just inside the tube can be detected, but the presence of the continuous two-phase interface makes it impossible to see into the vapor core. The first film strip is at a quality of approximately 1 percent, while that of the second film strip is approximately 5 percent. The increase in quality was produced by maintaining the Freon flow and increasing the hot air flow. The dark spots on the tube wall are dried dye left from previous tests; they have no effect on the flow or heat transfer process.

In the first film strip, some of the liquid stratifies into the bottom of the tube. Around the balance of the tube, a thin film of liquid covers the wall; heat is transferred by conduction through this liquid film. Although there are a number of active bubble nucleation sites, these probably have a negligible effect on the heat transfer rate. The heat transfer in annular flow is very similar to that for condensation inside a tube; it is probably valid to neglect the heat transfer to the stratified liquid and assume that all the heat is transferred by conduction through the thin liquid annulus.

Periodic flow surges occur in this film strip which must have been initiated in the plug flow regime, since the flow entering the tube was steady. The flow surges are detected by the deepening color, which indicates an increased liquid volume fraction. This flow regime is sometimes called slug flow, although the heat transfer mechanism is typical of annular flow.

In the second annular flow film strip, the quality is approximately 5 percent and the stratification of the liquid has essentially disappeared because the increased inertia forces now dominate gravity. The camera location was not changed as the quality was increased in order to observe the same active nucleation site which existed in the center of the previous film strip.

Although the vapor core cannot be seen through the liquid-vapor interface which forms the inner boundary of the liquid annulus, the high velocity vapor core contains many liquid droplets. The liquid-vapor interface exists just inside the tube, where the waves caused by the vapor shear are apparent.

Once aga n, while some nucleation sites exist, the dominant heat transfer mechanism is probably conduction through the thin liquid film. The vapor is generated primarily by vaporization from the liquid-vapor interface inside the tube and not by the formation of bubbles in the liquid. There is a significant amount of liquid dispersed throughout the vapor core as droplets, in addition to the liquid in the annulus on the wall.

The flow surges stil, occur at this quality. While the change in color of the fluid during the surge is not as obvious as at lower quality, the deepening pink indicates that the liquid volume fraction is increasing.

4. Mist Flow (Forced Convection Vaporization Burnout Condition)

The observation of the transition from annular to mist flow is of great interest, since this is presumably the point at which the evaporator heat transfer coefficient experiences the sharp decrease observed. Therefore, this transition is the cause of the forced convection vaporization burnout condition. A photograph of the partially dry wall taken from the last film strip is shown in Figure 36.

The flow surges which were apparent in the annular flow regime continue to persist in this transition regime. That is, the wall in front of the camera alternately becomes wet with liquid (along the bottom half in the movie) and then dry. This occurs about three times in the film strip.

The red line about halfway up the tube diameter is a thin strip of dye which presumably is less volatile than the Freon and tends to collect at high quality in the manner shown. Liquid droplets dispersed throughout the vapor core can be seen where the wall is dry. These droplets were formed downstream at lower quality and are carried along by the vapor. The velocity of these droplets is much higher than the velocity of the liquid film, and therefore gravity has a much smaller effect on them.

The following observations of the wall drying process are significant. A small dry spot forms and grows in all directions as the liquid vaporizes because of conduction heat transfer through the liquid. The small strips of liquid on the wall remain almost stationary relative to the high velocity vapor and the liquid droplets in the vapor core which can be seen flowing in the tube. The dominant heat transfer mechanism is conduction through the liquid film; nucleation may produce the initial dry spot on the wall, but has a small effect on heat transfer. This is the same drying process that would occur with a thin film of liquid in a hot pan whose temperature is not great enough to cause nucleate boiling. This transition occurs three times in the film strip, as described.

Beyond the point at which these film strips were taken, the wall is dry except when the liquid droplets in the vapor core impinge upon the wall. Most of the heat transfer is from the wall to the vapor. After the heat is transferred to the vapor, it is then transferred to the liquid droplets; the mist flow vaporization process actually takes place in the interior of the pipe, not at the wall. For this reason, the temperature of the vapor in the mist flow regime can be greater than the saturation temperature; thermal equilibrium may not exist in the tube.

The above description of the transition from annular to mist flow is in conflict with theories which postulate that the transition occurs when the thin liquid annulus becomes unstable owing to the effect of the high velocity vapor core (4). This was not observed in the high speed photographs. As a result of the visual observations of the transition process, it is concluded that the transition is simply due to the liquid film on the wall vaporizing as a result of conduction heat transfer through the liquid, while the vapor core contains a dispersion of liquid droplets. While the volume fraction of these droplets is very small, they account for a substantial mass fraction because of the high ratio of the liquid-to-vapor density.

This explanation is consistent with a theoretical stability analysis of a liquid film (8), whose predictions have been partially verified by experiment (9). This analysis predicts that a liquid film is stable for sufficiently small Reynold numbers, independent of the vapor velocity.

Since the liquid film Reynolds number decreases as the quality increases in a forced convection evaporator, the liquid annulus will be stable at sufficiently high quality, independent of the value of the vapor velocity. Therefore, the high quality burnout condition could not be due to an instability of the liquid film.

While annular two-phase flow is sometimes idealized so that all the liquid is in the annular film and all the vapor in the high velocity core, observations have shown that droplets of liquid generally exist in the vapor core. These droplets may or may not join the liquid annulus, depending on the magnitude of the turbulent vapor fluctuations and the transit time of the droplets through the evaporator. This is consistent with the stability analysis which predicts a high Reynolds number liquid film, such as exists at low quality, may be unstable.

In summary, the liquid droplets dispersed throughout the vapor core are produced as a result of a film instability at low quality. The transition from annular to mist flow occurs when the liquid annulus vaporizes as a result of conduction through the thin liquid film, while liquid droplets remain dispersed throughout the vapor core. The quality at the transition is determined by the mass of liquid contained in the droplets when the transition occurs.

IV SUMMARY OF CONCLUSIONS

The following conclusions appear to be valid based upon the observations of the forced convection vaporization process.

1. Throttling at the entrance of a forced convection evaporator tube yields steady flow into the tube.

2. Even though the flow into the tube is steady, the exit flow can fluctuate. This is probably due primarily to the periodic nature of plug flow combined with the compressible volume within the tube provided by the plug.

3. Nucleation of bubbles on the wall was observed whenever the wall was wet, in all flow regimes.

4. It is reasonable to correlate bubbly and plug-slug flow by superimposing liquid forced convection and nucleate pool boiling heat fluxes.

5. The dominant heat transfer mechanism in annular flow is conduction through the liquid film on the wall. The vapor formation process occurs primarily at the annulus liquid-vapor interface within the tube, not at the wall within the liquid annulus.

6. The transition from annular to mist flow (forced convection vaporization burnout) is simply the result of the annular liquid film vaporizing while liquid droplets, formed at low quality, remain dispersed throughout the vapor core.

7. Departure from thermal equilibrium is important in forced convection vaporization; bubbly flow can exist in a subcooled liquid and the vapor in mist flow can be superheated.

ACKNOWLEDGMENTS

The authors would like to acknowledge the valuable assistance of Mr. Les Meek and Mr. Ray Zink of the AiResearch Photo Lab, without whose creativeness films could not have been obtained; also Mr. Ronald Larson of the AiResearch Heat Transfer Lab who supervised building of the apparatus. This research was supported by the Aeronautical Systems Division of the Air Force through contract AF 33(657)-8954.

BIBLIOGRAPHY

1. Collier, J. G., "A Review of Two Phase Heat Transfer 1935-1957," AERE Report CE/R 2496, Harwell, Berkshire, England, 1958.

2. Griffith, Peter, "Two Phase Flow in Pipes," Massachusetts Institute of Technology, Course 2.529 Lecture Notes, July 1958.

3. Dengler, C. E., and J. N. Addoms, "Heat Transfer Mechanism for Vaporization of Water in a Vertical Tube," Chemical Engineering Progress Symposium Series, No. 18, Vol 52, 1956.

4. Groothuis, H., and W. P. Hendal, "Heat Transfer in Two Phase Flow," Chemical Engineering Science, Vol II, pp 212 to 220, 1959.

5. Sachs, P., and R. A. K. Long, "A Correlation for Heat Transfer in Stratified Two Phase Flow with Vaporization," Int. J. of Heat and Mass Transfer, Vol 2, pp 222-230, 1961.

6. Lowdermilk, W. H., Lanzo, C. D., and B. L. Siegel, "Investigation of Boiling Burnout and Flow Stability for Water Flowing in Tubes," NACA TN 4382, September 1958.

7. Rohsenow, W. M., and H. Y. Choi, Heat Mass and Momentum Transfer, Prentice-Hall, Inc., Englewood Cliffs, New Jersey, 1961, p 226.

8. Miles, J. W., "The Hydrodynamic Stability of a Thin Film of Liquid in Uniform Shearing Motion," J. of Fluid Mechanics, Vol 8, 1961, pp 592-610.

9. Charvonia, D. A., "An Experimental Investigation of the Mean Liquid Film Thickness and the Characteristics of the Interfacial Surface in Annular, Two Phase Flow," ASME Paper 61-WA-243.

Figure 28. Two-Phase Flow Regimes

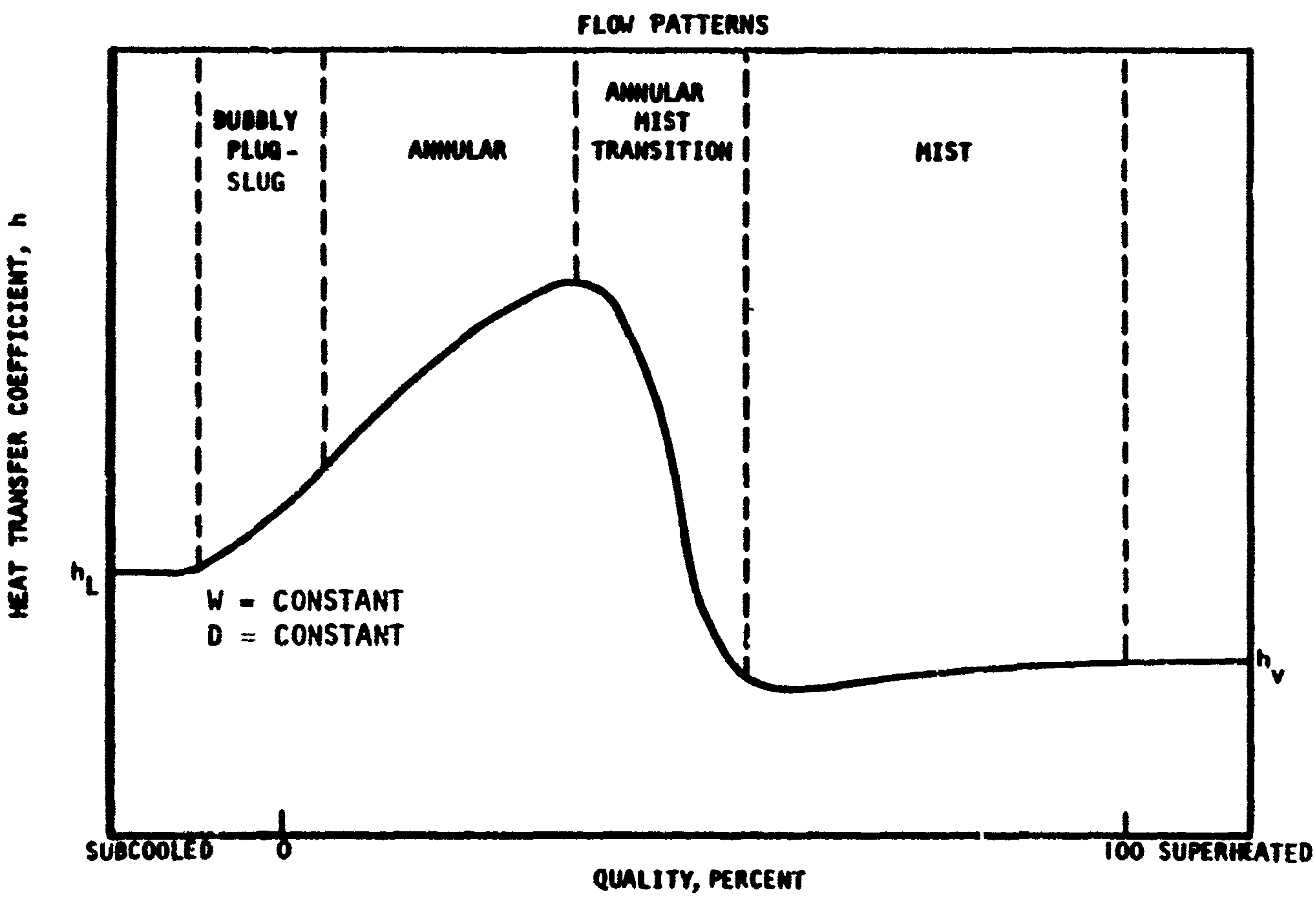

Figure 29. Characteristic Forced Convection Vaporization Heat Transfer Coefficient

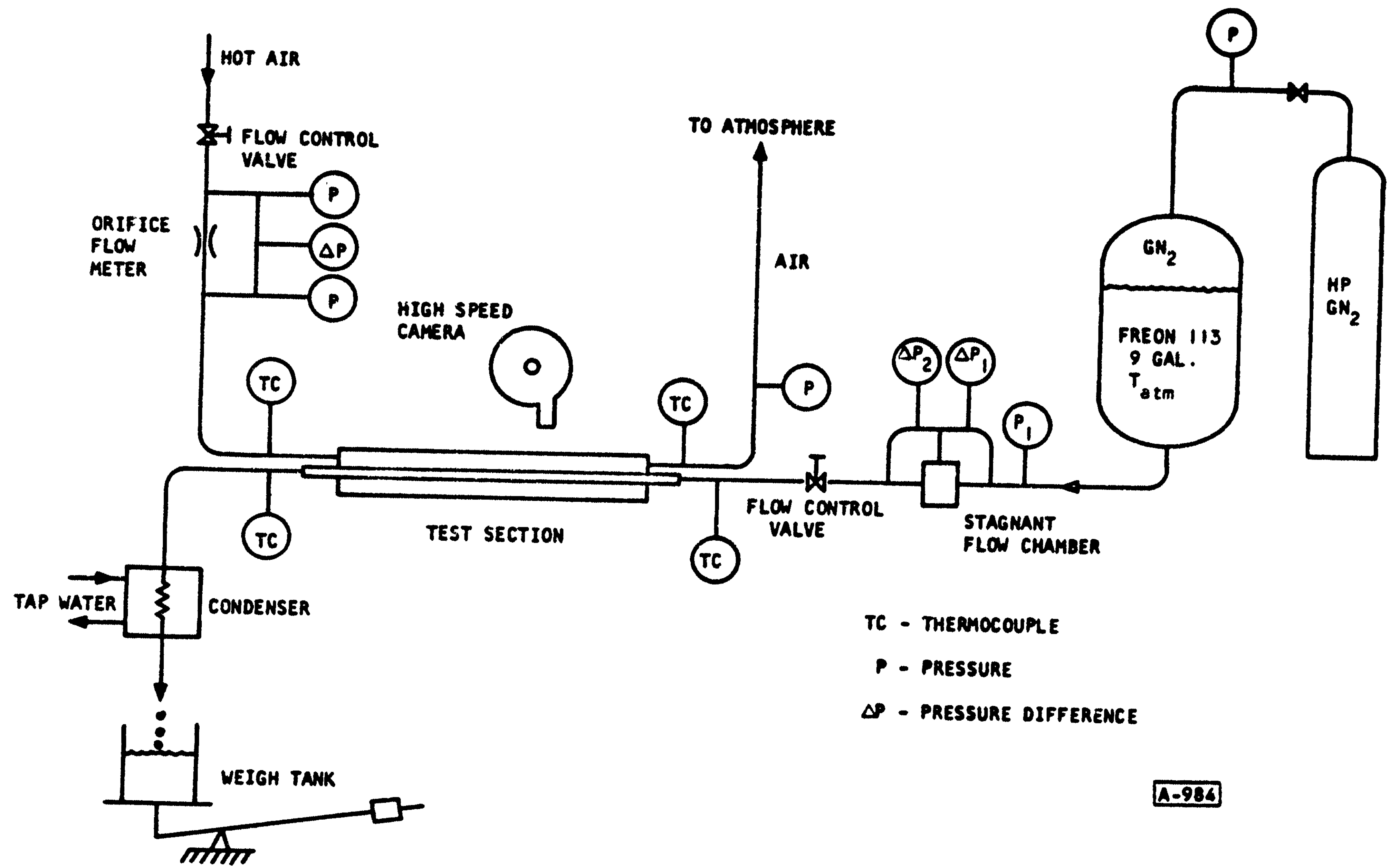

Figure 30. Test Apparatus Schematic

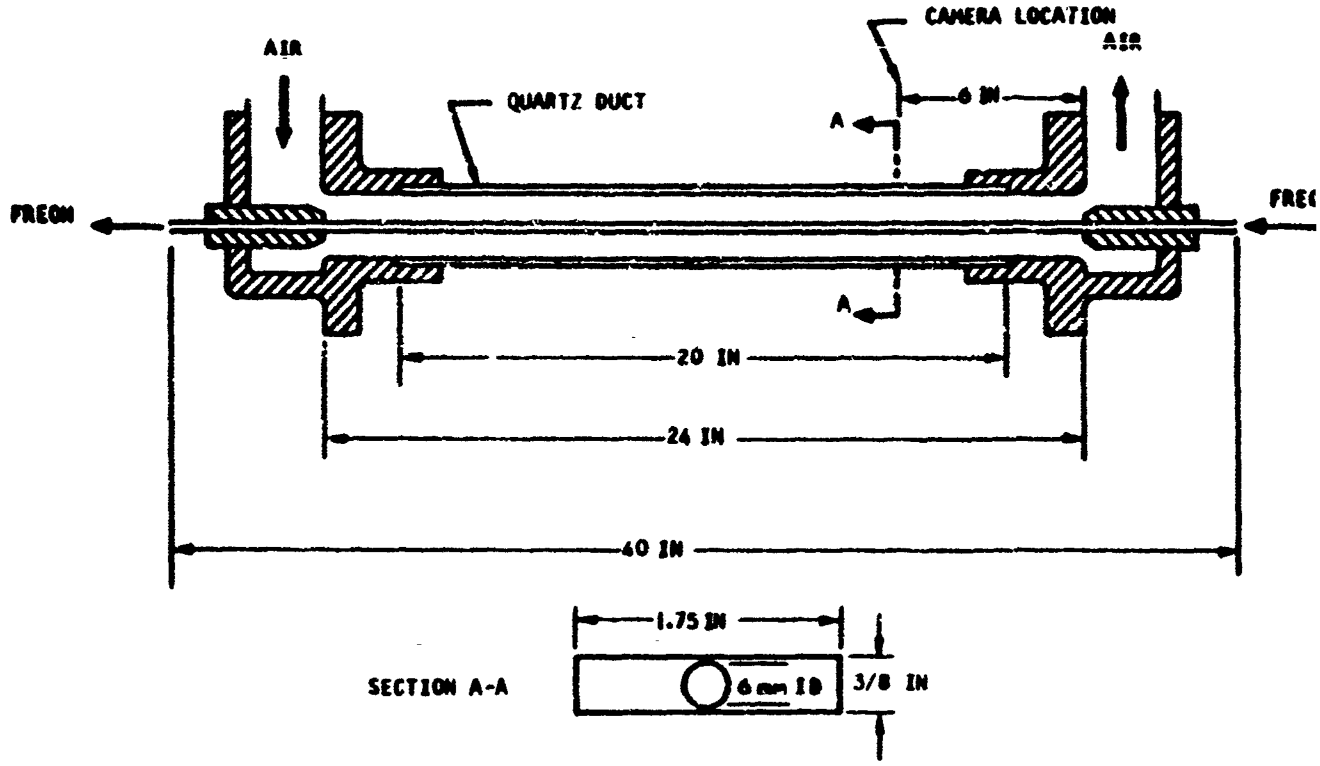

Figure 31. Test Section Geometry

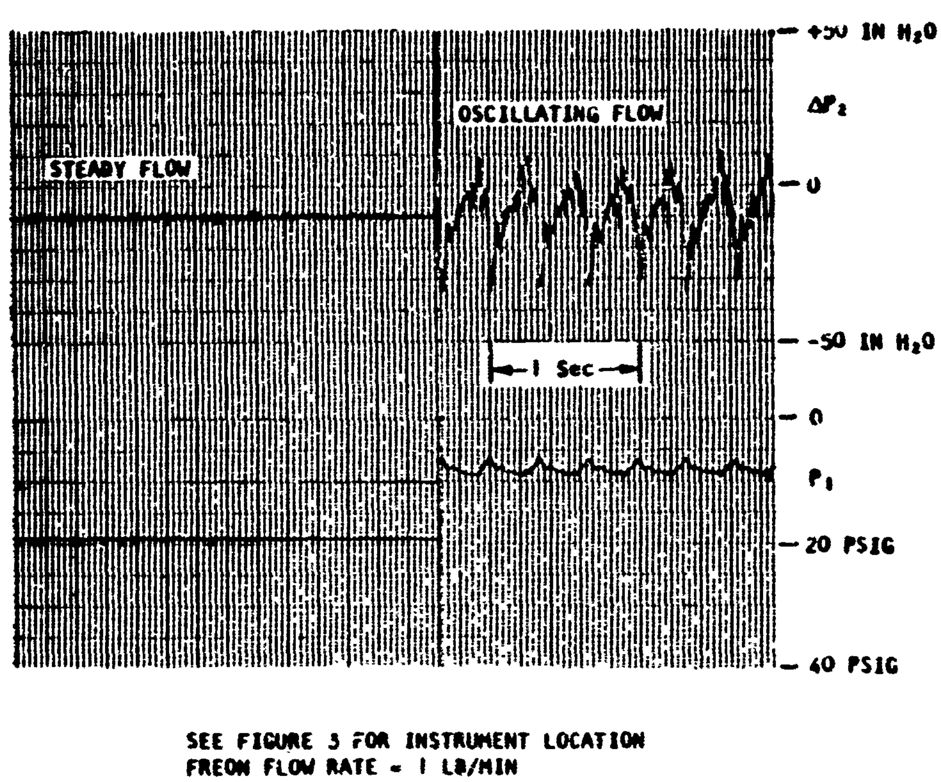

B-123

Figure 32. Typical Pressure Oscillations

FREON

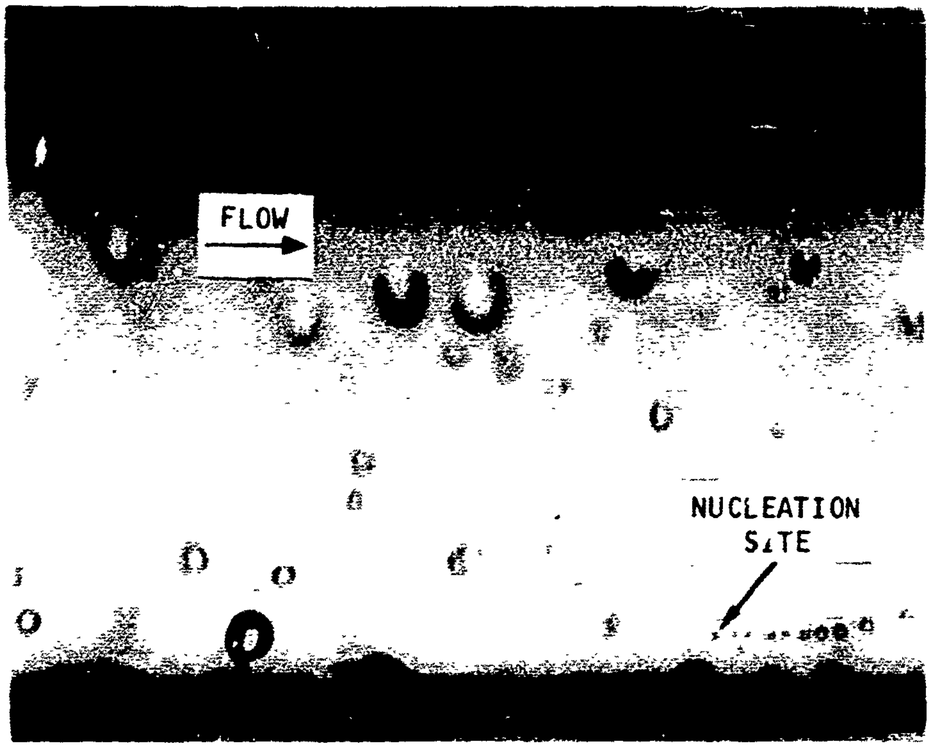

Figure 33. Bubbly Flow

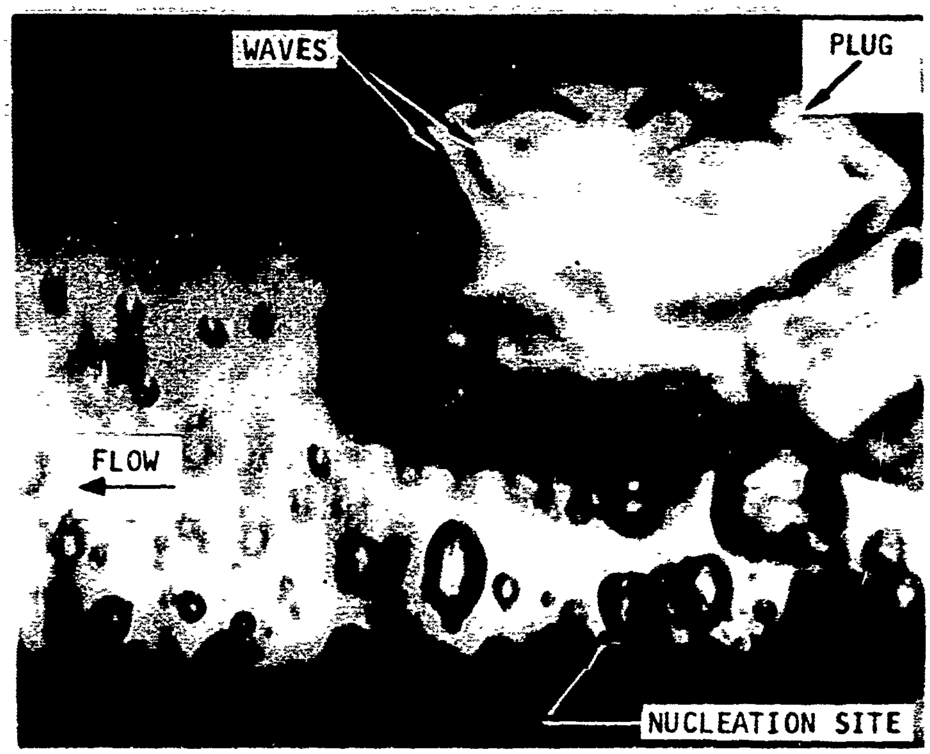

F-246

Figure 34. Plug Flow

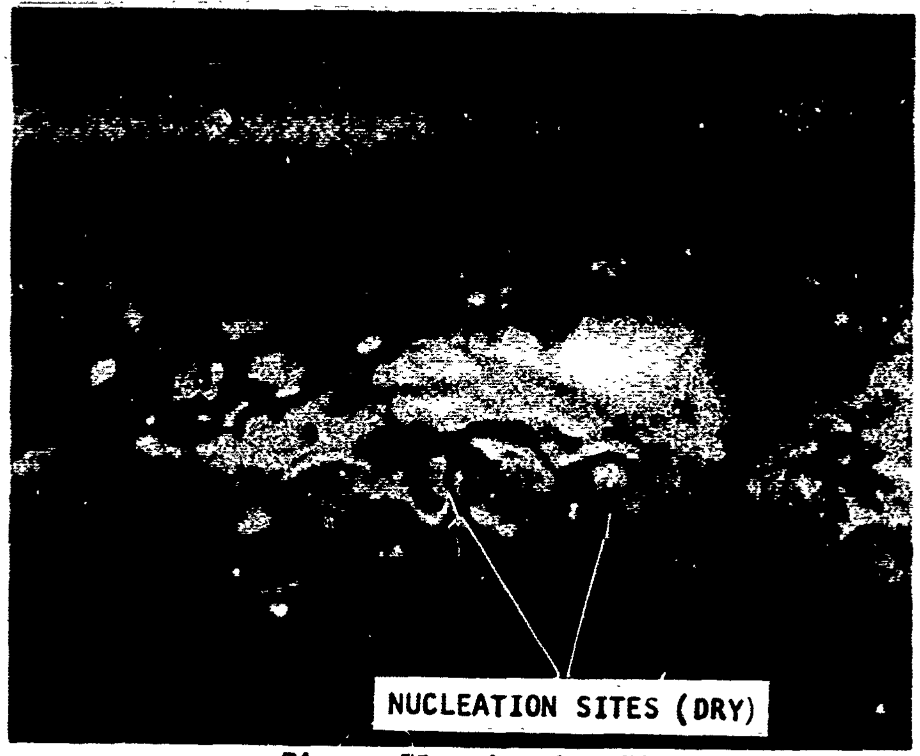

Figure 35. Annular Flow

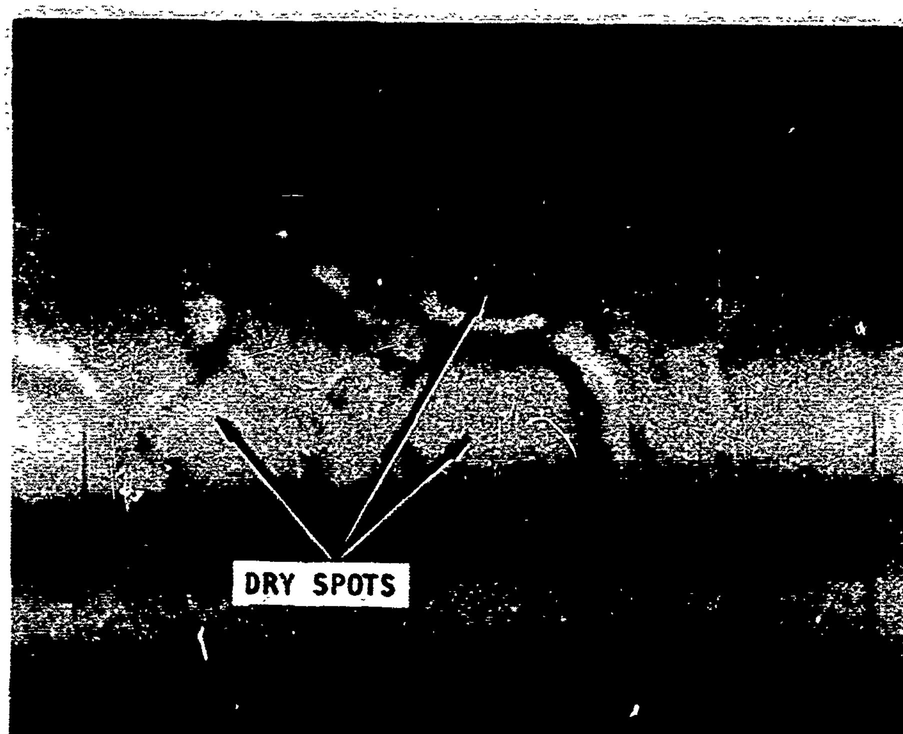

F-248

Figure 36. Annular-Mist Flow Transition